TOPICAL REPORT

PWR LATTICE PHYSICS METHODS

AT

FLORIDA POWER & LIGHT COMPANY

June, 1983

Prepared by: Olga Hanek
Olga I. Hanek
Engineer, Core Design Group

Prepared by: William G. Vernetson
William G. Vernetson, Phd.
Visiting Engineer, Core Design Group

Reviewed by: E. R. Knuckles
E. R. Knuckles
Senior Engineer, Core Design Group

Approved by: F. H. Southworth
F. H. Southworth
Supervisor, Core Design Group

Approved by: Allan E. Siebe
A. E. Siebe
Manager, Nuclear Fuel

DISCLAIMER OF RESPONSIBILITY

This document was prepared by the Fuel Resources Department of Florida Power & Light Company. This document is believed to be true and accurate to the best of our knowledge and information. However, it is authorized and intended for use and application only by Florida Power & Light Company.

FLORIDA POWER & LIGHT COMPANY, ITS OFFICERS, DIRECTORS, AGENTS AND EMPLOYEES SHALL NOT BE RESPONSIBLE OR LIABLE FOR ANY CLAIMS, LOSSES, DAMAGES OR LIABILITIES, WHETHER OR NOT DUE TO OR CAUSED BY THE NEGLIGENCE OF FLORIDA POWER & LIGHT COMPANY, RESULTING FROM THE USE OR MISUSE OF THIS DOCUMENT OR ANY INFORMATION CONTAINED HEREIN.

ABSTRACT

This report describes the methods used in the CHEETAH lattice physics model developed and implemented by the Florida Power & Light Company. Included in this report are descriptions of the methodology used in the CHEETAH model to generate fast and thermal cross sections for fuel and weak absorbers as well as the CHEETAH methodology used to model depletion and buildup of various isotopes. The basis for confidence in the CHEETAH model methodology and results is also presented to include comparisons with critical experiments, comparison with isotopic measurements and cross comparison of the CHEETAH methodology with other methodologies to provide an independent check of the CHEETAH methodology. Both experimental comparisons and comparisons with other calculational methodologies demonstrate the capability of the FPL CHEETAH model to produce fuel and weak absorber cross sections for input to diffusion theory codes and as a stand alone model for calculation of integral fuel lattice parameters.

TABLE OF CONTENTS

TOPICAL REPORT

PWR LATTICE PHYSICS METHODS AT FPL

LIST OF TABLES

LIST OF FIGURES

ACKNOWLEDGEMENTS

The authors gratefully acknowledge the assistance of F. H. Southworth, E. R. Knuckles and S. Lindauer of Florida Power & Light Company as well as K. Roach and S. Turner of the Southern Science Office of Black and Veatch.

1.0 INTRODUCTION

1.1 Purpose/Contents of Topical Report

The specific purpose of this topical is to document the benchmarking for the FPL model and methodology used to obtain lattice physics parameters for fuel and light absorber nuclides in FPL pressurized water reactor cores. As part of the basis for confidence in the FPL implementation and utilization of its CHEETAH lattice physics model, this report reviews the history of lattice physics efforts at FPL for its four operating reactors, along with the qualifications of those with primary responsibility for developing and implementing the lattice physics model. The input data base for such lattice physics calculations is described along with the generic aspects of the output. Both the cross section generation model and the depletion model used to account for burnup effects on the cross sections are presented, along with the experimental and theoretical basis for confidence in the methodology and its results.

1.2 History and Qualifications of the FPL Reactor Physics Group

The FPL Core Design and Methods Group has overall responsibility within FPL for the core designs implemented at FPL reactors. This group also has responsibility for FPL's reactor physics model and methodology development (including those for lattice physics). The FPL Reactor Physics functional organization is presented in Table 1.1. Involvement in lattice physics calculations began with Cycle 3 of the Turkey Point Units 3 and 4 at which point the FPL lattice physics was sufficiently developed and tested to provide FPL with adequate lattice

parameters (especially cross sections) with which to carry out reload physics verification and core follow analysis along with a variety of analyses on specific tests carried out on the Turkey Point Units 3 and 4 cores.

The FPL reactor physics experience is summarized in Table 1.2 and includes the following activities.

Lattice Physics Calculations - Lattice physics calculations to support reload physics determinations and core follow analyses have been performed for all reactor cores independently of the vendor analysis.

Reload Physics Design - The calculation of core lifetime, reactivity coefficients, and control rod effects for reload cores at Turkey Point Units 3 and 4, St. Lucie Unit 1 and St. Lucie Unit 2 have been performed independently of vendor analysis. As part of this activity, FPL engineers have reviewed startup physics tests at all four FPL nuclear units. In addition, using these models, loading patterns have been developed and implemented in joint efforts with the fuel vendors for each nuclear unit.

Core Follow - The analysis of in-core flux traces from Turkey Point Units 3 and 4, and St. Lucie Unit 1 has been performed. Assistance for the analysis of measurement data has also been provided to each plant. Core follow, for which the fundamental reason is verification of expected core behavior, requires a reliable lattice physics model to

produce the input necessary for such plant specific reactor physics analyses. The success with which the core follow analyses have tracked the core behavior further supports the fundamental adequacy of the CHEETAH lattice physics model.

Miscellaneous Reactor Physics Analyses - A statistical test model for core surveillance was developed based on assembly relative power distribution to determine significant departures in the expected core power distribution during power operation. In addition, the reactor physics analyses associated with a number of experiments have been performed successfully to include:

a. Measurement of Doppler and Moderator Temperature Coefficients During Turkey Point Unit 3, Cycle 4, At-Power Operation;

b. Prediction and corroborating measurement of Shoulder Gap Clearance Reduction on High Burnup Fuel Assemblies (35,000 MWD/MTU) resulting from fluence of neutrons with energies greater than about 1 MeV during St. Lucie Unit 1, Cycle 6 operation.

The Core Design and Methods Group at FPL currently includes a supervisor and six engineers. A number of supporting personnel such as programmers, technicians and co-op students are available. Present reactor physics related experience in the group totals about 75 engineer years, with degree levels including 2 PhD's, 2 M.S. degrees, and 3 baccalaureate degrees as well as one engineer with actual reactor operator experience. One member of the group has lectured (faculty) in

the University of Illinois Nuclear Engineering Program. Several members of the group have attended short courses and training seminars in fuel management and related areas of reactor physics. FPL engineers have also regularly attended user's group meetings on fuel utilization, fuel design, quality assurance and related areas. Finally, one engineer has been temporarily assigned as a resident engineer with a fuel vendor specifically to study and apply core reload methodology for FPL reload design activities. Overall, FPL reactor physicists have presented about a dozen papers in this area at ANS and other nuclear industry-related meetings. We expect to maintain experience levels comparable to those described above.

1.3 Summary Description of FPL Reactor Cores

1.3.1 Turkey Point Units 3 and 4

The Turkey Point Units 3 and 4 are essentially identical units[1]; each is designed to be a 2200 MWth pressurized water reactor located on the shore of Biscayne Bay twenty-five miles south of Miami, Florida. The nominal electrical rating of each plant is 760 MWe. The nuclear steam supply system (NSSS) is a three loop, three pump, three steam generator system supplied by Westinghouse Electric Corporation.

Each core is composed of 157 fuel assemblies which contain 15 x 15 arrays of Zircaloy-4 clad fuel pins. In addition to the chemical shim system, 45 full length, 20 finger, Ag-In-Cd alloy rod cluster control assemblies (RCCAs) are used to control the reactor. A

horizontal section of the core showing fuel assembly arrangement as well as location of control rods and instrumentation positions available to the incore moveable detectors (IMD) is shown in Figure 1.1.

Core power distributions are monitored in-core using a system consisting of five (5) moveable fission chambers which can monitor any of fifty (50) locations which are available to the system.

1.3.2 St. Lucie Unit 1

St. Lucie Unit 1 is a 2700 MWth pressurized water reactor located on Hutchinson Island in St. Lucie County between Ft. Pierce and Stuart on the east coast of Florida[2]. The nominal electrical rating of the plant is 890 MWe. The nuclear steam supply system is a two loop, four pump, two steam generator system supplied by Combustion Engineering, Inc. and has completed five cycles of operation.

The St. Lucie Unit 1 core is composed of 217 fuel assemblies which contain 14 x 14 arrays of Zircaloy-4 clad fuel pins. In addition to the chemical shim system, there are 73 full length control element assemblies (including eight with reduced poison loading) which are used to control the reactor. A horizontal section of the core showing fuel assembly arrangement as well as location of control rods and instrumentation is shown in Figure 1.2.

Core power distributions are monitored in-core using either the fixed self-powered neutron detector system or the moveable fission chamber system. The fixed self-powered detector (SPD) system is made up of 45 strings containing 4 detectors per string (each detector is 40 cm in length). The moveable fission chamber system consists of a single fission chamber, incore moveable detector (IMD), which can move to monitor 19 locations labeled in Figure 1.2.

1.3.3 St. Lucie Unit 2

St. Lucie Unit 2 is a pressurized water reactor, located adjacent to St. Lucie Unit 1, with a rated thermal power level currently of 2560 MWth for which the corresponding net electrical rating is 802 MWe[3]. This plant is in its first cycle of operation with a design thermal power level of 2700 MWth which is the maximum expected eventual output of the nuclear steam supply system. The NSSS is a two loop, four pump, two steam generator system supplied by Combustion Engineering, Inc.

The core is composed of 217 fuel assemblies which contain 16 x 16 arrays of Zircaloy-4 clad fuel pins. In addition to the chemical shim system, 83 control element assemblies (CEA's) are used to control the reactor. A horizontal section of the core showing fuel assembly arrangement as well as location of control rods and instrumentation is shown in Figure 1.3.

Core power distributions are monitored in-core using either the fixed self-powered neutron detector system or the moveable fission chamber system. The fixed detector system is made up of 56 strings (4 detectors per string) of 40 cm long self-powered neutron detectors (SPD) while the moveable fission chamber system consists of a single fission chamber, incore moveable detector (IMD), which can move to monitor 56 locations labeled in Figure 1.3.

1.4 Conservative Philosophy for Reactor Physics Calculational Methodology

The FPL Core Design and Methodology group applies physics methods and computer codes which are well-known and accepted within the nuclear industry. For example, fuel cross sections are generated with the CHEETAH[4][5] code which is an improved version of the well-known industry standard LEOPARD[6] code.

The FPL Core Design and Methodology group maintains the backup capability for more sophisticated calculations for the purpose of benchmarking design methods and for investigating the detailed effect of changes in design methods. This capability for more sophisticated calculations in lattice physics is illustrated by the cross comparison of the CHEETAH with the CASMO-2 and NULIF methodologies in Section 5.4 of this Topical Report.

The CASMO-2 and NULIF calculations wre performed independently by Southern Science Office of Black and Veatch, while the CHEETAH calculations were performed by FPL engineers.

Table 1.1

Nuclear Fuel Section Responsibilities Related to Reactor Physics

GROUP	RESPONSIBILITY
Core Design and Methods	"On-site" fuel management: overall responsibility for reload core design, development and implementation of lattice physics and other reactor physics to support reload design, core follow and experiment/test analysis for FPL operating reactors.
Reactor Support	Provides controlled core and assembly mechanical design data; overall responsibility for core performance verification, applies reactor physics to support reactor operations through core data book, startup physics and core follow analyses.
Fuel Supply	"Offsite" fuel management: overall responsibility for uranium procurement, conversion, enrichment and spent fuel disposal.
Systems Support	Provides computer and code systems configuration control and maintenance.
Thermal Hydraulics and System Analysis	Plant transient and accident analyses as well as other thermal-hydraulic analyses. Overall responsibility for Reload Safety Evaluations.

Table 1.2

FPL Reactor Physics Experience

Plant	Cycle	Reload Physics	Core Follow
Turkey Point 3	3	X	X
	4	X	X
	5	X	X
	6	X	X
	7	X	X
	8	X	X *
	9	X	
Turkey Point 4	3	X	X
	4	X	X
	5	X	X
	6	X	X
	7	X	X
	8	X	X
	9	X	X *
	10	X *	
St. Lucie 1	1	X	X
	2	X	X
	3	X	X
	4	X	X
	5	X	X
	6	X	X *
	7	X *	
St. Lucie 2	1	X	X *

*In Progress

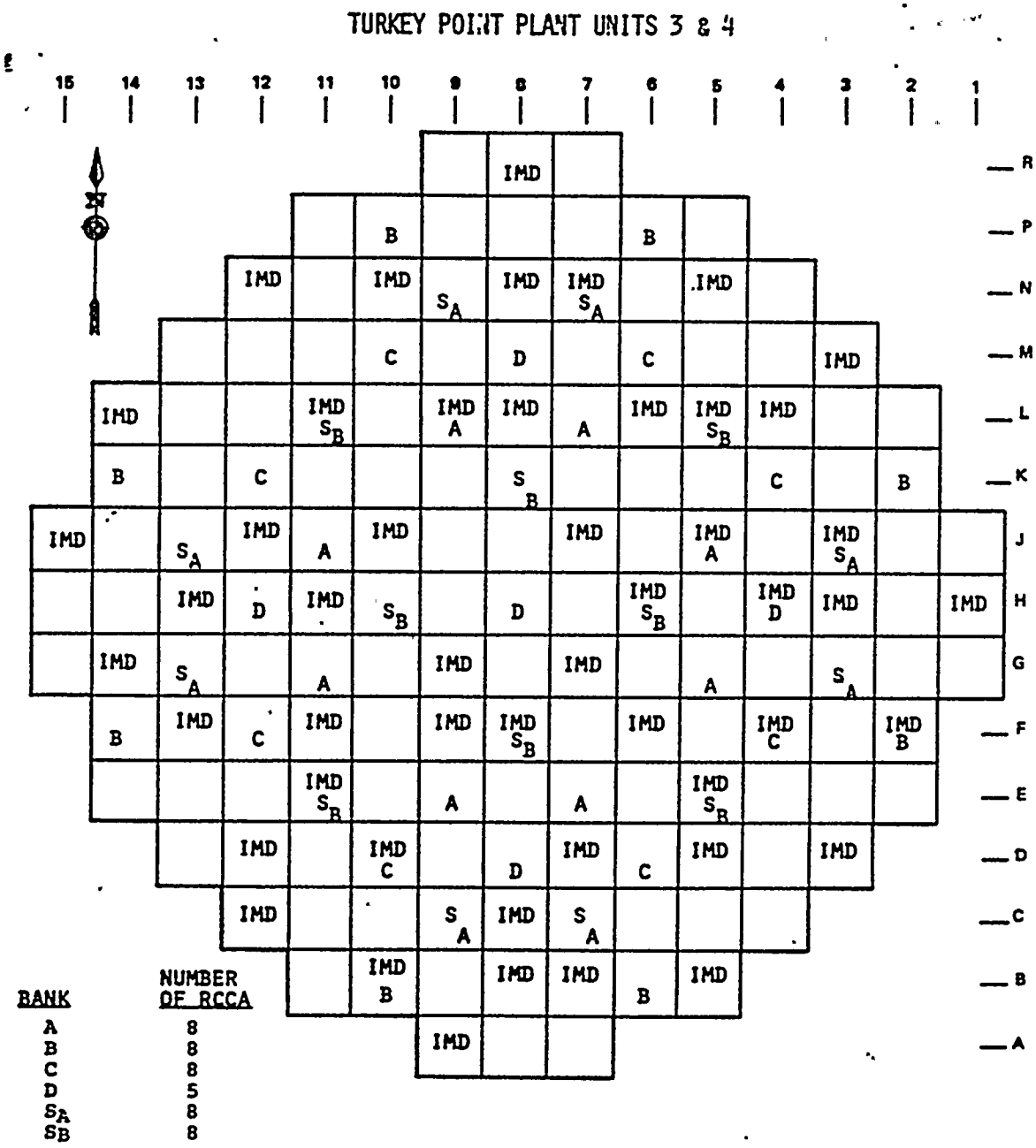

Figure 1.1 Horizontal Section of the Turkey Point Units 3 and 4 Cores.

ST. LUCIE PLANT UNIT NO. 1

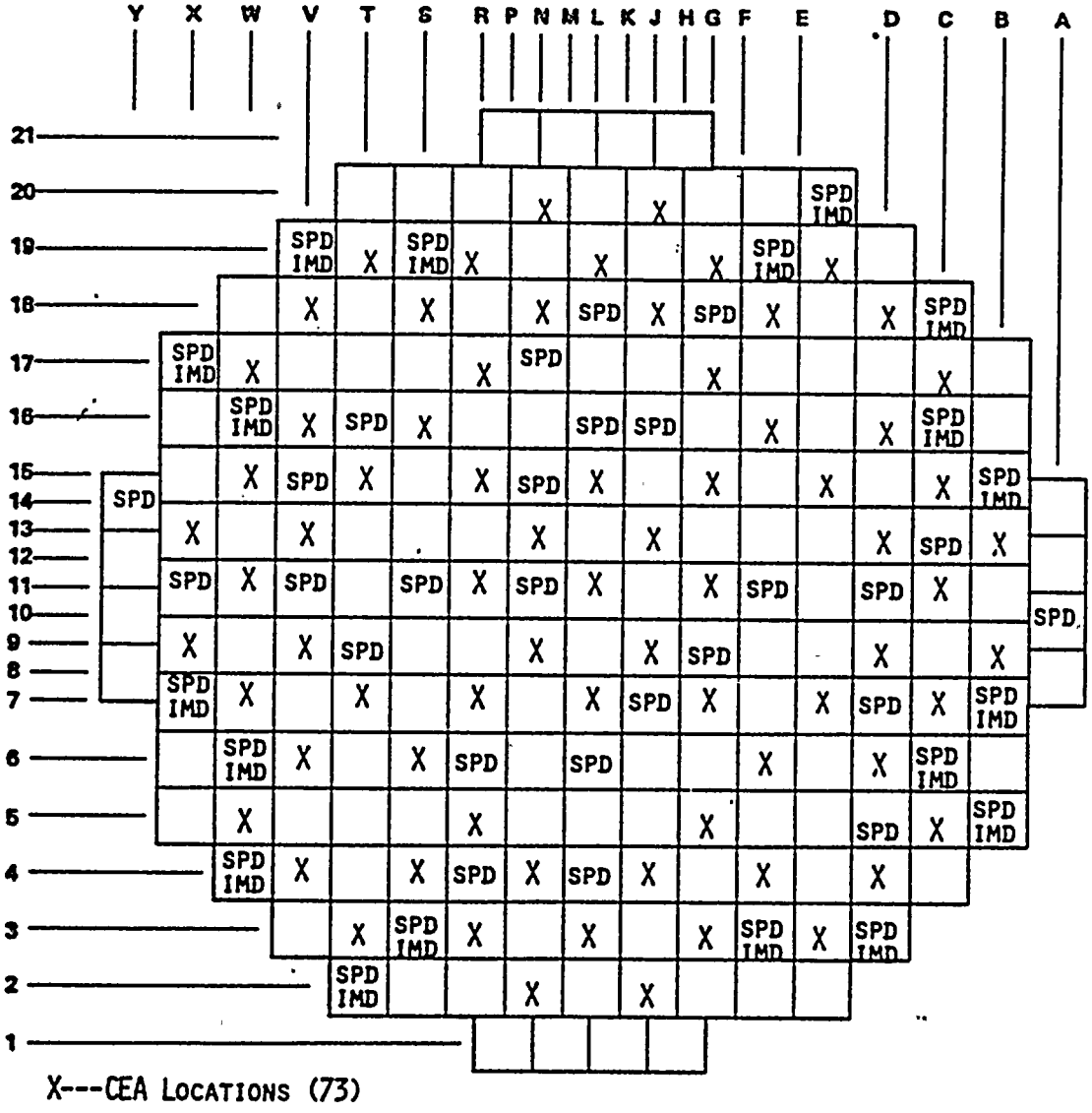

Figure 1.2 Horizontal Section of the St. Lucie Unit 1 Core.

ST. LUCIE PLANT UNIT NO. 2

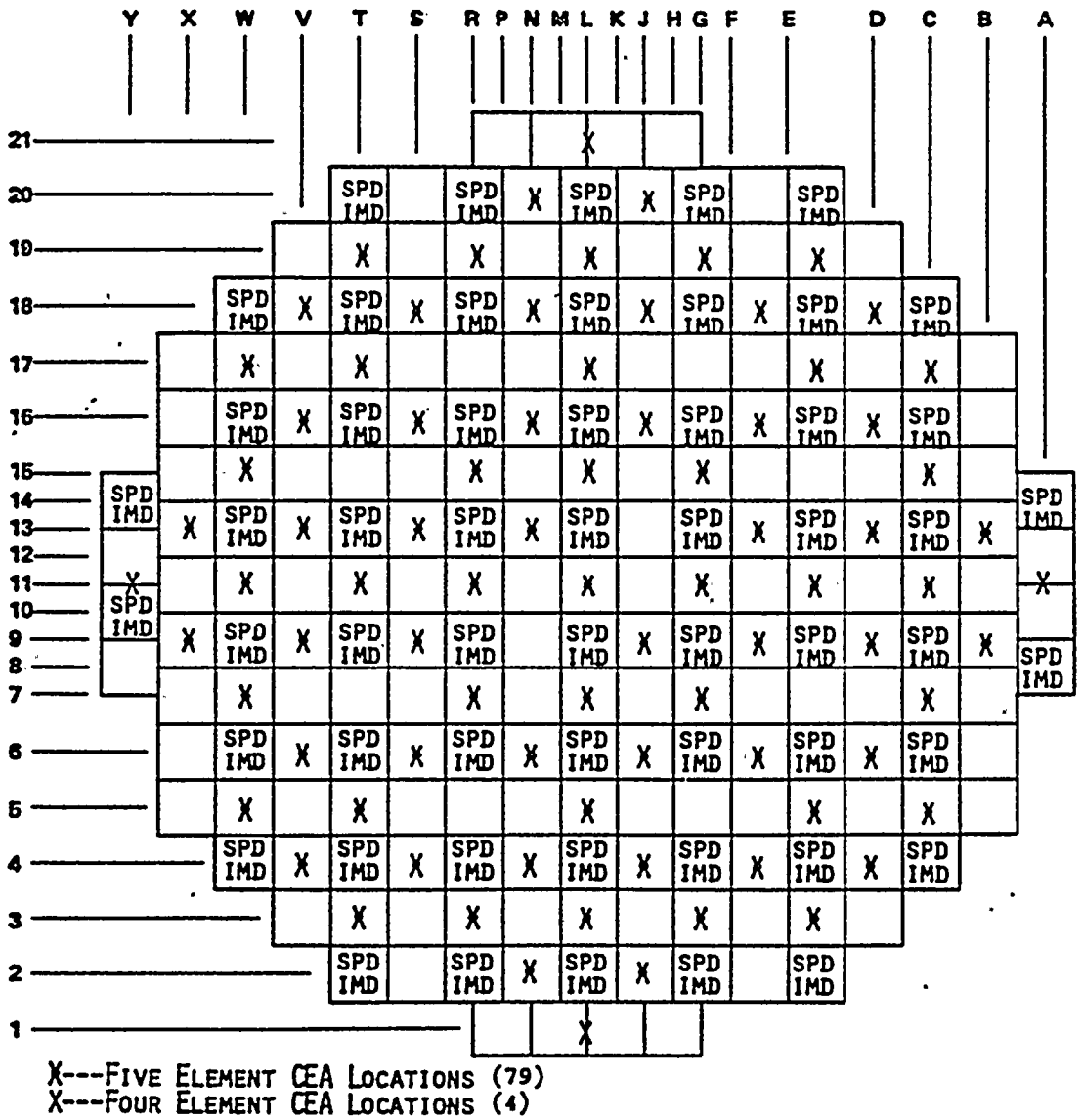

Figure 1.3 Horizontal Section of the St. Lucie Unit 2 Core.

2.0 OVERVIEW OF FPL CHEETAH LATTICE PHYSICS MODEL

This Lattice Physics Topical Report presents the generic CHEETAH model and methodology for lattice physics analysis on Turkey Point Units 3 and 4, and St. Lucie Unit 1; its application is currently being extended to the St. Lucie Unit 2 reactor. The generic aspects of the lattice physics model are addressed in Sections 3 and 4 of this Topical.

The workhorse for the FPL lattice physics model is the CHEETAH[4][5] code which is a Nuclear Associates International (NAI) improved version of the well-known industry standard code, LEOPARD[6]. The FPL CHEETAH code is used to generate fuel and weak absorber cross sections for all FPL reactor cores based upon computed fast and thermal spectra generated from input consisting of unit cell constituents, geometry and temperatures. In addition, CHEETAH contains a depletion model which is used to generate cross sections for various stages of burnup.

The basis for confidence in the lattice physics model and methodology is established by comparison to experimental data (critical experiments and isotopic measurements) as well as comparison with theoretical results generated with the same input using other methodologies.

CHEETAH has been applied to representative fuel in each of the FPL reactor cores. This application encompasses the full range of anticipated temperatures from cold critical to nominal hot full power conditions, enrichments from 1.5% to 4.5% and burnups from 0 MWD/MTU to 65,000

MWD/MTU. The CHEETAH model and associated methodology have been demonstrated to provide accurate and reliable lattice physics parameters with which accurate and reliable core-wide reactor physics analysis and core follow can be performed.

3.0 CHEETAH INPUT/OUTPUT

3.1 Input Description

The CHEETAH [4][5] Code requires a description of the unit fuel cell, various temperatures, pressures and, optionally, a description of the "extra" region. This "extra region" is a geometric approximation of the materials and volume in the reactor core not included in the fuel lattice, (e.g. instrument tubes, guide tubes and water gaps as well as the slots between assemblies) This material and volume is prorated over the individual fuel cell as the "extra" region. The over-all description can be derived from the "cold" mechanical design since CHEETAH optionally temperature-corrects the input dimensions and the number densities implicit in the input.

Input for the CHEETAH model consists of three generic types of information:

(a) Options Section detailing the type of problem to be run;

(b) Mechanical Data detailing the unit fuel cell and assembly geometry, composition and conditions for which cross section data are needed as well as the burnup steps to be run;

(c) Fine Group Cross Section Data selected from the CHEETAH Cross Section Library on the basis of material/isotope identification numbers specified in the input and used in the MUFT-SOFOCATE scheme.

3.2 Cross Section Data Library

The cross section data for the FPL CHEETAH code is stored in a 295 fine thermal group and 54 fine fast group structure. It is based upon ENDF/B-I ENDF/B-II and selected MILC data[5]. A material isotope is selected from the library for incorporation in the unit fuel cell or extra region by specifying its assigned identification number. The FPL CHEETAH identification numbers and corresponding material or isotope designation are presented in Table 3.1. No changes have been made to the CHEETAH library which was obtained from NAI along with the CHEETAH code.

3.3 Output Description

For ease of reference the CHEETAH output edits are discussed in their order of appearance on a typical printout. Output edits available with the FPL CHEETAH code are subdivided into the following seven (7) edit categories:

(a) .. Input Data Verification

(b) Cell Geometry and Neutron Spectrum-Related Parameters (includes U-238 resonance integral)

(c) .. Supercell Number Densities

(d) .Spectrum-Weighted, Few-Group Microscopic Cross Sections

(e) Macroscopic Nuclear Parameters (includes relative fluxes and infinite multiplication factor)

(f) Depletion Information

(g) . Punched Tape Output

The first output of the FPL CHEETAH code is an edit of the input data which provides ease of checking to assure that the desired problem was run including use of the proper non-lattice volume fraction and corresponding non-lattice peaking factor to account for non-fuel lattice core volumes in the supercell.

The first calculated output gives temperature, cell dimensions, unit cell volume fractions and various outputs that are indicative of how well moderated the cell is. This section of the output edit also contains the omega search parameters and the U-238 resonance integral along with the Doppler contribution and the Dancoff correction. In addition, this section contains water and fuel densities, system pressure, the input buckling along with key neutron spectrum parameters including the Wigner-Wilkins 1/v factor, the Maxwellian 1/v factor, the non-uniform Dancoff correction factors, the infinite multiplication factor and the four flux group contributions to k_{oo}. This section also contains the power density and absolute flux levels.

Next the supercell volume-weighted and flux-weighted number densities along with isotopic disadvantage factors are edited along with the improved removal cross sections derived from the improved removal treatment (IRT) for the three fast groups as abstracted from the Greuling and Goertzel approach[5] utilizing the moderating ratio and absorption in the energy region where resonance capture has been smoothed and averaged to assure it is slowly varying. The flux weighted number density is computed using region and energy

dependent disadvantage factors to reflect absorption profiles as well as geometric location. In addition, the heterogeneous number densities and effective energy per fission may be edited.

Next, the spectrum-weighted elemental microscopic cross sections are edited to include the transport, absorption, nu-fission and fission cross sections; one for each fast group and two for the thermal group, one averaged over the Wigner-Wilkins spectrum, the other over a Maxwellian spectrum using Breen's Mixed Number Density (MND) model[9]. For the Group 3 absorption cross section, both a smooth and a resonance cross section are output; the total group 3 absorption cross section is the sum of these two.

The FPL CHEETAH code also edits one fast group microscopic cross sections for possible use in a later 2-group PDQ-7 or other calculation followed by neutron balance data giving the probability that a fission neutron will be absorbed in each element or leak out of the cell based on material buckling.

The macroscopic edit provides volume weighted lattice parameters (D, Σtr, Σa, Σr, $\kappa \Sigma f$, Σf, $\nu \Sigma f$,) and the relative flux for three fast groups and/or for a single fast group as well as for two thermal weightings, the conventional and the MND model. This edit also includes conversion ratios and four-group k_{oo}'s computed from the macroscopic constants for Xenon only removed, for Xenon and soluble poison removed, and also for Xenon, soluble poison and Doppler removed. Next, CHEETAH

also edits the optional cell homogenized number densities plus disadvantage factors.

The output of CHEETAH includes the "Cell Only Macroscopic Edit" and the "Extra Region Only Macroscopic Edit" and additional edits for the so-called Sub-Extra Regions if such are specified in the input; up to five additional regions are allowed to provide a fine breakdown of the extra region. Since the cell "extra" region represents a composite of all the non-lattice regions encountered in the infinite assembly array, the "sub-extra" regions consist not only of the various specific non-lattice region descriptions but can include regions outside the infinite assembly array such as the baffle and reflector over which spectral averaging can be performed These can be obtained by including an additional subregion in the extra region over which an edit is performed. Multiplication factors reported are two-group values.

For depletion cases, mass conversions per unit of original fuel loading are computed and listed for each time step and for the total time since beginning of life. These conversions are based on the original fuel loading and the changes in number densities during depletion.

Power sharing by individual fissionable isotopes is also computed and edited for each time step of a depletion calculation as well as for the total elapsed time span of the depletion calculation.

Optionally, CHEETAH also provides the following punched tape output:

a. Macroscopic and microscopic cross sections for PDQ-7 input including 2-group or 4-group; conventional or MND thermal data;

b. Fast and thermal flux data for further flux spectrum weighting calculations;

c Fuel number densities along with burnup (MWD/MTU) at each time step in a depletion case.

Table 3.1 CHEETAH Input Identification

IDENTIFICATION NUMBER	MATERIAL OR ISOTOPE
1	Hydrogen
2	Oxygen
3	Zr-2
4	Carbon
5	Iron
6	Nickel
7	Aluminum
8	Chromium
9	Manganese
10	Uranium-235
11	Uranium-236
12	Uranium-238
13	Plutonium-239
14	Plutonium-240
15	Plutonium-241
16	Samarium-149
17	Xenon-135
18	Fission Products
19	Boron-10
20	Neptunium-237
21	Plutonium-238
22	Americium-241
23	Natural Gadolinium
24	Uranium-234
25	Plutonium-242
26	Promethium-149
27	Iodine-135
28	UO2
29	PuO2
30	ThO2
31	H2O
32	D2O
33	SS-304
34	SS-316
35	SS-348
36	—
37	Inconel-718

Note 1: The nuclides Np-237, Pu-238 and Am-241 have not been incorporated into the CHEETAH depletion model.

Note 2: The Boron-10 scattering cross sections are artifically inflated to account for the other isotopes present in natural boron.

4.0 THE CHEETAH MODEL

4.1 Features of the FPL CHEETAH

The FPL CHEETAH model is based upon the CHEETAH[4][5] code which is an NAI-improved version of the industry standard LEOPARD[6] code which is used to generate the nuclear parameters, primarily broad group cross sections, of a particular fuel assembly dependent upon its enrichment and burnup in order to support criticality, burnup, isotopic composition and other core-wide calculations. The CHEETAH Code is a zero-dimensional, pin-cell, multigroup, point depletion code wich is used to obtain homogenized cell constants as a function of burnup. Fast and thermal neutron spectra are calculated from a modified MUFT-SOFOCATE[7][8] model using a self-consistent B-1 approximation in the fast region and a modified Amouyal-Benoist (ABH) method [10] in the thermal range. This B-1/ABH theory code does not explicitly account for spatial variations in the flux. CHEETAH assumes the reactor consists of an infinite array of unit fuel cells arranged uniformly in either a square or hexagonal lattice. Each cell contains fuel, clad and moderator regions; lattice irregularities can be accounted for by defining an extra fictitious fuel cell region which includes the fraction of the reactor core that is not unit fuel cells. This extra region allows spectral effects due to lattice irregularities to be included in the CHEETAH spectral averaged cell cross sections.

4.2 Cross Section Generation Model

Spectrum calculations are performed by CHEETAH on the equivalent unit cell including the extra region; the complete four region unit cell

is referred to as the "supercell". The size of the fictitious extra region is determined by entering a non-lattice (non-fuel cell) fraction which is defined as the fraction of the total core that is not unit fuel cells. The objective here is to account for spectrum effects, and hence effective cross section variations, on the fuel cell due to constituents of the fuel assembly which are not fuel cells such as guide tubes, instrument tube, spacer grids, water gaps between assemblies, etc.

4.2.1 Thermal Spectrum

The CHEETAH thermal spectrum is computed using the Wigner-Wilkins approximation as in SOFOCATE[8] with the option of utilizing 172 or 295 fine groups and with one important feature added for the treatment of the thermal disadvantage factors. In SOFOCATE the disadvantage factors had to be input or determined by a separate routine using the output from a prior SOFOCATE run. In CHEETAH, the flux variation across the unit fuel cell is accounted for through a modified Amouyal-Benoist[10] disadvantage factor calculation. The disadvantage factors are energy dependent through the energy dependence of the cross sections that appear in them and inherent in the spectrum calculation. In addition, provision is made to weight non-fuel unit cell regions of the supercell by a factor to account for non-uniform thermal neutron flux distribution within the overall fuel assembly containing non-fuel unit cells.

The FPL CHEETAH model computes the thermal spectrum utilizing one of two thermal energy cutoff options, either 172 fine groups with a thermal cutoff at 0.625 ev or 295 fine groups with a corresponding cutoff at 1.855 ev. The higher cutoff option was incorporated into the NAI-improved LEOPARD[4] specifically to improve the treatment of the large Pu-240 resonance at 1.056 ev. When this higher cutoff option is selected, this low-lying Pu-240 resonance can be included in the thermal spectrum calculation where a more detailed method for computing spatial self-shielding is used. With the 1.855 ev cutoff option, the Amouyal-Benoist integral transport theory procedure is used to treat the 1.056 ev Pu-240 resonance rather than the L-factor self-shielding calculation used by MUFT in the fast spectrum calculation for this resonance.

When the 1.855 ev thermal cutoff is selected, the energy mesh across this resonance in CHEETAH is 0.01 ev and Doppler broadening of the cross sections is explicitly incorporated using the input resonance effective temperature that is also used for U-238.

The effect of including the Pu-240 resonance in the thermal spectrum calculation (and consequently using ABH theory to determine the self-shielding) has been investigated by analyzing the results of various plutonium critical experiments as well as comparison with other computer code models. The general

agreement reported supports the validity of the 1.855 ev thermal cutoff option where the Pu-240 resonance is included in the CHEETAH thermal spectrum calculation[4]. Plutonium critical experiment comparisons reported in Chapter 5 of this report were run using both thermal cutoff options. No significant difference was observed. Similarly, depletion calculations for Turkey Point fuel assemblies were performed using each option. No significant differences in reactivity or isotopics were seen. The FPL CHEETAH model therefore, is not restricted in its choice of cutoff, as long as consistency with other sources of cross-sections is maintained.

The energy-dependent, disadvantage factors are computed from the integral transport theory method as proposed by Amouyal and Benoist with the energy-dependence incorporated via the fine group cross sections. The CHEETAH model also accounts for the clad which had been assumed to be void in the original work. Basically, the theory uses diffusion theory in the moderator and the method of successive generations (utilizing escape and collision probabilities) in the fuel region with a transport boundary condition, based upon the applicable transport boundary correction and linear extrapolation distance, applied at the inside of the moderator[6][10][11][12].

The expressions used to calculate the flux disadvantage factors refer to the pellet average flux; however, the code renormalizes

all the fluxes to a cell average of unity as a more useful reference. When an extra region is defined, the moderator disadvantage factor is arbitrarily assigned to this region. The code, however, has a provision for adjusting the "extra" region importance to account for flux variations in the non unit fuel cell regions in the fuel assembly. In all cases, the disadvantage factors are renormalized to give an average flux of unity.

The macroscopic cross sections at each energy level are then computed by summing the flux weighted number densities and microscopic cross sections over all elements and all regions in the cell.

4.2.2 Fast Spectrum

The CHEETAH fast (non-thermal) spectrum is calculated using a consistent B-1 approximation for each of the 54 fine groups spanning the energy range from 10 MeV down to the thermal cutoff at 0.625 eV as in the MUFT[7] code or 50 fine groups spanning the range down to 1.855 ev when the higher thermal cutoff is selected. Since the spatial distribution for the fast and epithermal flux in MUFT is not explicitly treated, special procedures are incorporated to account for important heterogeneous effects. Two corrections are considered: one is applied in the fast energy region, usually group 1 (E>0.821 MeV) in a 4-group calculation; the other is applied in the resonance or epithermal energy region, usually groups 2 and 3 (thermal cutoff

to 0.821 MeV) in a 4-group calculation.

For the fast energy region, a correction could be incorporated to the fast fission rate of U-238 in terms of a flux advantage factor since the U-238 in the pellet sees a preferentially higher fast flux, especially above the fission threshhold. However, Strawbridge[11] has found that this correction is negligible so it is not included in the CHEETAH model, nor was it included in the antecedent LEOPARD code.

For the epithermal energy region, the second correction considered is a most important correction incorporated into the CHEETAH model to account for resonance effects in the epithermal region. The important heterogeneous effect in the resonance region is the lumping effect of the resonance absorbers and the resultant reduction in the absorption reaction rate. As part of the CHEETAH model, a self-shielding factor is applied to the cross sections to account for the reduced absorption. The self-shielding is assumed to be negligible for all elements except for U-238 providing the Pu-240 resonance at 1.056 ev is included in the thermal spectrum calculation with the cutoff at 1.855 ev. Otherwise a self-shielding effect is calculated or assigned for both U-238 and Pu-240.

The importance of self-shielding effects in fissionable isotopes is reduced due to the fact that both fission and absorption rates

change resulting in negligible changes in the multiplication factor. In addition, since the concentration of such isotopes as U-235 and Pu-239 is relatively low, the importance of considering resonance effects in these isotopes is further reduced. Therefore, no significant errors are introduced by neglecting self-shielding effects in fissionable isotopes.

The resonance absorption calculation (with accounting for spatial self-shielding) consists of three sets of calculations where correct results from one set are directly dependent on the results of the previous set. The three sets of calculations to obtain a spectrum suitable for use in spectral weighting of fast few group constants are:

1. Calculation of the U-238 resonance escape probability,
2. Calculation of a self-shielding factor for U-238 using a "2-step w-search" procedure [12],
3. Calculation of the CHEETAH fast spectrum (MUFT Spectrum) followed by spectral weighting to obtain the fast few group constants.

4.2.2.1 The Resonance Escape Probability

As the first set of calculations, the resonance escape probability for U-238 is computed from the familiar Wigner expression[4][12] using U-238 density and scattering powers homogenized or averaged over the pellet, clad, moderator, and "extra" regions. The resonance integral is computed

from the "metal-oxide correlation" developed by Strawbridge [11] which has been found to agree well with Hellstrand's correlations for isolated rods[13][14]. The correlation has also been found to agree with Hellstrand's temperature correlations[15].

A shadowing correction, the Dancoff factor, due to close-packed lattice effects is also applied to the resonance integral. This shielding correction is simply the blackness of the moderator. The Dancoff correction applied for the CHEETAH fast spectrum model is calculated by Sauer's method[16] with a further correction factor applied to reduce the Dancoff Factor to account for partial transparency of the fuel rod[17].

4.2.2.2 The U-238 Self-Shielding Factor

The calculational procedure used for determining the U-238 self-shielding factor (L-238) is referred to as the "2-step w-search" procedure after Barry[6]. The objective of this procedure is to isolate and then calculate the energy self-shielding effect of the U-238 in the fuel cell on the cell energy spectrum. The w-parameter on which the search is performed is defined as the ratio of non-thermal neutron captures in U-238 to neutron removals to the thermal group which means this is a key nonthermal lattice parameter in determining the multiplication as well as the conversion

ratio of the core.

The two steps in the "2-step w-search" procedure refer to two calculations of the w-parameter. First, the reference w-parameter is calculated for a reactor which has negligible neutron leakage and neutron captures except those in U-238. The results for the resonance escape probability obtained in the first set of calculations outlined in Section 4.2.2.1 are used in this omega calculation.

The second step in this w-search procedure consists of a "modified MUFT" calculation in which the capture cross section in all elements except U-238 is set to zero along with the leakage (buckling $B^2=0$). The modified MUFT iterates on (adjusts) the U-238 self-shielding factor (L-238) until the reference w-parameter calculated in Step 1 is satisfied; that is, each resonance escape probability for U-238 is adjusted by this L-factor and the L-factor is then varied until the resonance integral for U-238, when calculated assuming zero absorption for all other elements, agrees with the Strawbridge and Barry correlation[12]. The resultant U-238 self-shielding factor is the end result of this second set of calculations; this L-238 is then used in MUFT to determine the CHEETAH (MUFT) fast spectrum and the fast few group constants in the third set of calculations presented in Section 4.2.2.3.

The major assumption in this search procedure is that the U-238 self-shielding factor (L-238) is unaffected by absorption in other isotopes and by fast neutron leakage, both of which are present in the reference w-parameter calculation. This assumption is reasonable since the resonances of various isotopes interact only slightly as demonstrated in studies analyzing the effect of U-235 enrichment change on the U-238 self-shielding factor[18].

4.2.2.3 Calculation of Nonthermal Group Constants

Using the "converged" L-factor for U-238 from the 2-step w-search procedure and a self-shielding factor of unity for all other isotopes (provided the 1.855 ev thermal cutoff is selected), MUFT is rerun after restoring the buckling and all absorption cross sections. Optionally, MUFT performs a buckling or poison search until the effective multiplication factor is unity. The fast, non-thermal, few-group microscopic cross sections are then averaged over the computed MUFT spectrum.

When the lower thermal cutoff is selected the CHEETAH code utilizes one of two options to determine a resonance self-shielding factor (L-240) for Pu-240. The first option is to assisgn the same value for L-240 as is determined by the two-step omega-search procedure for U-238. The second option involves a separate calculation of the L-240 factor.

The resultant L-240 is based upon the appropriate L-240 correlation from those incorporated into the CHEETAH code. In either usage case, the resonance self-shielding effect of the Pu-240 is accounted for in the FPL CHEETAH model when the 0.625 ev thermal cutoff is selected. The resultant L-factor (L-240) is used along with the L-238 self-shielding factor in the MUFT fast spectrum calculation to determine nonthermal group constants.

4.3 Cross Sections for Fuel and Weak Absorbers

4.3.1 Cross Sections for Fuel Cells

CHEETAH is used in the FPL reactor physics model to generate the cross sections for all fuel regions in the reactor and for all non-fuel regions except for those in which a strong parasitic neutron capture takes place such as in burnable poison pins and control rod fingers. The few-group cross section data generated is part of the input needed to the diffusion theory, two-dimensional, fine mesh and nodal models used for reactor physics design and core follow calculations.

In addition the built-in CHEETAH polynomial fits for fission product cross section, with an appropriate scaling factor, are used in all CHEETAH depletion calculations. For CHEETAH, the fuel in the assembly lattice is explicitly described as a four-region supercell consisting of pellet, clad, moderator and an extra region composed of the constituents of the assembly which are not unit

fuel cells.

A CHEETAH depletion calculation is performed over the expected burnup and temperatures the assembly will experience during its lifetime in the reactor. These depletion calculations then yield few group cross sections for fuel and weak absorbers in the fuel cell that span the expected lifeltime of the fuel. These various CHEETAH calculations provide the few group cross section data for unit fuel cells for use in HARMONY or PDQ-7 calculations.

4.3.2 Cross Sections for Weak Absorber Cells

CHEETAH is also used to generate cross sections for the instrument tubes, guide tubes baffle, and moderator non-fuel cell regions in the reactor. These non-fuels are also treated in a unit cell fashion which includes a fuel, clad and moderator region; these are included as the extra region in the supercell. All the materials/isotopes which constitute a non-fuel region are distributed within the supercell extra region with cross sections to be weighted over the resultant spectrum.

4.4 The Depletion Model

4.4.1 Generic Model and Methodology

The FPL CHEETAH code performs burnup calculations to account for variations of neutron spectra with depletion. This accounting is achieved by first performing the spectrum calculation for a specified supercell system, then calculating the fuel depletion for

a given time increment followed by a recalculation of the spectrum. This procedure is repeated until the desired burnup level is reached. This procedure assumes that the energy integrated flux remains constant throughout the burnup time step which is not valid during xenon buildup since the code does not provide for a thermal poison removal as the xenon builds in. This restriction is overcome by initially running one or two short burnup time steps.

The FPL CHEETAH depletion model considers the following groups (chains) of related elements and accounts for isotopic changes in the supercell during burnup:

a. Uranium-235 Chain (includes U-234, U-235 and U-236)

b. Uranium-238 Chain

c. Lumped Fission Products

d. Xenon-135 and Samarium-149 Production

e. Boron-10

The absolute fluxes needed for reaction rates are obtained implicitly from the user-supplied power density. By definition, this must equal the product of the internally calculated energy generation per fission based on stored data, the macroscopic fission cross section (which is directly calculable from CHEETAH-generated number densities) and volume weighted cross sections and the absolute flux.

4.4.2 Isotopic Accounting Groups

4.4.2.1 Fissionable Isotopes

An exact solution is used for both the U-235 chain and for the U-238 chain; the solution is based on Laplace transforms of the set of equations describing nuclide concentrations. Initial number densities are included directly at the beginning of a depletion step as needed for the initial spectrum calculation. For the FPL CHEETAH model, the U-235 chain actually begins with U-234 (the first nuclide in the linear chain) and runs single pass through U-236 which is arbitrarily assumed to end the chain when capturing a neutron. The U-238 chain begins with U-238 and runs single pass through to Pu-242 which is arbitrarily assumed to end the chain when capturing a neutron. A constant energy-integrated flux is assumed through the burnup time step. Since this assumption is invalid unless a thermal poison is removed as the xenon builds in, several short initial burnup/time steps are utilized to avoid violating this restriction; FPL has found steps at about 110 and 380 hours to be effective.

The FPL CHEETAH includes the isotopes Np-237, Pu-238 and Am-241 in its microscopic cross section library. These isotopes were not present in the original LEOPARD library and have not been incorporated into the CHEETAH depletion model[4].

4.4.2.2 Lumped Fission Products

All fission products except those involved in the Xe-135 chain (I-135 and Xe-135) and the quickly saturating Sm-149 chain (Pm-149 and Sm-149) are lumped into a single pseudoelement which is accrued at the rate of one per fission event. Burnup-dependent, effective cross section polynomial correlations for this pseudoelement are included in the depletion model for the fast group and for the thermal group cross sections respectively.

4.4.2.3 Xenon and Samarium Chains

The CHEETAH model incorporates the CANDLE[19] code treatment of the xenon and samarium chains. Having calculated the depletion of the various fissionable isotopes, CHEETAH calculates the average yields of I-135, Xe-135 and Pm-149 based on the average density of the applicable fissionable isotopes and the stored fission yields.

4.4.2.4 Boron-10

The FPL CHEETAH depletion model does not distinguish between soluble (shim) and fixed (burnable) poisons. Basically the only distinction is in where the poison (Boron-10) is located within the supercell. Boron-10 in the pellet or clad region is automatically burnable; Boron-10 in the moderator or the extra region is not burnable. With the exception of B-10, all isotopic changes due to depletion are assumed to take place in the pellet region.

5.0 BASIS FOR CONFIDENCE

5.1 Introduction

This section contains the basis for confidence in the FPL CHEETAH lattice physics model and methodology. In order to verify that the calculations performed by the CHEETAH code are sufficiently accurate for fuel assembly reactivity isotopic predictions, comparisons have been made with data from various critical experiments and with measured isotopics as a function of exposure. In addition, a cross comparison of the CHEETAH methodology with other methodologies has been performed to provide independent verification of the CHEETAH methodology.

5.2 Comparison of CHEETAH Results with Critical Experiments

The first step toward establishing a basis for confidence is to compare the results of CHEETAH calculations with data from well-defined clean critical experiments. The capability to calculate such experiments is a strong indication of the range of applicability of CHEETAH. For this purpose, three groups of clean critical experiments have been analyzed with the CHEETAH code, as follows:

(a) Strawbridge and Barry [12]

(b) SNUPPS Zircaloy Clad Experiments[20]

(c) Mixed Oxide Critical Experiments[21]

The data comparison involves determining the CHEETAH-calculated effective multiplication factor (keff) as a function of six parameters which are significant in reactor design (enrichment, fuel density, lattice

pitch, critical buckling, soluble boron concentration and water-to-uranium volume ratio) for the three groups of experiments. The calculated k_{eff} values were then compared in each case with the experimentally determined values of unity to check for the possibility of systematic errors in the CHEETAH model.

5.2.1 Strawbridge and Barry Experiments[12]

The first group of data was selected from the paper by Strawbridge and Barry[12]. The Strawbridge and Barry experiments selected for comparison are the light water moderated, uranium dioxide criticals with either aluminum or stainless steel clad. The k_{eff} for each of 40 experiments (all Strawbridge and Barry Critical Experiments except those utilizing heavy water moderator) was calculated using the measured buckling as input to CHEETAH. These experiments covered a broad range of enrichments, fuel densities, lattice pitches, critical bucklings, moderator boron concentrations and water-to-fuel volume ratios. The enrichment varied from approximately 1.31 to 4.02 weight percent U-235 while the fuel density varied from 7.53 to 10.53 gm/cm^3; lattice pitch varied from approximately 0.405 to 1.31 inches; the critical buckling varied from 17.2 to about 95.7 m^{-2}; finally, the soluble boron concentration varied from 0 to 3389 ppm while the water-to-uranium volume ratio varied from 2.06 to 10.38.

These data include the cold critical operating range for Turkey Point Units 3 and 4 as well as St. Lucie Units 1 and 2, so these experiments provide a good basis for evaluating the FPL CHEETAH model. As indicated by Strawbridge and Barry [12], the experimental lattices used in this comparison represent a severe test of any calculational procedure. The variation of the CHEETAH calculated effective multiplication factor versus each of the six selected parameters is presented in Figures 5.1 through 5.6. The data is also listed in Table A.1 of Appendix A for reference. As indicated on the figures, the CHEETAH k_{eff} results are in good agreement with the experimental data (k_{eff} = 1.0) over the wide range of critical experiments considered. A statistical analysis on this group of calculations yielded k_{eff} = 1.0034 $\pm$ 0.0082 where the quoted error corresponds to one standard deviation about the mean.

While there is a general bias to predict k_{eff} greater than 1, the quoted error and bias is deemed to be very acceptable. There appears to be no systematic trends in Figures 5.1 through 5.6 indicating a consistent and reliable treatment over the ranges examined for the plotted variables.

5.2.2 SNUPPS Zircaloy Clad Experiments[21]

The second group of clean critical experiments analyzed with the CHEETAH code had identical fuel (UO2) to that of Strawbridge and Barry but with a single enrichment set at 2.719 w/o U-

$235^{(21)}$. This group of 14 experiments covered a broad range of water-to fuel volume ratios and boron concentrations in the moderator on relatively small (radial dimension) experimental arrays of fuel pins; the radius of the fuel region was varied approximately from 17.6 cm to 26.5 cm for a constant active fuel height of about 121.9 cm. No measured bucklings were reported for these experiments - only the critical number of fuel pins from which the critical radius can be inferred.

For these zircaloy clad experiments the pitch was varied from 0.600 to 0.976 inches; the water-to-uranium volume ratio was varied from 3.04 to 12.66; the critical buckling varied from 55.72 to 97.25 m^{-2} and the soluble boron concentration varied from 0 to 727.7 ppm. The key difference in this set of critical experiments was the investigation of low absorption clad; all fuel in this group was clad with Zircaloy-4 as the basis for the SNUPPS cores.

Analyses using CHEETAH and material bucklings given in the reference (20) indicated a possible bias of about 1.5% in k_{eff}. In order to reduce the possible effects of experimental error and the resultant bias in k_{eff} associated with the material bucklings for these small assemblies, one-dimensional radial calculations were performed on this group of experiments using diffusion equation coefficients for both fuel and reflector regions calculated with the CHEETAH code. With the calculated radial leakages, the

one-dimensional calculations provided a much better correlation. The variation of the calculated effective neutron multiplication factor versus the six selected parameters is also presented in Figures 5.1 through 5.6 for this group of experiments. The data is also listed in Table A.2 of Appendix A for reference. A statistical analysis on the one-dimensional calculations yielded $k_{eff} = 1.007 \pm 0.0019$ where again the quoted error is one standard deviation.

5.2.3 Mixed Oxide Critical Experiments[21]

The third group of clean critical experiments consisted of 14 experiments selected from two larger sets of experiments conducted at the Westinghouse Reactor Evaluation Center as reported by Babcock and Wilcox[21]. One set was conducted as part of the Saxton plutonium evaluation program[22], the other was conducted later, partly to investigate the effects of Pu-240 isotopic fuel content on analytical evaluation of critical experiments[23]. Of the fourteen critical experiments analyzed in this group, eleven were mixed oxide fueled (zircaloy clad) while three were fueled with enriched UO_2 clad with stainless steel. Like the SNUPPS critical experiments, these experiments are also characterized by small assembly radius ranging from only 12.94 cm to 27.22 cm; in addition, the height of these assemblies is small also (about 92.96 cm) making these experiments even more sensitive to leakage and experimental uncertainties in axial and radial buckling measurements.

All eleven mixed oxide criticals selected from the two sources had PuO_2 in natural UO_2 and covered a range of pitches varying from 0.52 to about 1.06 inches. These eleven experiments may be subdivided into two categories according to the PuO_2 content (w/o) in the fuel. The fuel in the five Saxton experiments[22] was 6.6 w/o PuO_2. The fuel in the six isotopically varying experiments [23] was all 2.0 w/o PuO_2. For the six 2.0 w/o PuO_2 experiments, two subsets of experiments were selected. The plutonium in four experiments contained approximately 8 w/o Pu-240; these four experiments covered a small range of water volume fractions (0.737-0.777) and a moderate range of soluble boron concentrations (0-526 ppm). The plutonium in the other two experiments was approximately 24 w/o Pu-240; these two experiments also covered a small range of moderations (H_2O volume fraction of 0.737 and 0.777) but with no soluble boron.

The final three experiments considered in this group of mixed oxide experiments were connected with the Saxton Plutonium program but the fuel was UO_2 enriched to 5.74 w/o U-235, with no plutonium content. Again the experiments covered a range of water-to-fuel volume fractions (0.495 - 0.782).

Attempts to correlate these experiments using CHEETAH and measured bucklings yielded relatively high k-effective results. This is partially attributed to experimental errors in measured buckling values due to the small size of the assemblies in this

group of experiments. A statistical analysis on the eleven plutonium bearing experiments yielded k_{eff} = 1.0138 ±0.0073. To account for possible buckling errors in the smallest dimension, one-dimensional radial calculations were performed on this group of experiments using diffusion equation coefficients for both fuel and reflector regions calculated with CHEETAH. The one-dimensional calculations provided a similar correlation as a statistical analysis on the eleven plutonium-bearing experiments yielded k_{eff} = 1.0138 ±0.0092. However, the excess in keff above unity was indicated to be better correlated with the type of experiment involved within the three subgroups of plutonium bearing criticals as well as for those three experiements fueled only with UO_2. In particular, the CHEETAH 1-D k-effective results for the fourteen plutonium criticals fall within four distinct groups corresponding to the four types of fuel used as shown in Table 5.1.

To determine the sensitivity effect of the Pu-240 resonance treatment on the calculation of the eleven plutonium-bearing critical experiments (4 through 14), CHEETAH calculations were performed using the option for a thermal cutoff at 1.855 ev. A statistical analysis on these eleven zero-dimensional calculations yielded k_{eff} = 1.0103 ±0.0094 which shows a slightly better k-effective result but an even larger standard deviation than for zero dimensional CHEETAH calculations performed with the 0.625 ev cutoff. The comparative results for k_{eff} obtained with

each of the thermal cutoffs in the CHEETAH calculations and also with the 1-D CHEETAH-based calculations are summarized in Table 5.2.

Although the CHEETAH calculations with the 1.855 ev cutoff produce a slightly better overall agreement with experiment, this does not appear to be significant since the standard deviation is also larger by nearly as much as the average keff is reduced toward unity.

The summary of the results of the one-dimensional calculations of all fourteen plutonium critical experiments in Table 5.1 does indicate some correlation of the experiments. As discussed earlier, the results for the four distinct types of fuel correspond reasonably closely, though in some cases, such as the five 6.6 w/o PuO_2 experiments (4 through 8), the average deviation from the experimental measurement of unity is larger. One possible implication of these more tightly bunched subgroups of keff is that there is a source of experimental error that varies from one experimental subgroup to another. The obvious candidate to account for this error is the measured leakages (bucklings). This hypothesis is supported by several considerations.

First, the 1-D calculations using CHEETAH-produced constants provide reasonably consistent results for k-effective for each separate set of plutonium criticals (see Column 4 of Table 5.1),

though the average value is above unity. However, the first three critical experiments contain no plutonium but also show a high calculated k_{eff} = 1.01127. In addition, the calculation of plutonium criticals with the higher thermal cutoff (1.855 ev) in the FPL CHEETAH eliminates the treatment of the Pu-240 resonance from consideration as the source of a significant amount of the disagreement. However, analysis of the Strawbridge and Barry and the SNUPPS criticals loaded with UO2 clearly shows that CHEETAH gives reasonably good results for such cases. Therefore, since the keff calculated for such small assemblies is extremely sensitive to leakage measurements, the parameters most likely to account for such experimental errors are the measured leakages.

As a second indication that the measured leakages are responsible for the lesser agreement on the plutonium critical experiments, the consistent results within the experiment subgroups may be attributed to four unique sets of experimental conditions. These considerations support leakage measurement errors in these extremely small critical experiments which could easily account for the disagreement in calculated values of keff.

The variation of the calculated keff versus the six selected parameters is presented in Figures 5.1 through 5.6 for the one-dimensional results calculated with CHEETAH constants at the 0.625 ev cutoff. The data is also listed in Table A.3 of Appendix

A for reference. A statistical analysis on the one-dimensional calculations yielded $k_{eff} = 1.0138 \pm 0.0073$ where the quoted error is one standard deviation and the points are scattered about the mean with no apparent trend in any of the Figures. Considering the small size of these critical experiments, and the comparative importance of experimental leakage measurements, these results show adequate agreement and further verification of the CHEETAH lattice physics calculational model.

5.3 Comparison of CHEETAH Results with Isotopic Measurements

5.3.1 Comparison with Yankee Rowe Isotopic Measurements

In addition to comparison with critical experiments, the results of the CHEETAH model have also been compared with the isotopic measurements made on the Yankee Rowe I spent fuel as part of the Yankee Core Evaluation Program[24]. The FPL CHEETAH depletion uranium and plutonium isotopics are presented in Figures 5.7 through 5.13 in comparison with specific isotopic production or destruction in the Yankee Rowe asymptotic neutron spectrum. This spectrum is found in those regions of the core which are well removed from and unaffected by the perturbations occurring near water slots which surrounded the cruciform control rod positions in Yankee Rowe Core I and near the core reflector. Graphic results presented in Figures 5.7 through 5.13 show the variation of seven isotopes in the asymptotic neutron spectrum with burnups up to about 28,000 MWD/MTU as follows:

1. U-235 Net Destruction

2. U-236 Net Production

3. U-238 Net Destruction

4. Pu-239 Net Production

5. Pu-240 Net Production

6. Pu-241 Net Production

7. Pu-242 Net Production

For each isotopic net production or destruction presented, data are presented from the Yankee Rowe I spent fuel measurements along with Yankee Atomic calculations based on the Yankee LEOPARD unit cell model calculation. The FPL CHEETAH isotopics are shown to agree very well in all cases, though there is a slight underprediction of the fissile plutonium isotopics at the higher burnups. In general the FPL CHEETAH-calculated isotopics agree well with the measured and LEOPARD-calculated isotopics.

5.3.2 Comparison with Turkey Point Unit 3 Isotopic Measurements

A primary objective of the Department of Energy (DOE) National Waste Terminal Storage Program is to develop and demonstrate the technology for safe disposal of spent commercial reactor fuel. A major requirement is a performance prediction model for spent fuel disposal to support disposal technology and licensing of nuclear waste disposal repositories. Performance modeling must be based on data obtained from field disposal and from separate laboratory tests on fuel which has undergone significant burnup. Performance is established by comparing pre- and post-test

conditions, which are qualified and quantified by a series of nondestructive and destructive tests on the respective fuel assemblies and rods[25]. To establish the burnup level of the test assemblies, rods are selected from representative assemblies and experimental analysis and corroborative theoretical calculations are conducted to establish the burnup level isotopic composition of the burned fuel[26].

As part of this program, five highly-burned fuel rods (G7, G9, H6, J8 and I9) were removed from the B17 fuel assembly (2.559 w/o enrichment) used during the first two operating cycles of the FPL Turkey Point Unit 3 reactor. Nondestructive examination of the B17 fuel assembly and rods showed all five rods selected for burnup analysis to be of sound integrity prior to destructive testing. The experimental methodology used to prepare the samples and perform the measurements is detailed elsewhere[25][26]. A total of eight fuel rod sections were subjected to experimental burnup analysis — four sections from rod G7 and one from each of the other rods. Five of the samples were taken at the same distance from the fuel rod bottom. The sample identification numbers and axial locations are listed in Table 5.3 along with the experimental results of the HEDL (Hanford Engineering Development Laboratory) burnup determination and the comparative FPL CHEETAH-calculated results.

The average measured burnup for the eight samples was determined to be 26,150 MWD/MTU ranging from 19,800 MWD/MTU at the top of the G7 rod to 27,700 MWD/MTU at the middle of the H6 and J8 fuel rods. Samples taken from all five rods at identical locations varied from 26,600 to 27,700 MWD/MTU. The experimental determinations of burnup in these eight samples were augmented with detailed measurements of fissile and fertile fuel isotopics[26]. As a result, the FPL lattice physics depletion methodology can be applied to calculate isotopic consitituents for comparison with the isotopic measurements at the measured burnup. For each fuel sample section, the FPL CHEETAH was run to the measured burnup limit to predict the resultant discharge U-235 and fissile plutonium gain. The measured and calculated isotopics are recorded in Table 5.3. In each case there is excellent agreement between the CHEETAH-calculated isotopics and the HEDL-measured isotopics; in most cases the measured and the calculated isotopic compositions differ by a few percent or less.

The two samples (H6-13 and J8-13) determined to have the same burnup at 27,700 MWD/MTU were selected as a typical case to illustrate the agreement of measured isotopics with calculated isotopics. As for all cases, the FPL CHEETAH-predicted discharge U-235 content is lower than the average HEDL-measured value: 0.6841 w/o U-235 versus 0.7165 w/o U-235. In contrast, the FPL CHEETAH-predicted fissile plutonium content

is somewhat higher: 70.10 w/o versus 68.35 w/o. Although the disagreement on fissile fuel content in each case is small, the overall effect on reactivity is even smaller. For the two cases cited, the CHEETAH predictions on U-235 are about 0.31 Kg/T low and those on fissile plutonium are about 0.14 Kg/T high. Therefore, the net difference in fissile fuel is approximately 0.17 Kg/T low which corresponds to only about 0.017 w/o difference on the fissile content of the fuel at 27,700 MWD/MTU. Because this enrichment corresponds to less than 0.2% uncertainty in reactivity (less than 1% in power), the excellent agreement of these isotopic comparisons is further substantiated as it supports confidence in CHEETAH to model FPL reactor cores.

As part of the continuing DOE program on spent fuel disposal, additional Turkey Point Unit 3 fuel rods were analyzed to determine their burnup as well as fertile and fissile isotopic composition, essentially repeating the types of analysis performed on the Cycle 2 fuel. These burnup measurements were performed as part of the pre-test characterization of the Turkey Point Unit 3 fuel assemblies (3-cycle burnup) for the Climax - Spent Fuel Test (C-SFT) which involves placement of PWR spent fuel assemblies into a granite formation at the NEVADA Test Site[27].

For the burnup analysis, five 3-cycle fuel rods from the Turkey Point Unit 3 were destructively examined to include rods G9, G10 and H9 from assembly D01 and rods G9 and G10 from assembly

D04. Burnup analyses were performed and reported on fuel from one section (1/2 in) of each of the five rods[27]. The sections were all taken from approximately the same axial location, 66 inches from the rod bottom. Again the sample preparation, experimental methodology and analytical techniques are detailed elsewhere[25][26][27].

Analytical burnup measurements were performed on all five samples. The sample identification numbers and fuel rod locations are listed in Table 5.4 along with the experimental results of the burnup and isotopic analysis and the comparative CHEETAH calculated results for the isotopics. The measured burnup values ranged from 30,510 MWD/MTU for sample D01-G10 to 31,560 MWD/MTU for sample D01-H9. The spread in measured burnup levels is small because all sample sections were removed from about the same axial location. The average of the five burnup measurements is 31,073, somewhat higher than the results of burnup measurements on the Cycle 2 Turkey Point Unit 3 fuel samples reported in Table 5.3.

The isotopic results are again presented in two categories: discharge U-235 (w/o) in total uranium and fissile plutonium (w/o) in total plutonium. For each case, the FPL CHEETAH was run to the measured burnup limit and the discharge U-235 and net fissile plutonium gain was extracted from the CHEETAH output as reported in Table 5.4. Comparison of the HEDL isotopic

measurements with the FPL CHEETAH isotopic calculations presented in Table 5.4 indicates excellent agreement between measured (HEDL) and calculated (FPL CHEETAH) fissile isotope discharge quantities at relatively high fuel burnup for both types of fissile isotopes and for all five samples. The estimated reactivity worth of the average difference in measured versus calculated fissile fuel content for these five samples is less than 0.1% reactivity showing even better agreement than for the Cycle 2 cases.

In general both sets of the FPL CHEETAH-calculated isotopics show excellent agreement with the HEDL measurements. This agreement further supports the FPL lattice physics model and as well as provides further support for concluding that measurement errors are the cause for the deviations reported in Section 5.2.3 for some of the plutonium critical experiments.

5.4 Cross Comparison of CHEETAH Methodology

5.4.1 Methodologies Used for CHEETAH Cross Comparison

To assure that the CHEETAH methodology is appropriate for the FPL lattice physics model, cross comparisons were carried out using other selected methodologies. Essentially the cross comparison of the CHEETAH methodology was directed toward two other independent methodologies whose codes produce unit cell output similar to that of the CHEETAH code.

As presented in Section 4.0, the FPL CHEETAH model uses a modified B-1/ABH zero-dimensional code to produce lattice constants and k_{eff} for an infinite array of unit cells. For the cross comparison of the CHEETAH methodology, two independent methodologies were selected which span a great deal of the analytical sophistication available for producing lattice physics constants. One methodology, as implemented in the NULIF code,[28] is based on theory similar to the CHEETAH model in that both CHEETAH and NULIF are zero-dimensional, spectral averaging, pin/unit cell codes whose primary objective is to provide burnup-dependent, spectrum-weighted, few-group neutron cross sections for fuel cells for use in a spatial diffusion code such as PDQ-7. NULIF, however, uses the P-1 equations for fast and thermal spectra calculations and has a more sophisticated treatment of the U-238 resonance. NULIF, like the similar option in CHEETAH, has a higher thermal group cutoff at 1.855 eV which allows it to incorporate the 1.05 eV Pu-240 resonance into the thermal spectrum calculation. The NULIF library utilizes 80 thermal groups and 31 epithermal groups. The NULIF code was run with the LIFT6 model option which uses the Fermi Age model for all elements except hydrogen in the epithermal spectrum calculation.

In contrast, the other independent methodology, as implemented in the CASMO-2 code[29] is based on a much different theory since CASMO-2 is a two-dimensional, multigroup (69 fine groups)

transport code for the calculation of eigenvalues, spatial reaction rate distributions and depletion of light water reactor fuel assemblies. CASMO-2 uses a fast transmission probability methodology based on integral transport theory. The program has flexible output and produces few-group parameters for the whole assembly or any specified subregion for use in global reactor diffusion theory calculations.

The CASMO-2 code was also selected for the independent methodology comparison because of its broad applicability for generating cross sections, not only for fuel cells and water tubes but also for heavy absorber cells. In this regard, the CASMO-2 model is a well-accepted industry standard for the generation of such heavy absorber constants. The CASMO-2 code is the basis for the complete Yankee Atomic lattice physics model and methodology presented in the Yankee Benchmark Report (30) which has received full regulatory acceptance.

With these two independent methodologies, two types of comparison calculations were performed. The first type of calculation applied the three codes to analyzing the variation of keff with burnup and enrichment. At the theoretical level, these calculations are similar to the experimental critical assembly measurements reported and analyzed in Section 5.2. The second type of calculation applied the three codes to analyzing and predicting fuel isotopic variation with burnup and enrichment.

Again, at the theoretical level, this application is similar to the Yankee Rowe Isotopic Measurements analysis presented in Section 5.3.1 and similar Turkey Point Unit 3 Isotopic Measurements presented in Section 5.3.2.

5.4.2 Results of CHEETAH Methodology Cross Comparison of k_{oo}

For the actual methodology cross comparison calculations, two types of fuel were analyzed for a range of burnups and for a range of enrichments to encompass the expected CHEETAH range of application in the Turkey Point and St. Lucie 1 Units. For Turkey Point, the variation of k_{oo} with burnup was investigated for 9 enrichments in the range from 1.5 to 4.5 w/o U-235; for St. Lucie 1, the variation of k_{oo} with burnup was investigated for 7 enrichments in the range from 1.8 to 4.5 w/o U-235. All depletion calculations were run from 0 to 50,000 MWD/MTU while the three highest enrichments in each plant were run to 65,000 MWD/MTU. The variation of k_{oo} with enrichment was also investigated for two assumed burnups for each reactor unit -- one at 150 MWD/MTU and one at 50,000 MWD/MTU.

All cases considered in this series are summarized in Table 5.5; for each of the parametric cases delineated in Table 5.5, results of k_{oo} calculations with the FPL CHEETAH and NULIF were generated. In addition, as the more sophisticated methodology, CASMO-2 results were generated for selected cases spanning the entire range of enrichments and burnups for which the other two

methodologies were applied. These applications are also summarized in Table 5.5.

For the cases listed in Table 5.5, graphs showing the results of all three methodologies in calculating k_{oo} are presented as Figures 5.14 through 5.33. In general, the CASMO-2 and NULIF calculations are in good agreement with the CHEETAH results, deviating a small amount at the high and low enrichments, probably due partly to library differences among the codes. In addition, the NULIF and CASMO-2 consistently agree more closely on k_{oo} values at higher burnups than do CHEETAH and CASMO-2 (though all are close); this is explained by the better treatment of the Pu-240 poison effects in these two codes. These small discrepancies are not considered to be of great significance and overall the cross comparison of the CHEETAH methodology is successfully demonstrated.

5.4.3 Results of CHEETAH Methodology Cross Comparison of Fuel Isotopics

Two types of fuel were also analyzed for the cross comparison of calculated fuel isotopics to include five enrichments for the Turkey Point Units and four enrichments for St. Lucie Unit 1. The range of enrichments analyzed for each type of fuel encompasses the expected CHEETAH model range of application for the FPL nuclear units. The cases analyzed and the methodologies applied for each are summarized in Table 5.6.

Again CHEETAH and NULIF were run for all cases to calculate discharge U-235 (w/o) and fissile plutonium (Pu-239 and Pu-241) gain (Kg/T) while CASMO-2, as the more sophisticated methodology, was run for fewer cases but still spanning the entire range of enrichments. In addition, all fuel isotopic calculations were run from 0 to 50,000 MWD/MTU with the three highest enrichments for each plant being run to 65,000 MWD/MTU to assure coverage of the entire expected range of application of the CHEETAH methodology.

The results of the fuel isotopic calculations for Turkey Point Unit enrichments are presented in Figures 5.34 through 5.43; those for St. Lucie Unit 1 are presented in Figures 5.44 through 5.51. In general, the results show excellent agreement among all three methodologies for the calculated discharge U-235 for all enrichments over the entire burnup range considered.

The calculated results for fissile plutonium gain are in lesser agreement, especially at higher burnups where the highest discharges are predicted by NULIF with CASMO-2 and CHEETAH yielding progressively lower predicted discharges. Library differences are the cause of some of this difference, though again the primary cause is the better treatment of the Pu-240 poison effects in NULIF and CASMO-2. Better agreement is indicated between the isotopic results of the sophisticated methodology (CASMO-2) and CHEETAH than between the NULIF and

CHEETAH methodologies. The divergence is not large and is not considered significant in either case. In general, the fuel isotopics calculated with the independent methodologies agree well with those calculated with the FPL CHEETAH methodology.

5.5 Summary of Basis for Confidence

The basis for confidence in the FPL CHEETAH model and methodology has been established for the intended range of PWR application utilizing both experimental checks and methodology comparisons. For the comparisons with critical experiments in Section 5.2, the capability of the FPL CHEETAH model to analyze successfully a wide range of experiments from the UO_2 fueled (clad with aluminum and stainless steel) experiments of Strawbridge and Barry[12] to the SNUPPS critical experiments on zircaloy clad fuel[20] and various mixed oxide critical experiments [21] has been demonstrated.

There is no apparent trend in the plots of k_{oo} variation with the six selected lattice physics parameters. The Strawbridge and Barry and SNUPPS critical experiments show excellent agreement with the CHEETAH-based results. The k_{oo} for the mixed oxide group of experiments shows a bias in the resultant k_{eff} but this is explained by the small size and resultant uncertainty associated with axial buckling measurements in these assemblies. The comparisons with critical experiments have demonstrated that the FPL CHEETAH model is capable of analyzing a wide range of experiments with good agreement utilizing only basic fuel assembly mechanical design data.

As presented and discussed in Section 5.3.1, the FPL CHEETAH model results agree well with the Yankee Rowe isotopic measurements and predictions[24] obtained with the Yankee asymptotic neutron spectrum. Good agreement was also demonstrated between the CHEETAH model predictions and the results of the Turkey Point Unit 3 isotopic measurements as presented in Section 5.3.2.

Finally, as presented in Section 5.4, the FPL CHEETAH methodology comparison with the NULIF[28] and CASMO-2[29] methodologies has verified good agreement on k_{oo} and fuel isotopic calculations over a broad range of burnups and enrichments characteristic of expected FPL CHEETAH applications in the Turkey Point and St. Lucie Units.

Table 5.1

Correlation of Zero and One-Dimensional

CHEETAH Calculations of Plutonium Critical Experiments

Experiment Number	Fuel Loading Description	K-Effective Range Zero-D	K-Effective Range One-D
1-3	5.74 w/o UO_2 - no PuO_2	1.003-1.016	1.006-1.015
4-8	6.6 w/o PuO_2	1.011-1.022	1.020-1.026
9-12	2.0 w/o PuO_2 (8 w/o Pu-240)	0.9994-1.015	1.0007-1.0065
13-14	2.0 w/o PuO_2 (24 w/o Pu-240)	1.010-1.013	1.0101-1.012
	Average k_{eff}	1.01375	1.01377

Table 5.2

Results of CHEETAH Calculations of Eleven

Plutonium-Bearing Critical Experiments

Methodology Used	Thermal Cutoff	K-Effective
CHEETAH (O-D)	0.625 ev	1.01375±0.00727
CHEETAH (1-D)	0.625 ev	1.01377±0.00918
CHEETAH (O-D)	1.855 ev	1.0103±0.0094

Table 5.3

Comparison of HEDL Isotopic Measurements

With FPL CHEETAH Depletion Calculations

on Turkey Point Unit 3, Cycle 2, Assembly B17 Fuel Rods

			Discharge U-235/U-Total (w/o)[3]		Fissile Pu/Pu-Total (w/o)	
Sample	Location[1] (in)	Measured[2] Burnup MWD/MTU	HEDL Measured	FPL CHEETAH	HEDL Measured	FPL CHEETAH
G7-35	134.5-135.0	19,890	1.0448	1.0291	74.84	75.45
G7-6	16.5-17.0	25,580	0.7920	0.7676	70.17	71.50
I9-13	70.0-70.5	26,660	0.7090	0.7243	68.32	70.78
G9-13	70.0-70.5	26,940	0.7890	0.7133	68.85	70.60
G7-30	116.5-117.0	27,170	0.7456	0.7044	69.33	70.45
G7-15	70.0-70.5	27,540	0.7278	0.6902	68.82	70.20
J8-13	70.0-70.5	27,700	0.7189	0.6841	68.39	70.10
H6-13	70.0-70.5	27,700	0.7140	0.6841	68.30	70.10

Note 1: Location refers to axial distance in inches measured from the bottom of the fuel rod for 1/2 inch long fuel rod samples.

Note 2: Samples are arranged in order of increasing measured burnup for ease of comparison.

Note 3: Original assembly B17 enrichment was 2.559 w/o.

Table 5.4

Comparison of HEDL Isotopic Measurements

With FPL CHEETAH Depletion Calculations

On Turkey Point Unit 3, Cycle 3 Fuel Rods

Sample	Location (in)1	Measured2 Burnup MWD/MTU	Discharge U-235/U Total (w/o)3		Fissile Pu/Pu-Total (w/o)	
			HEDL Measured	FPL CHEETAH	HEDL Measured	FPL CHEETAH
D01-G10-4	65.5-66.0	30,510	0.5915	0.5854	66.66	68.42
D01-G9-15	65.75-66.25	30,720	0.6113	0.5784	67.01	68.29
D04-G9-9	65.75-66.25	31,260	0.5747	0.5608	66.90	67.97
D04-G10-7	65.5-66.0	31,310	0.5905	0.5592	66.60	67.94
D01-H9-7	65.5-66.0	31,560	0.5826	0.5512	66.90	67.79

Note 1: Location refers to axial distance in inches measured from the bottom of the fuel rod for 1/2 inch long fuel rod samples.

Note 2: Samples are arranged in order of increasing measured burnup for ease of comparison.

Note 3: Original assembly D01 and D04 enrichment was 2.556 w/o.

Table 5.5

Cases Analyzed for CHEETAH, NULIF, CASMO-2

Methodology Comparison of k_{oo} Calculations

K-Infinity Versus Burnup

		Methodology Used		
Plant	Enrichment(w/o)[1]	CHEETAH	NULIF	CASMO-2
TP4	1.5	x	x	x
TP4	1.9	x	x	
TP4	2.3	x	x	
TP4	2.7	x	x	
TP4	3.104	x	x	x
TP4	3.5	x	x	
TP4	3.9*	x	x	
TP4	4.2*	x	x	
TP4	4.5*	x	x	x
SL1	1.80	x	x	x
SL1	2.75	x	x	
SL1	3.03	x	x	x
SL1	3.35	x	x	
SL1	3.67*	x	x	
SL1	4.00*	x	x	
SL1	4.50*	x	x	x

K-Infinity Versus Enrichment

		Methodology Used		
Plant	Burnup (MWD/MTU)	CHEETAH	NULIF	CASMO-2[2]
TP4	150	x	x	x
TP4	50000	x	x	x
SL1	150	x	x	x
SL1	50000	x	x	x

Note 1: All depletion calculations run from 0 to 50000 MWD/MTU. Starred(*) higher enrichment cases were run to 65000 MWD/MTU.

Note 2: Seven enrichments were used as ordinate values for which k_{oo} was calculated. All enrichments were calculated with CHEETAH and NULIF but only the lowest, middle and highest enrichments were calculated with CASMO-2.

Table 5.6

Fuel Isotopics Cases Analyzed

for Independent Methodology Comparison

of Predicted Discharge U-235 and Fissile Plutonium Gain

		Methodology Used		
Plant	Enrichment(w/o)[1]	CHEETAH	NULIF	CASMO-2
TP4	1.5	x	x	x
TP4	2.3	x	x	
TP4	3.104	x	x	x
TP4	3.9*	x	x	
TP4	4.5*	x	x	x
SL1	1.80	x	x	x
SL1	3.031	x	x	x
SL1	3.67*	x	x	x
SL1	4.50*	x	x	x

Note 1: All fuel isotopic calculations were run from 0 to 50,000 MWD/MTU; the two highest enrichments (*) for each plant were run to 65,000 MWD/MTU.

Figure 5.1

Variation of Calculated K-Effective with Enrichment
for Three Sets of Critical Experiments

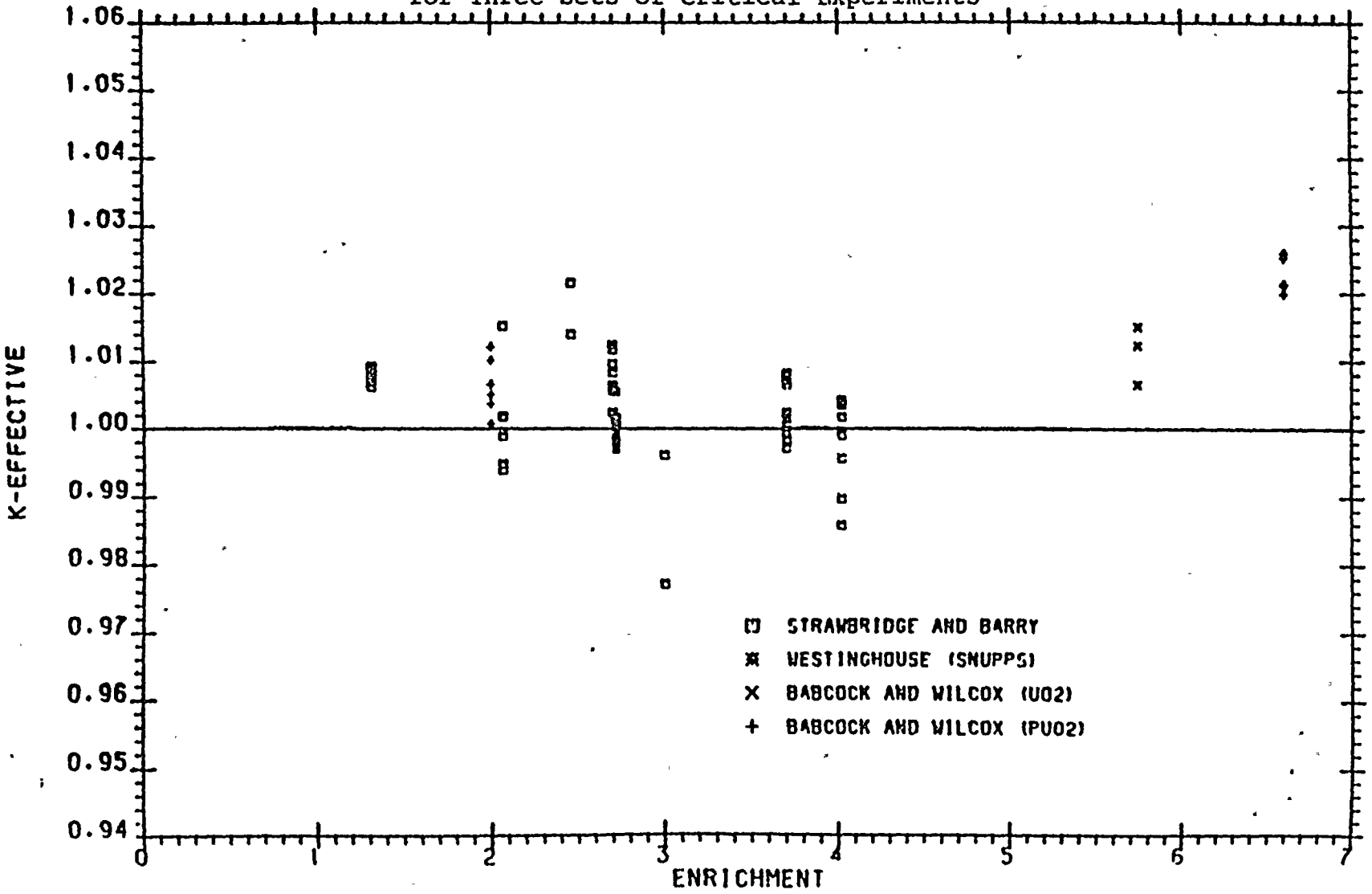

Figure 5.2

Variation of Calculated K-Effective with Fuel Density
For Three Sets of Critical Experiments

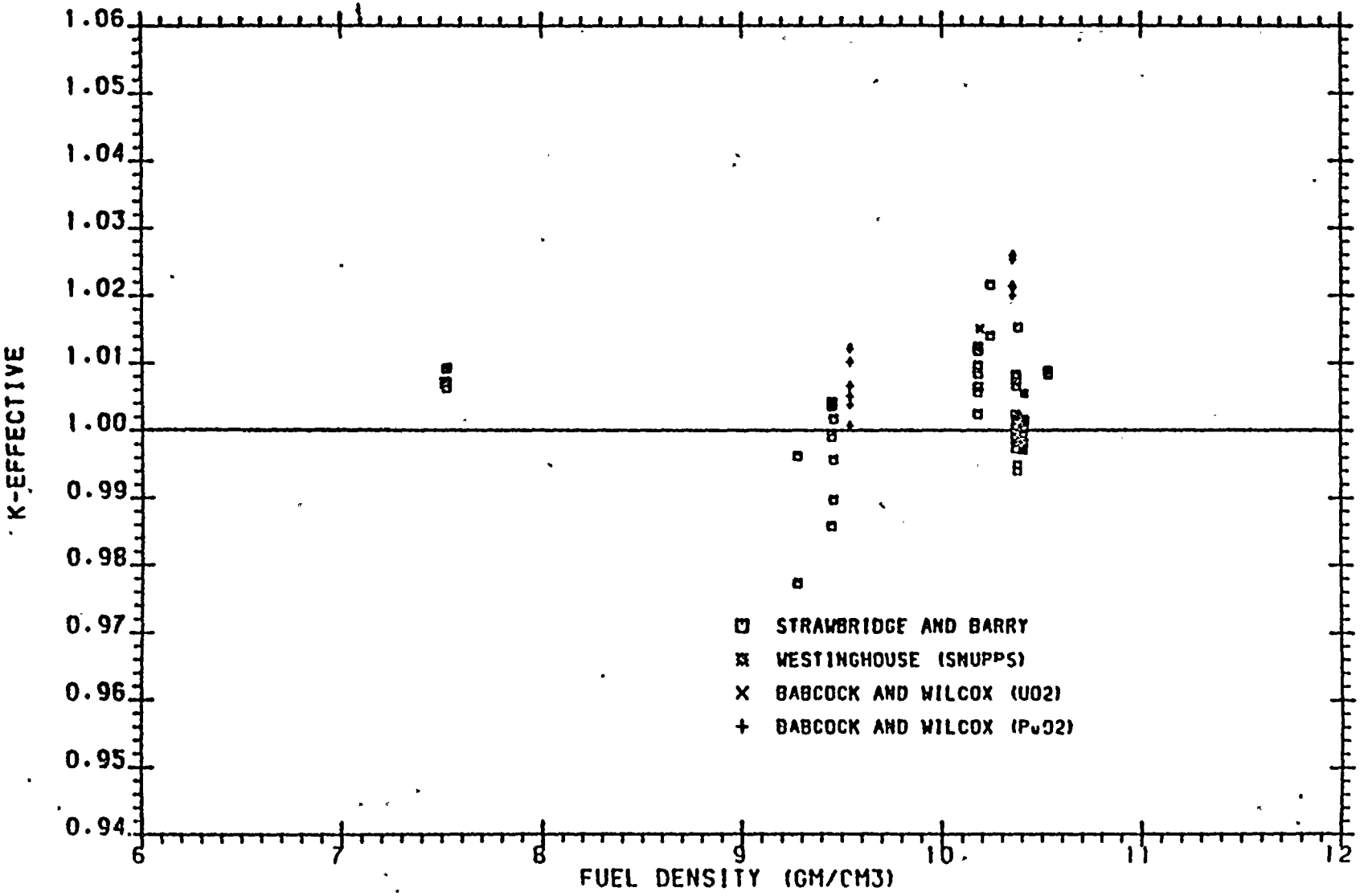

Figure 5.3

Variation of Calculated K-Effective with Lattice Pitch
For Three sets of Critical Experiments

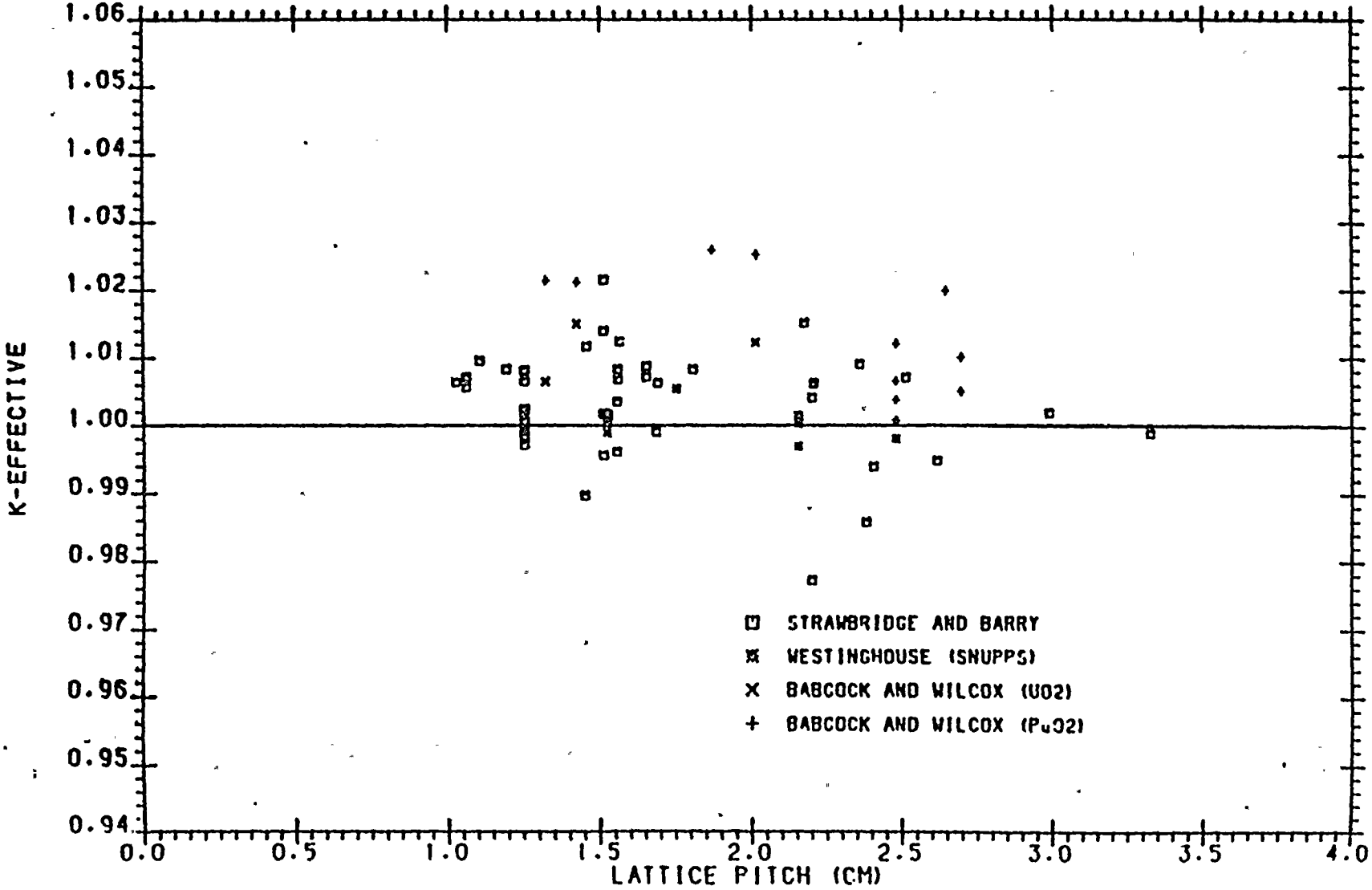

Figure 5.4

Variation of Calculated K-Effective With Critical Buckling
For Three Sets of Critical Experiments

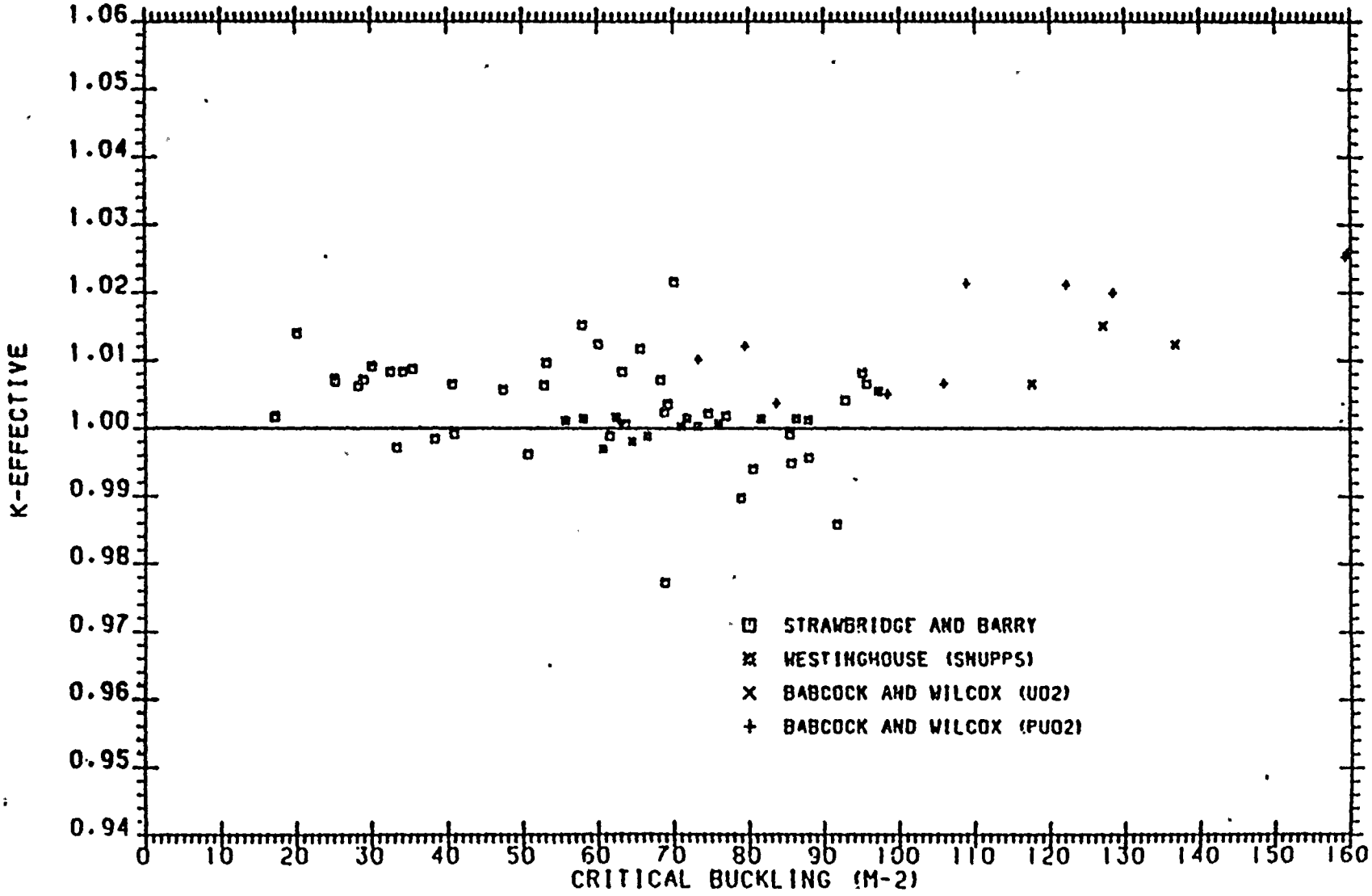

Figure 5.5

Variation of Calculated K-Effective with Soluble Boron Concentration for Three Sets of Critical Experiments

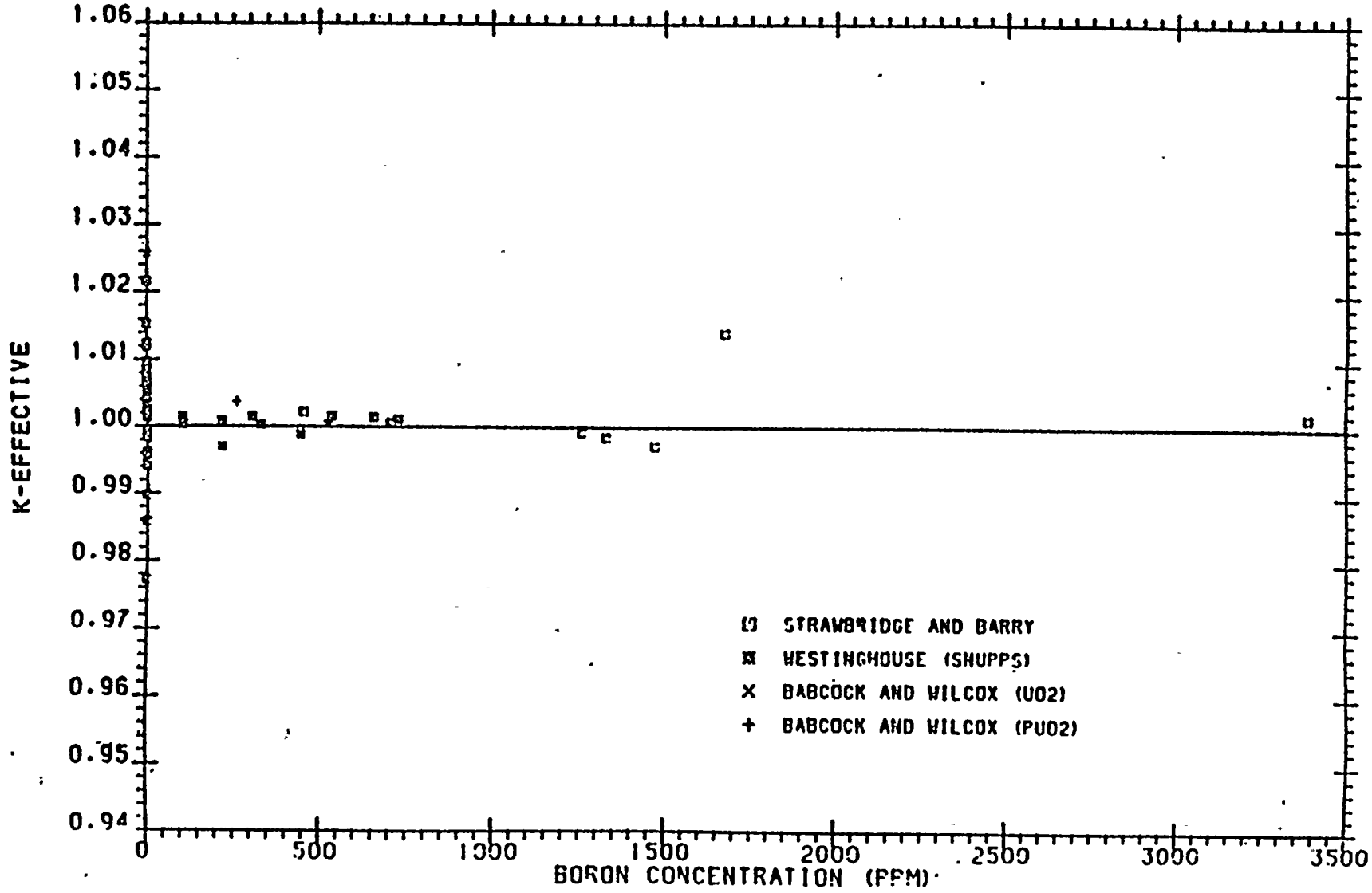

Figure 5.6

Variation of Calculated K-Effective with water-to Fuel Volume Ratio for Three Sets of Critical Experiments

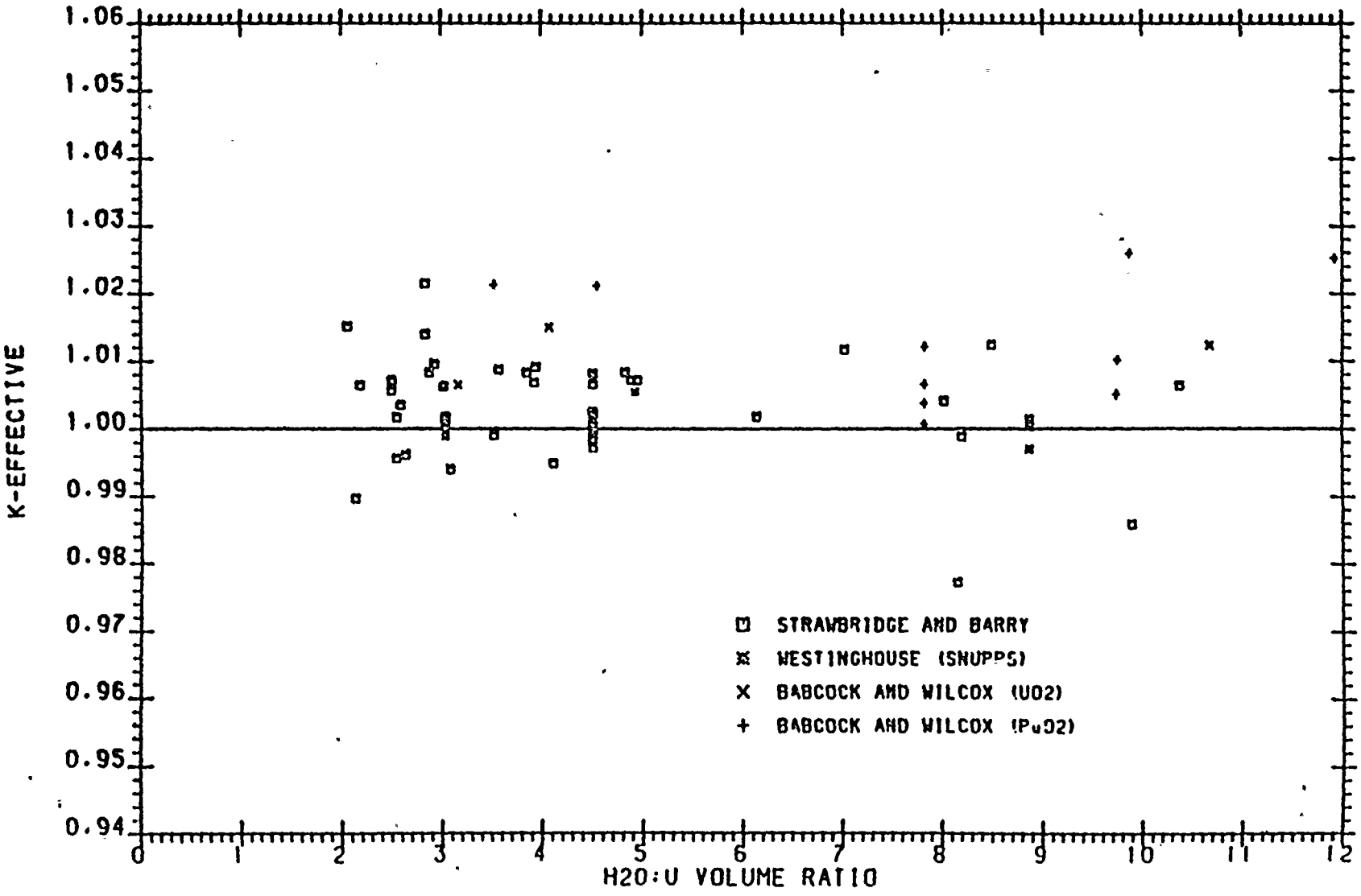

Figure 5.7

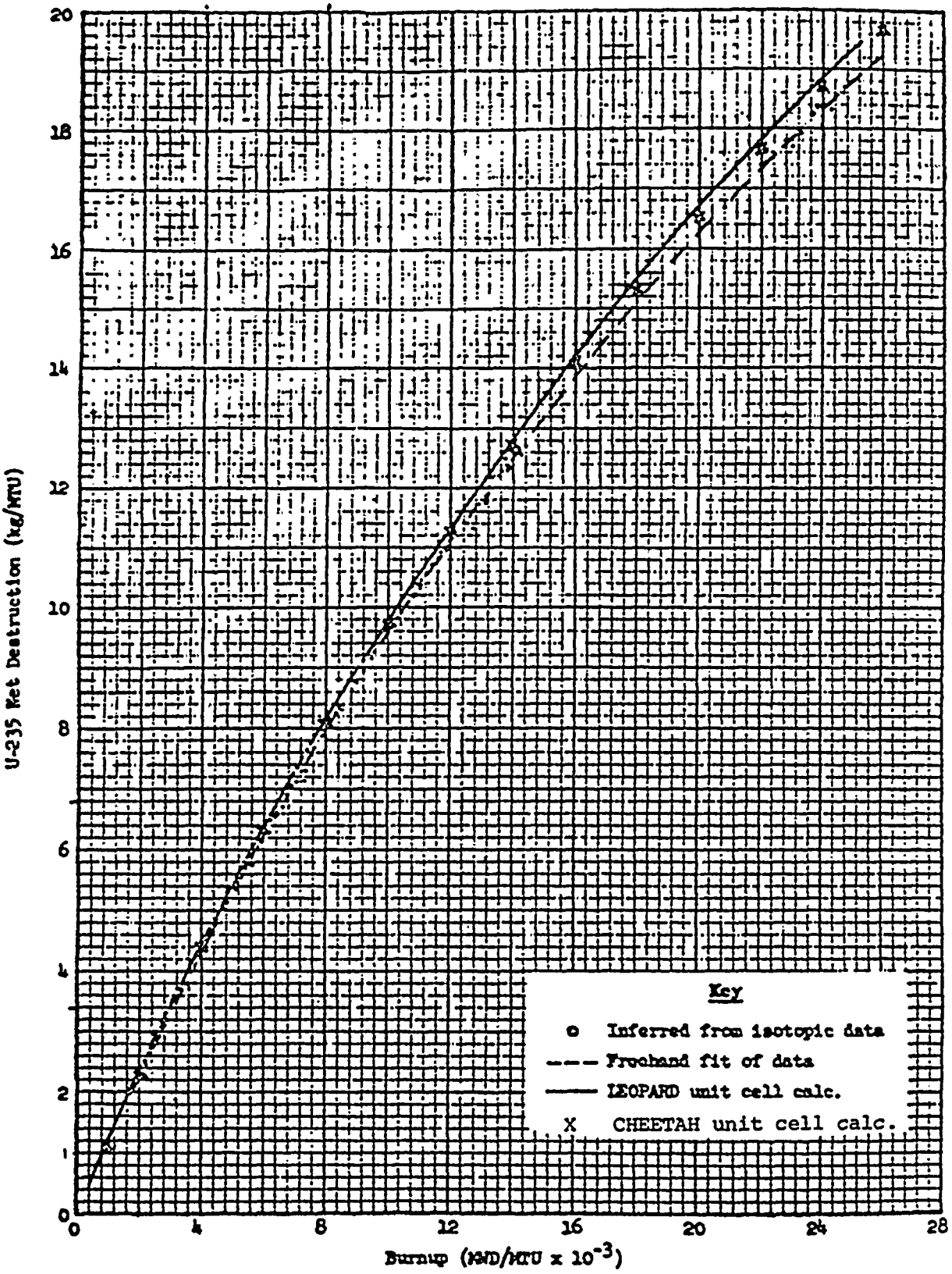

Net Destruction of U-235 Versus Burnup
in the Yankee Asymptotic Neutron Spectrum (Ref. 24)

Figure 5.8

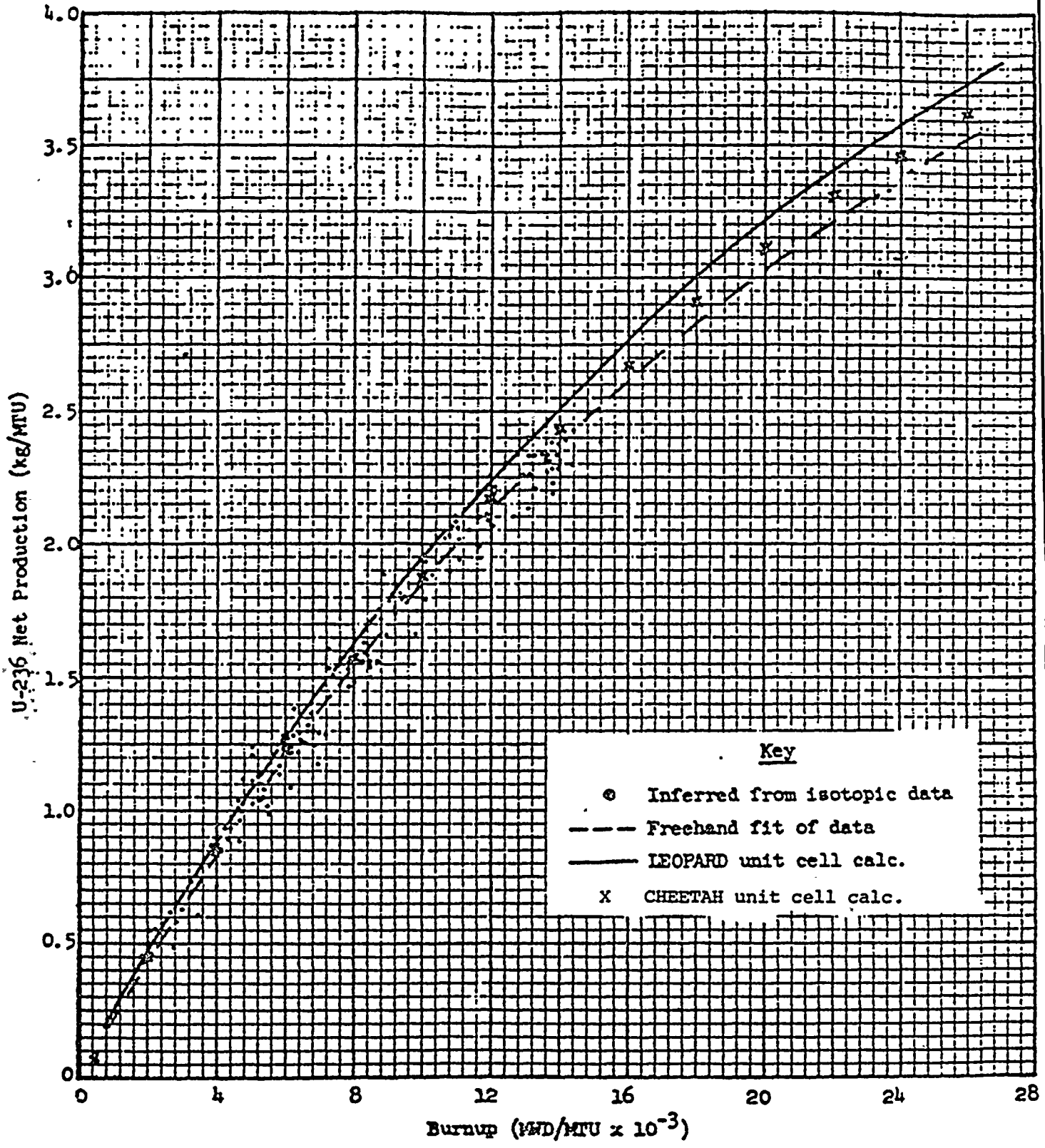

Specific Production of U-236 Versus
Burnup in the Yankee Asymptotic Neutron Spectrum (Ref. 24)

Figure 5.9

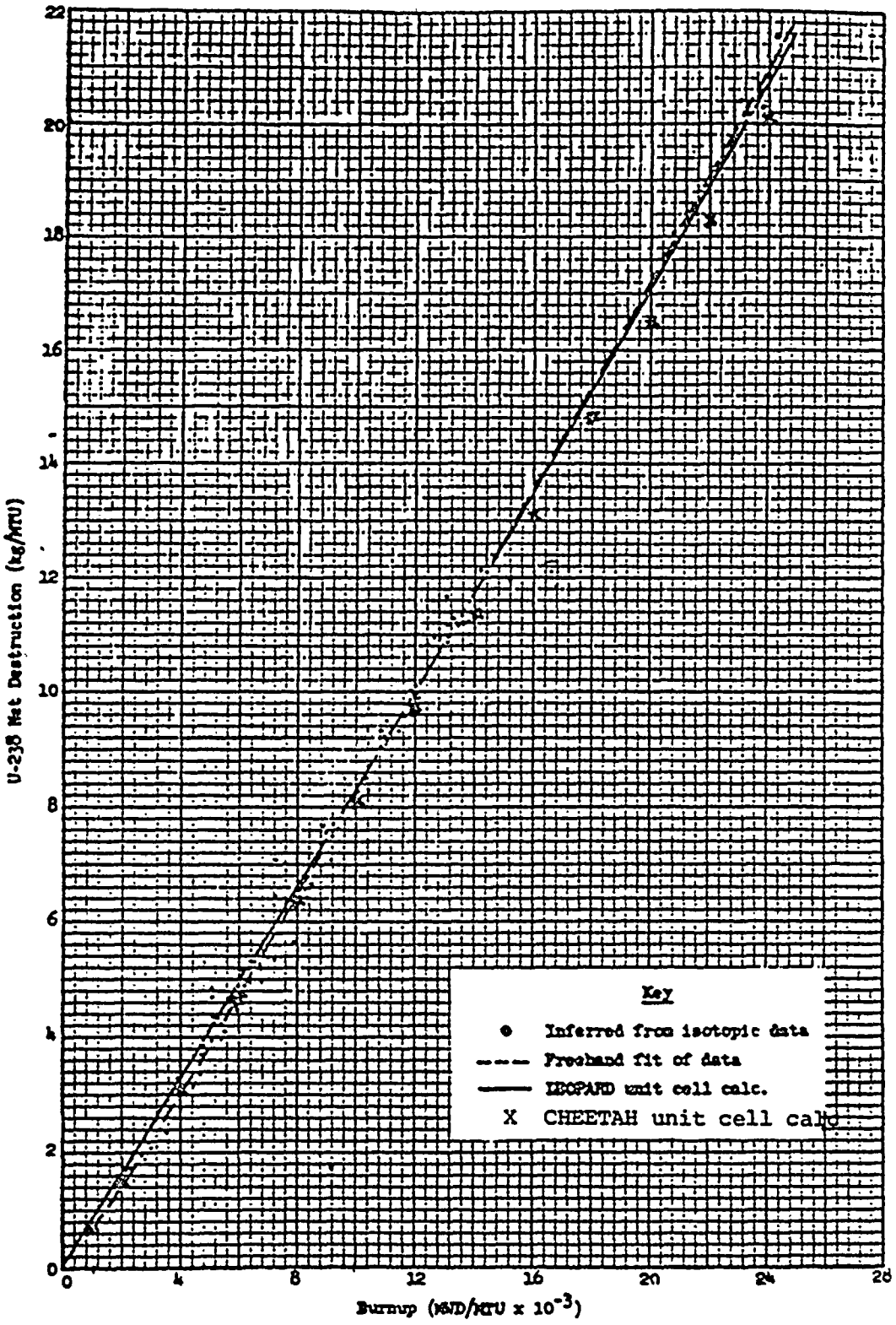

Net Destruction of U-238 Versus Burnup
in the Yankee Asymptotic Neutron Spectrum (Ref. 24)

Figure 5.10

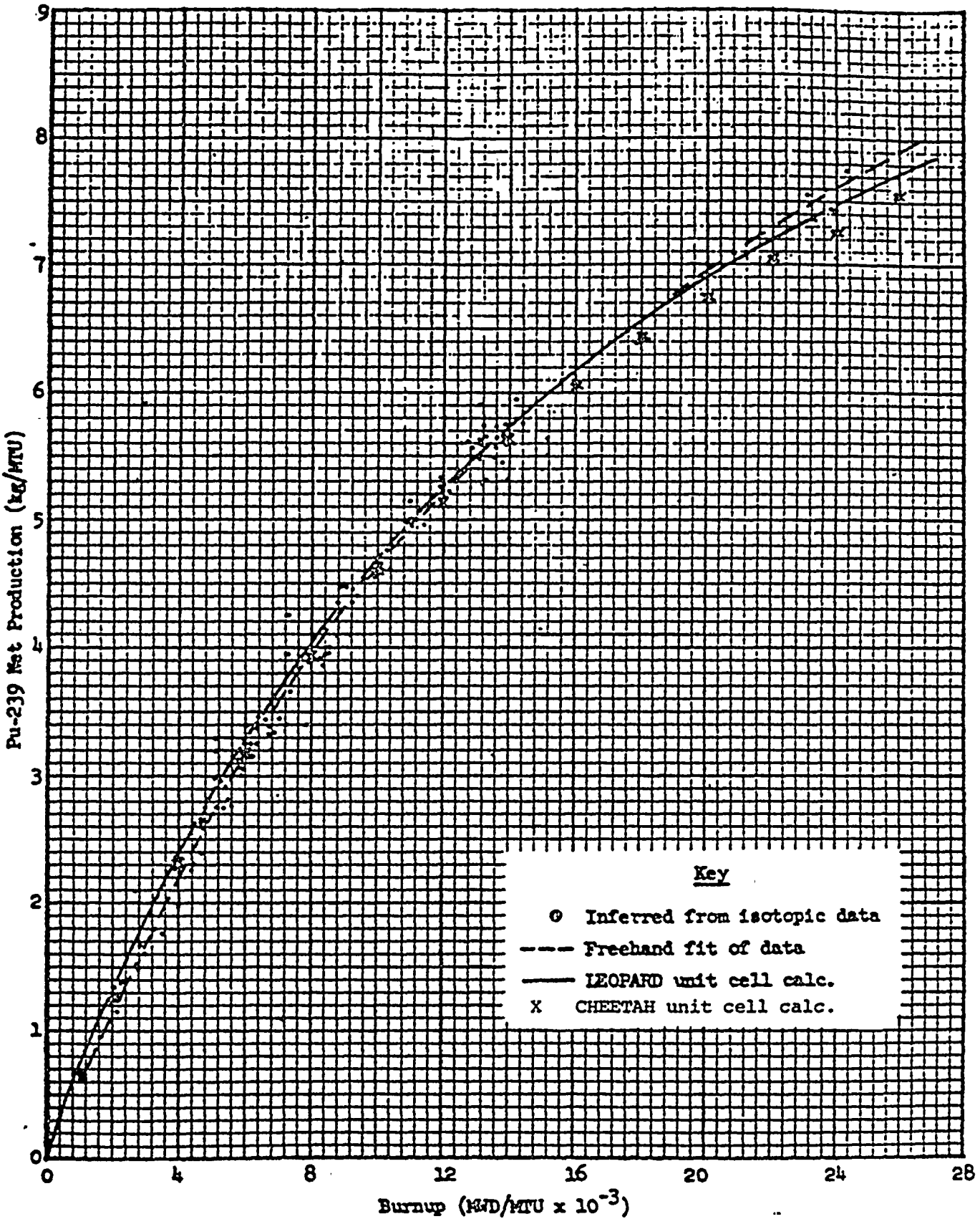

Specific Production of Pu-239 Versus Burnup in the Yankee Asymptotic Neutron Spectrum (Ref. 24)

Figure 5.11

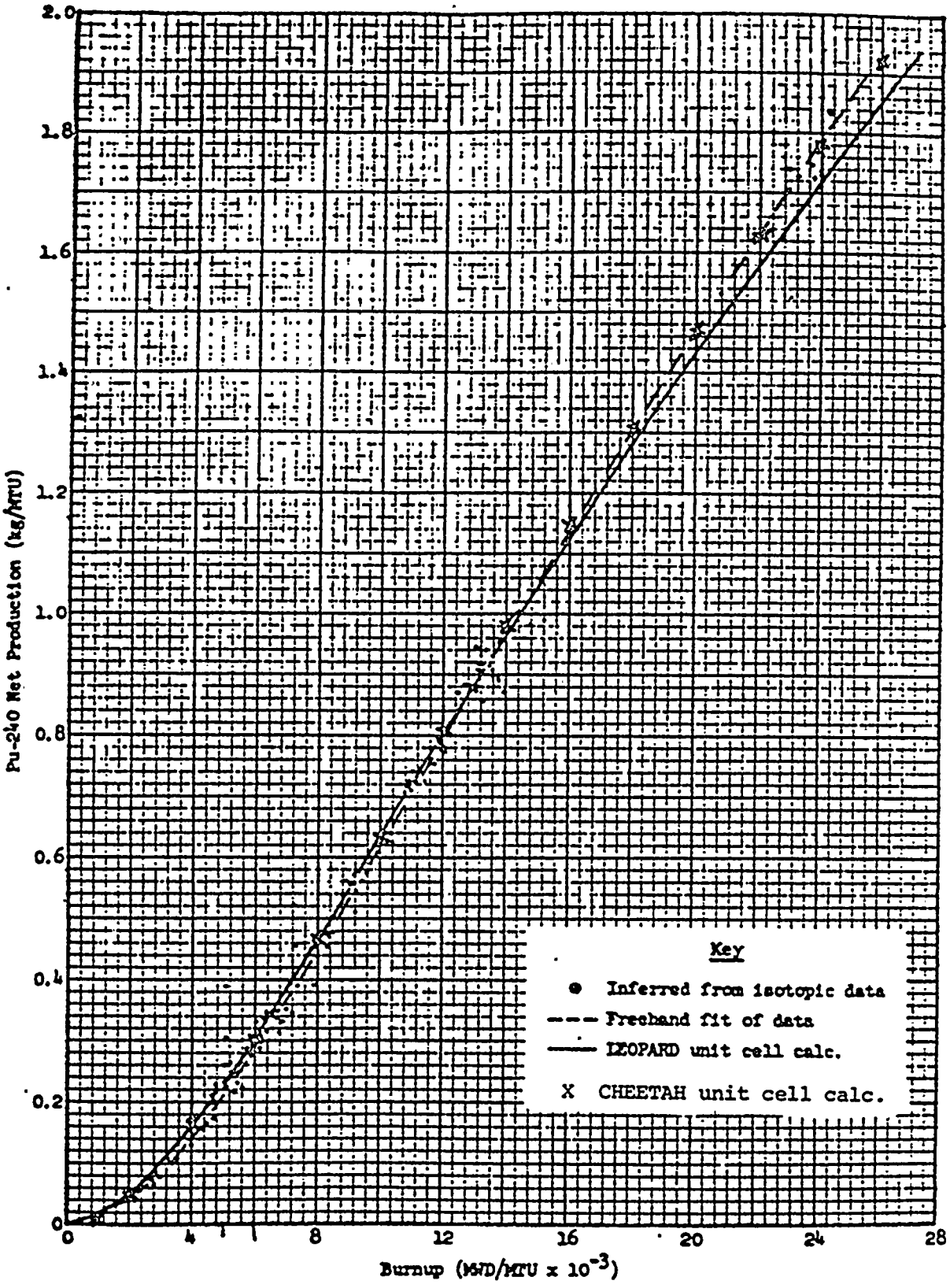

Specific Production of Pu-240 Versus Burnup in the Yankee Asymptotic Neutron Spectrum (Ref. 24)

Figure 5.12

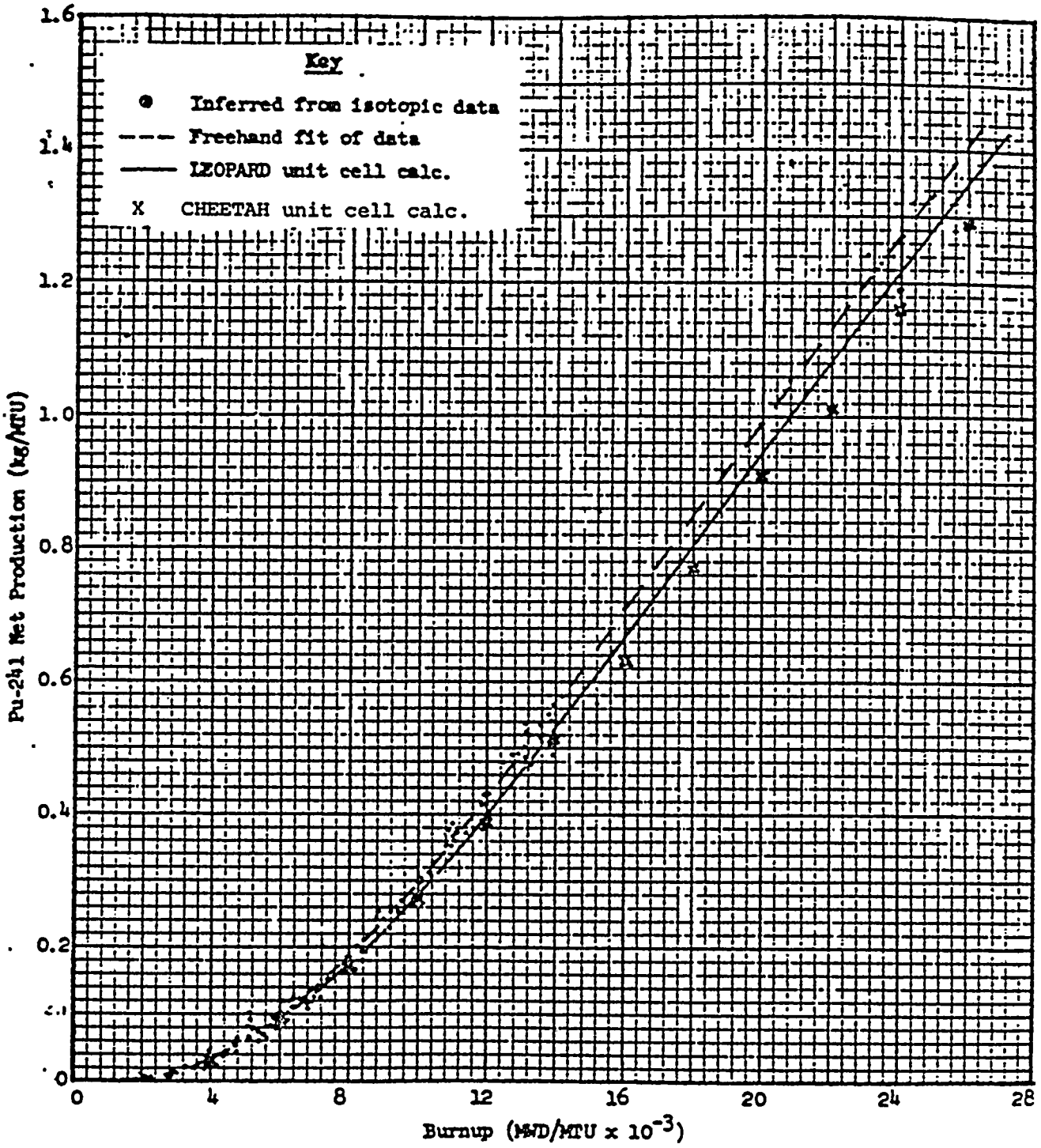

Specific Production of Pu-241 Versus Burnup in the Yankee Asymptotic Neutron Spectrum (Ref. 24)

Figure 5.13

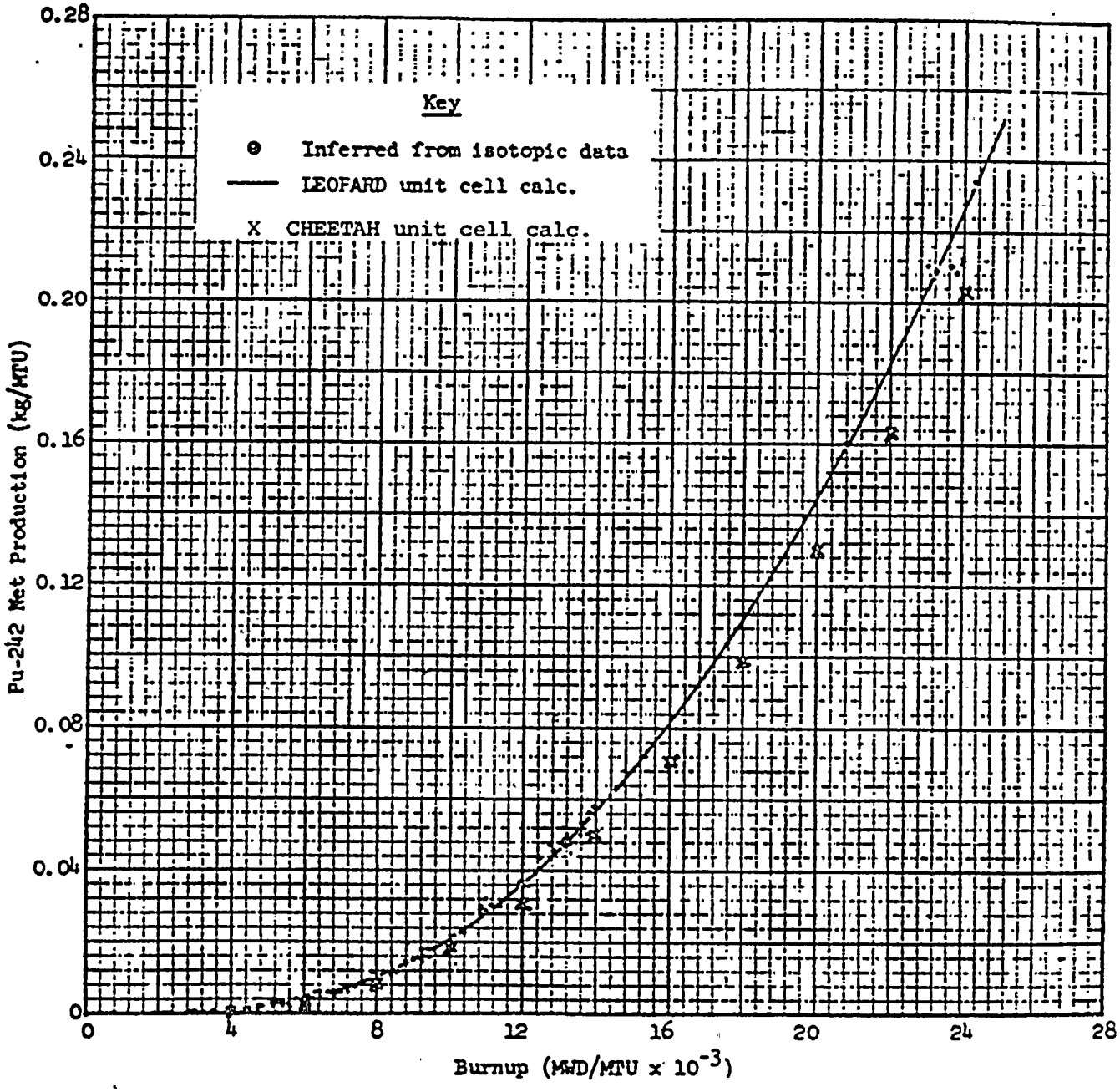

Specific Production of Pu-242 Versus Burnup in the Yankee Asymptotic Neutron Spectrum (Ref. 24)

Figure 5.14

TP 4 Nuclear Plant

K Infinity vs. Burnup at 1.5% enrichment

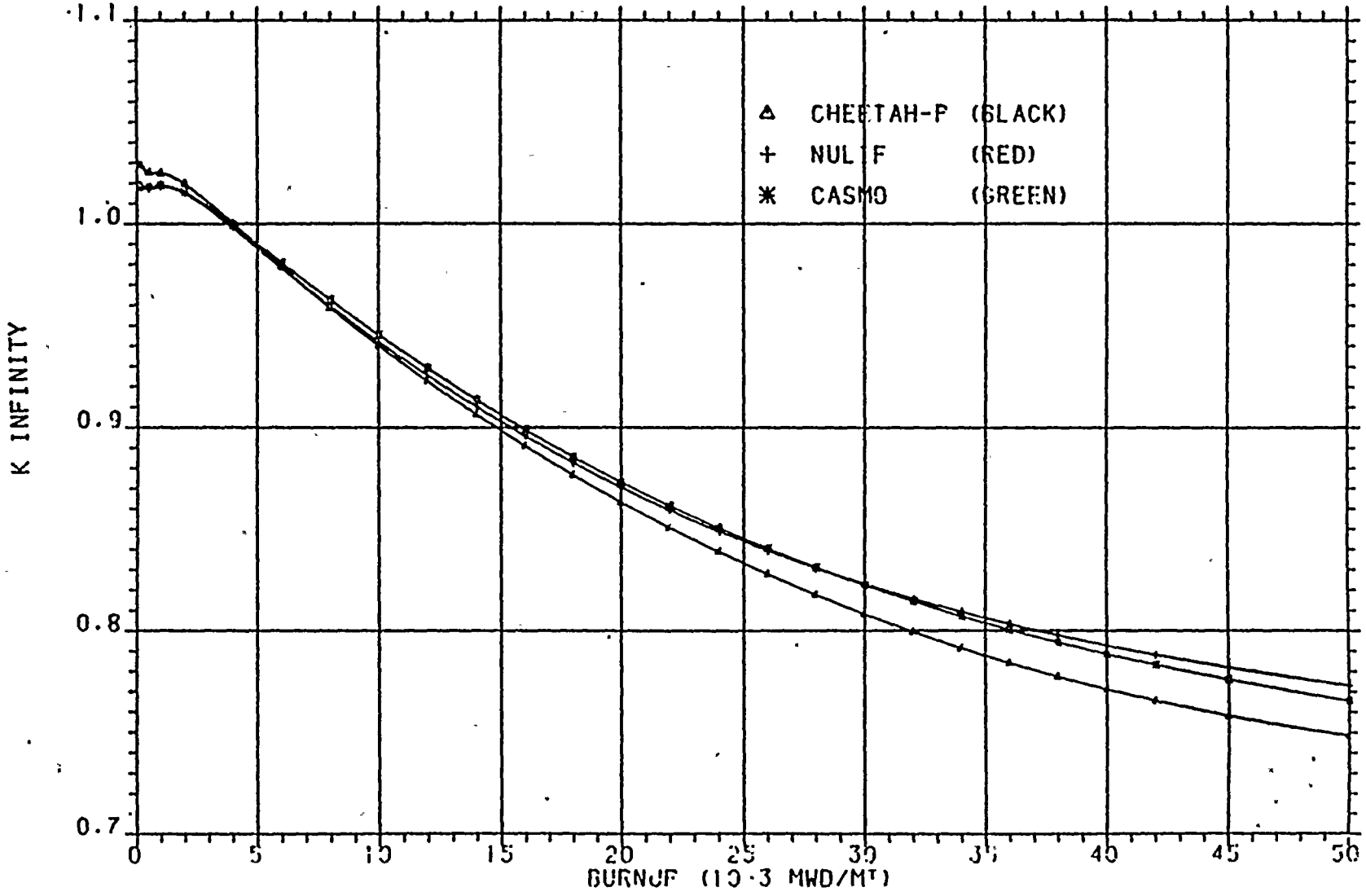

Figure 5.15

TP 4 Nuclear Plant

K infinity vs. burnup at 1.9% enrichment

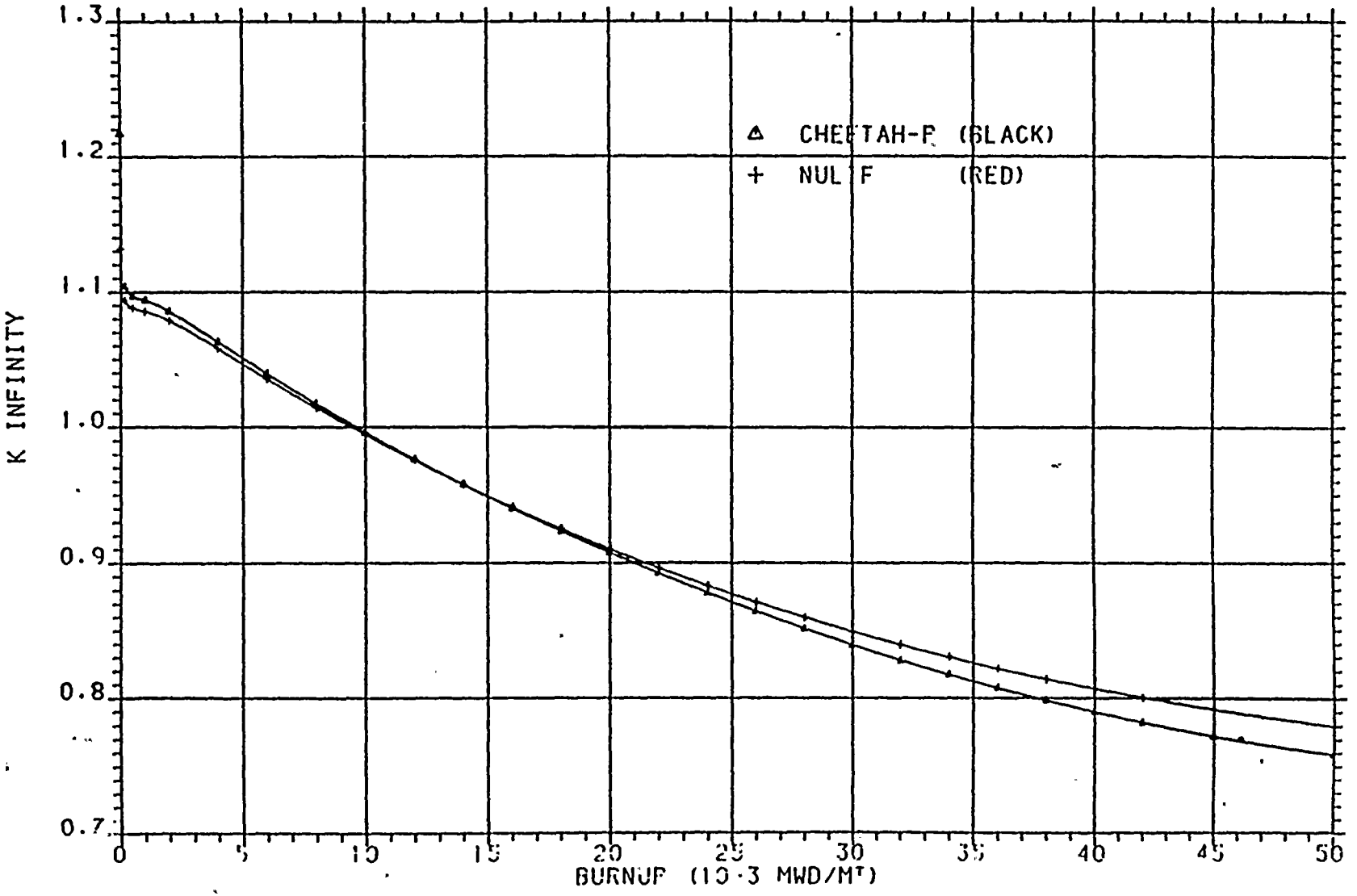

Figure 5.16

TP 4 Nuclear Plant

K infinity vs. burnup at 2.3% enrichment

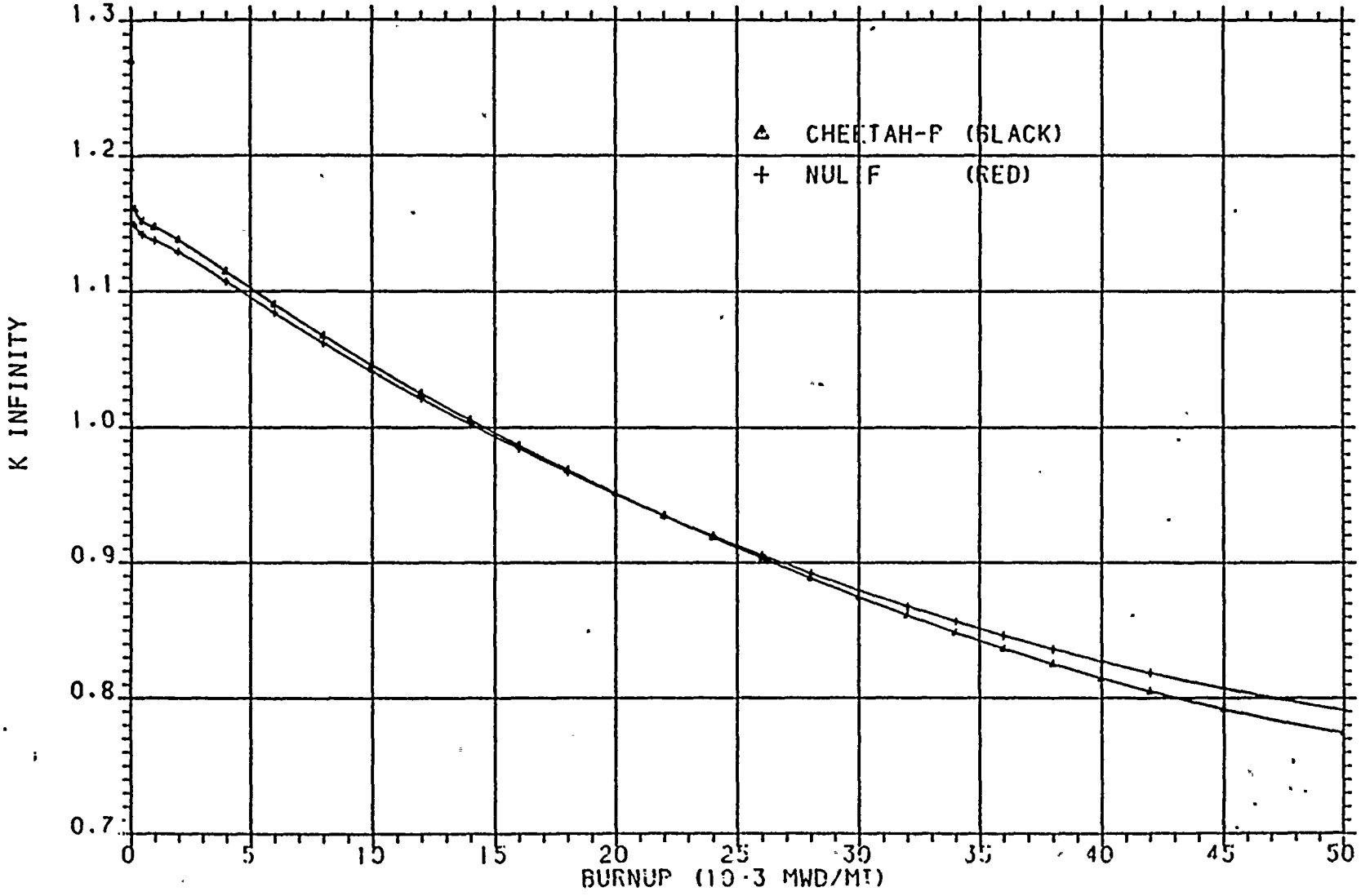

Figure 5.17

TP 4 Nuclear Plant

K infinity vs burnup at 2.7% enrichment

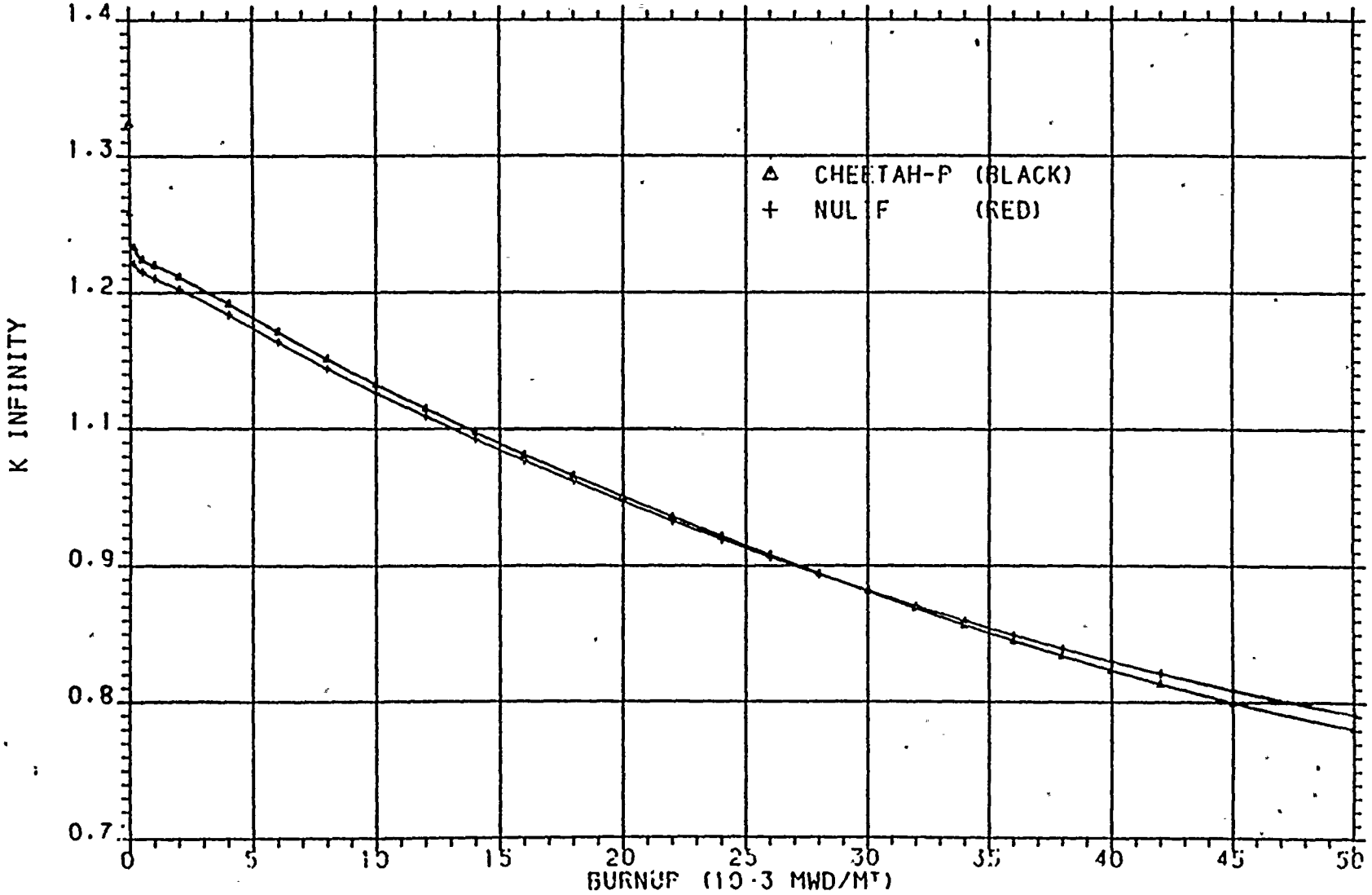

Figure 5.18

TP 4 Nuclear Plant

K-infinity vs. burnup at 3.10% enrichment

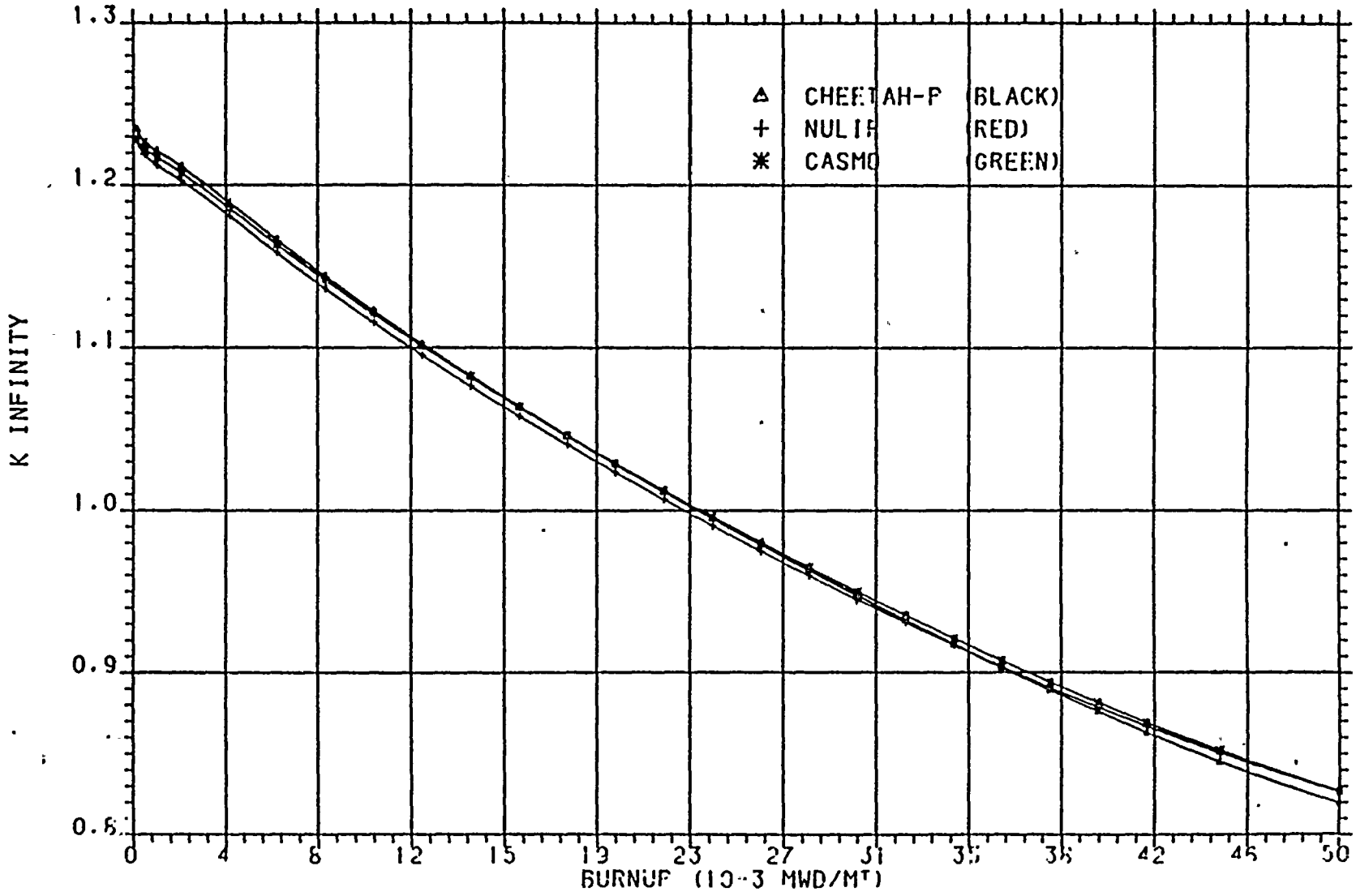

Figure 5.19

TP 4 Nuclear Plant

K-infinity vs. burnup at 3.5% enrichment

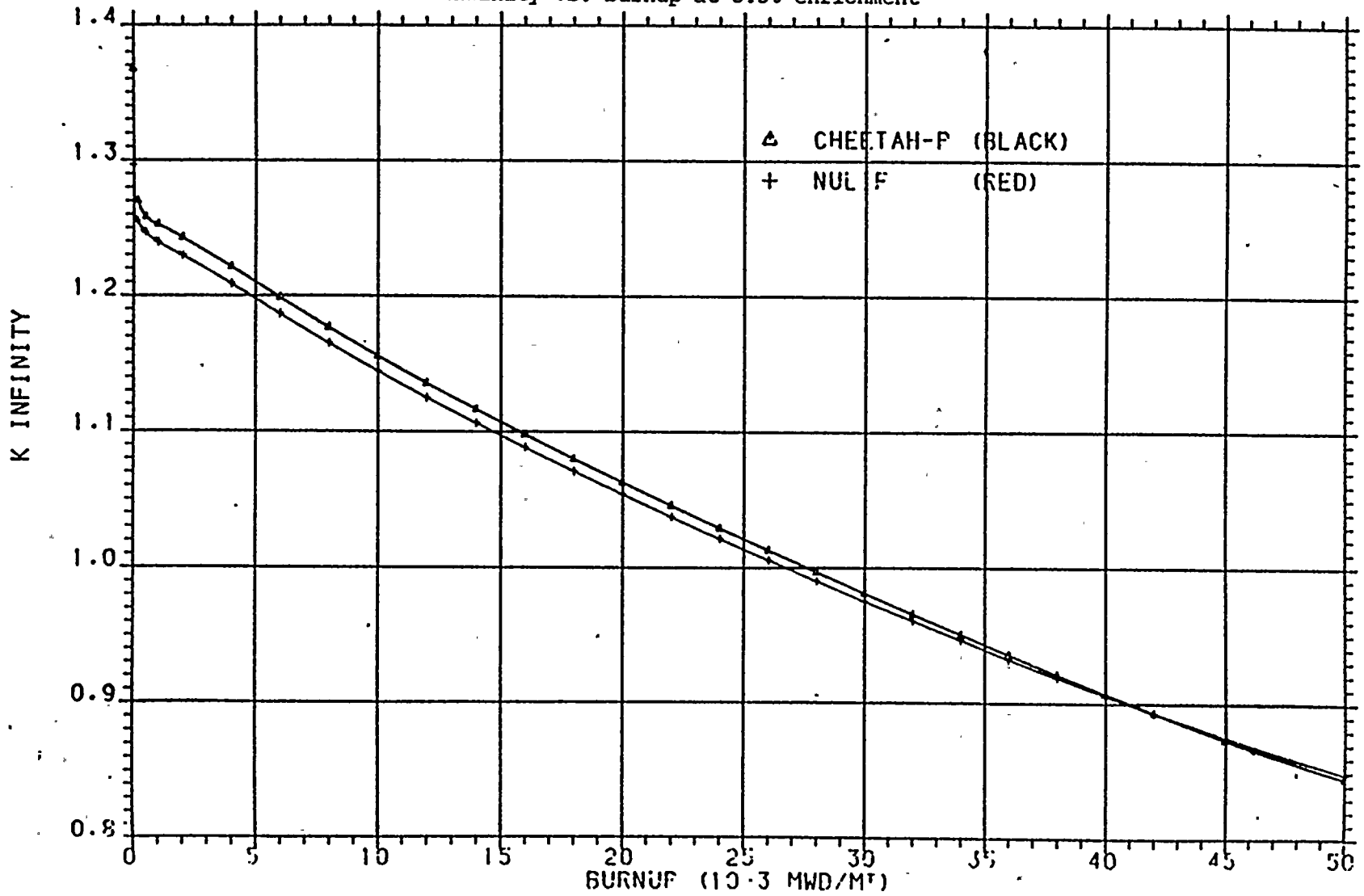

Figure 5.20

TP 4 Nuclear Plant

K-infinity vs. burnup at 3.9% enrichment

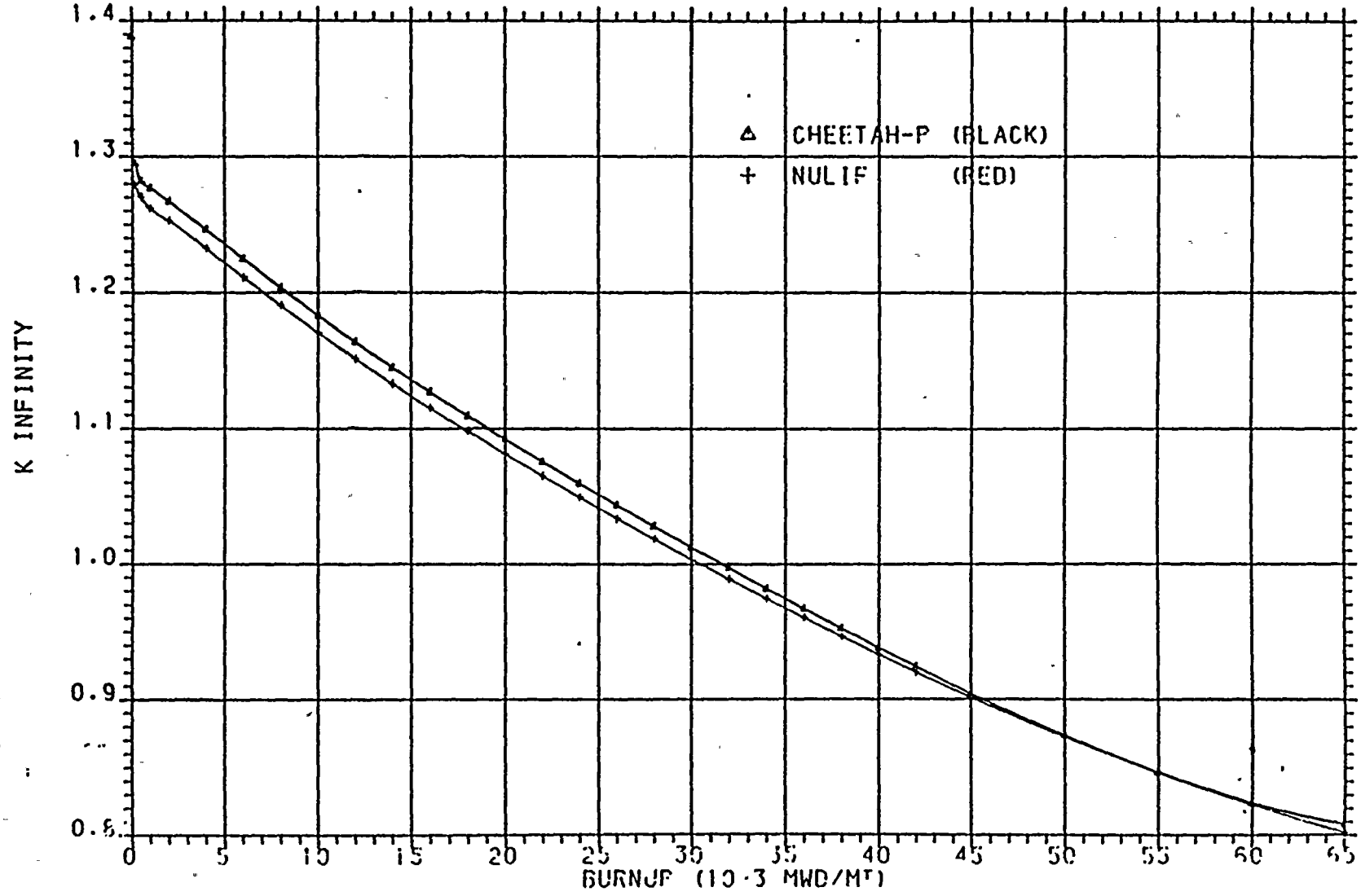

Figure 5.21

TP 4 Nuclear Plant

K-infinity vs. burnup at 4.2% enrichment

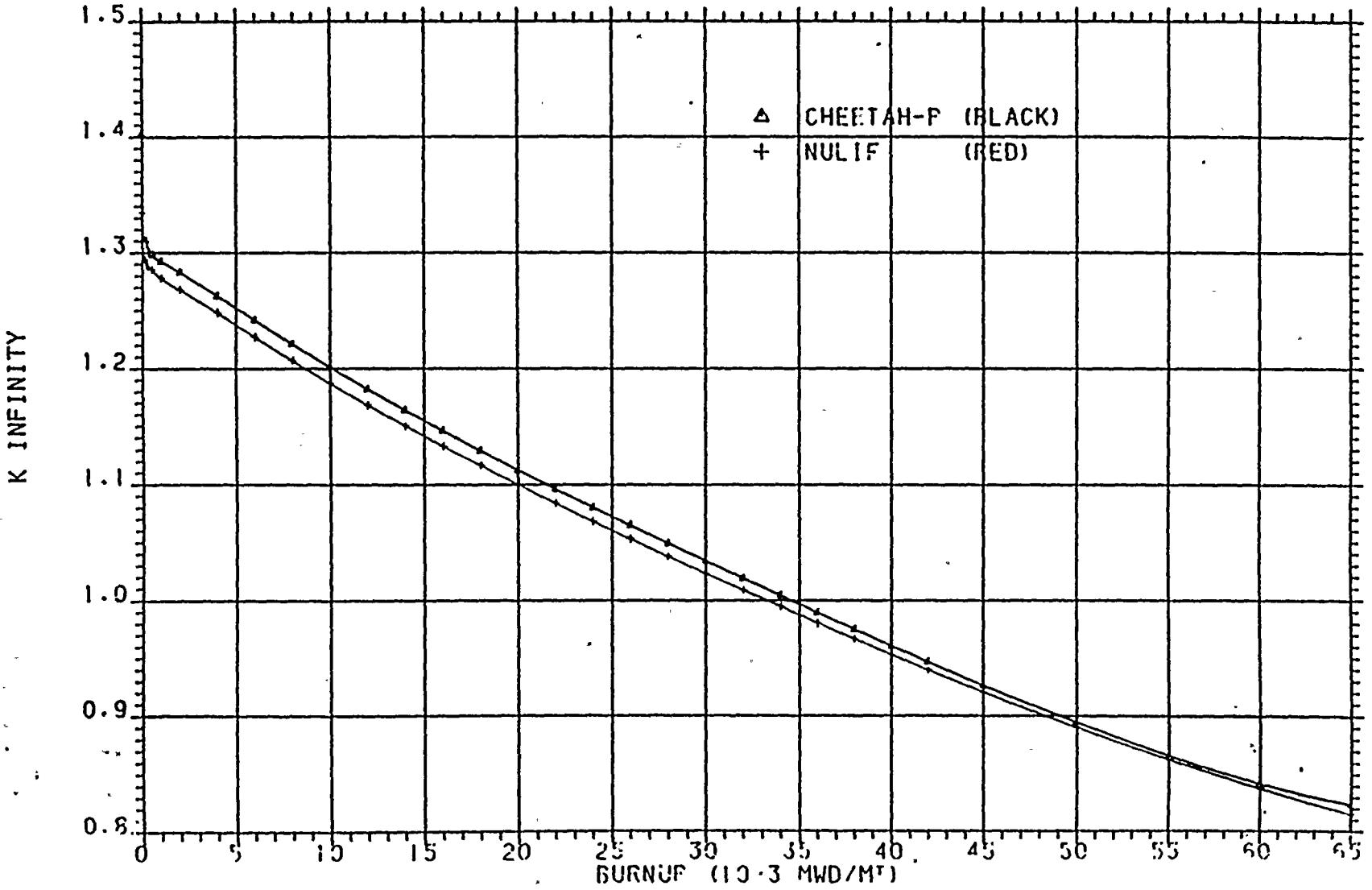

Figure 5.22

TP 4 Nuclear Unit

K-infinity vs. burnup at 4.5% enrichment

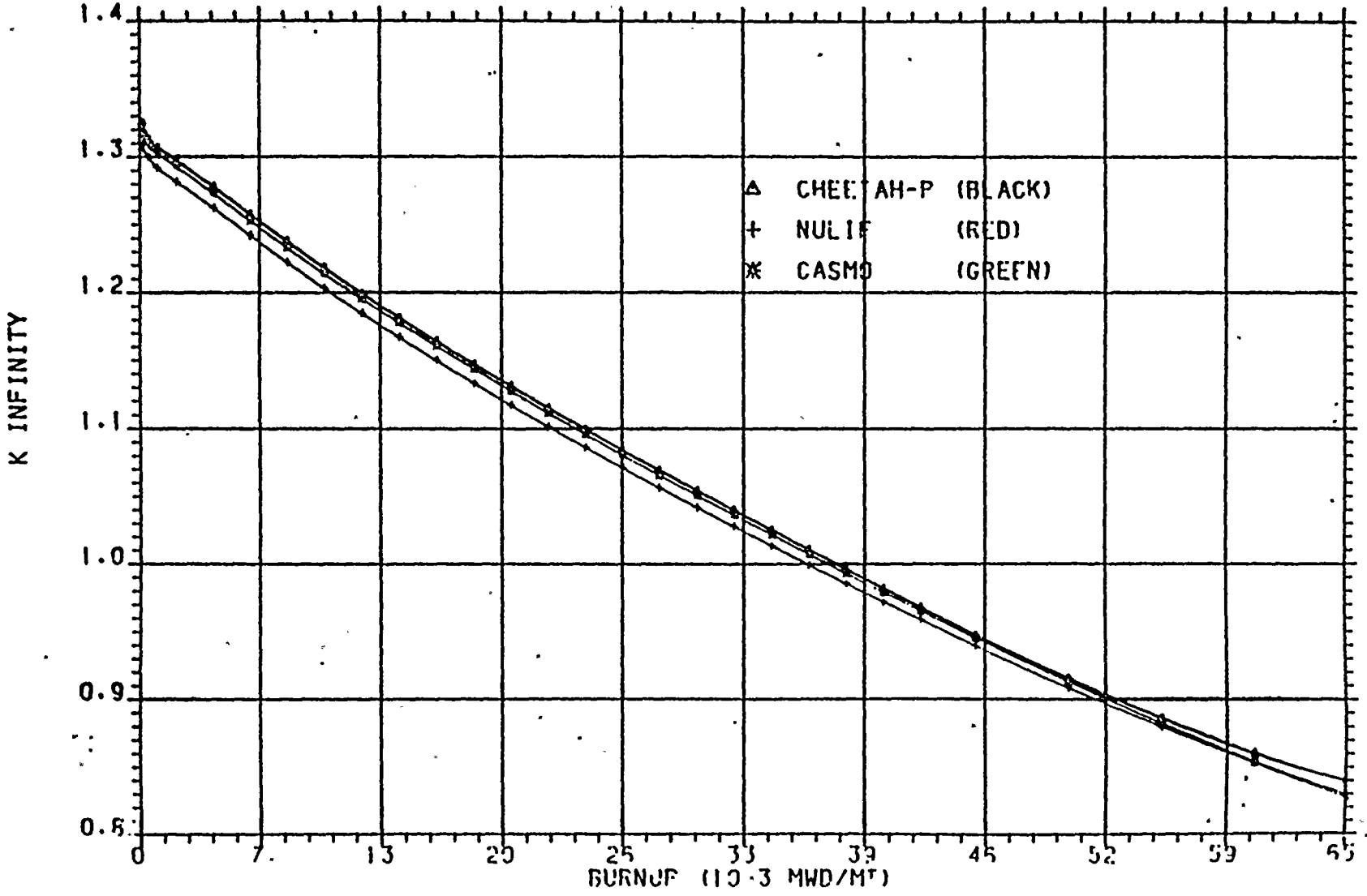

Figure 5.23

SL 1 Nuclear Unit

K-infinity vs. burnup at 1.80% enrichment

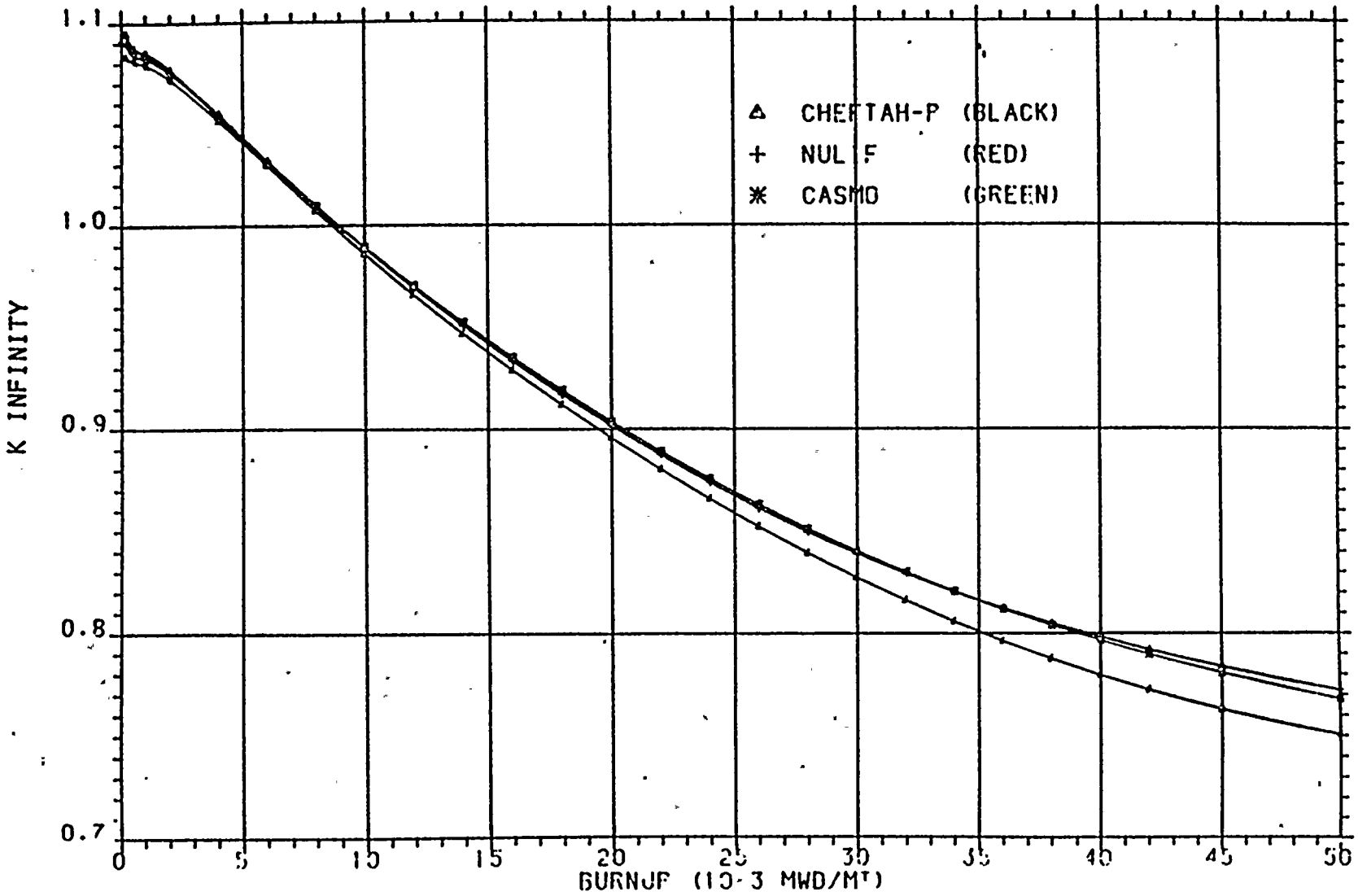

Figure 5.24

SL 1 Nuclear Unit

K infinity vs burnup at 2.75% enrichment

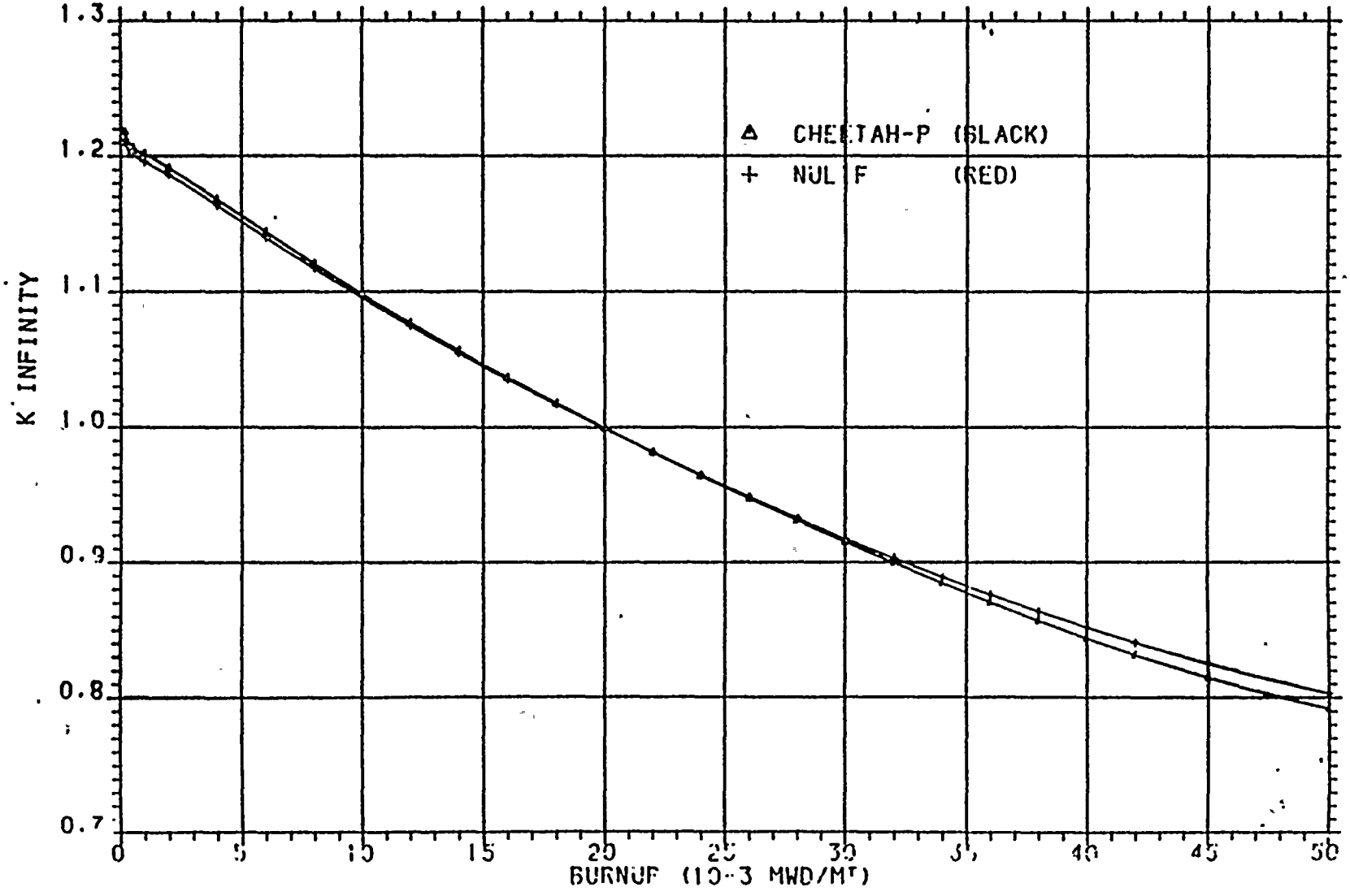

Figure 5.25

SL 1 Nuclear Unit

K infinity vs. burnup at 3.03% enrichment

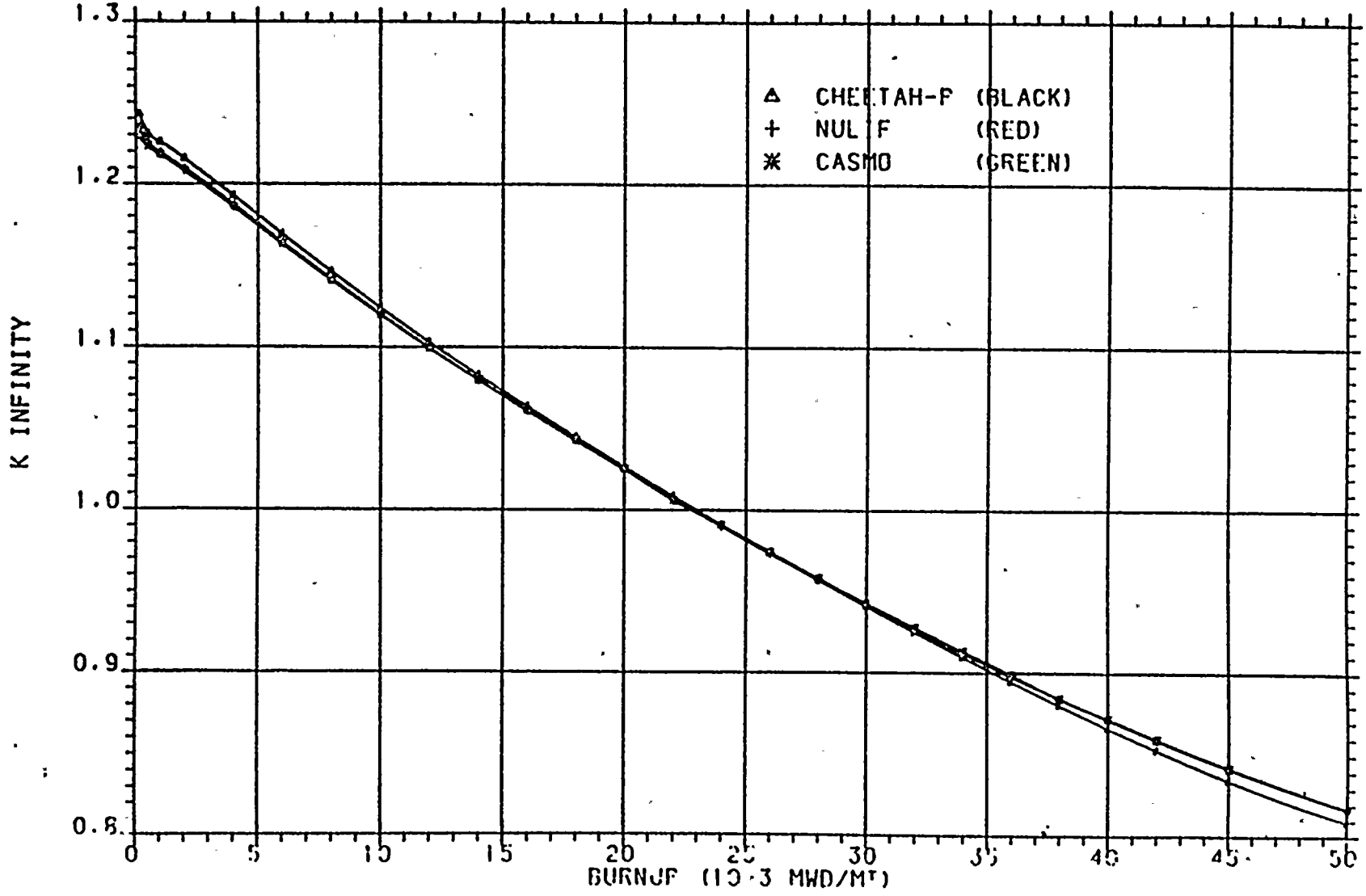

Figure 5.26

SL 1 Nuclear Unit

K infinity vs burnup at 3.35% enrichment

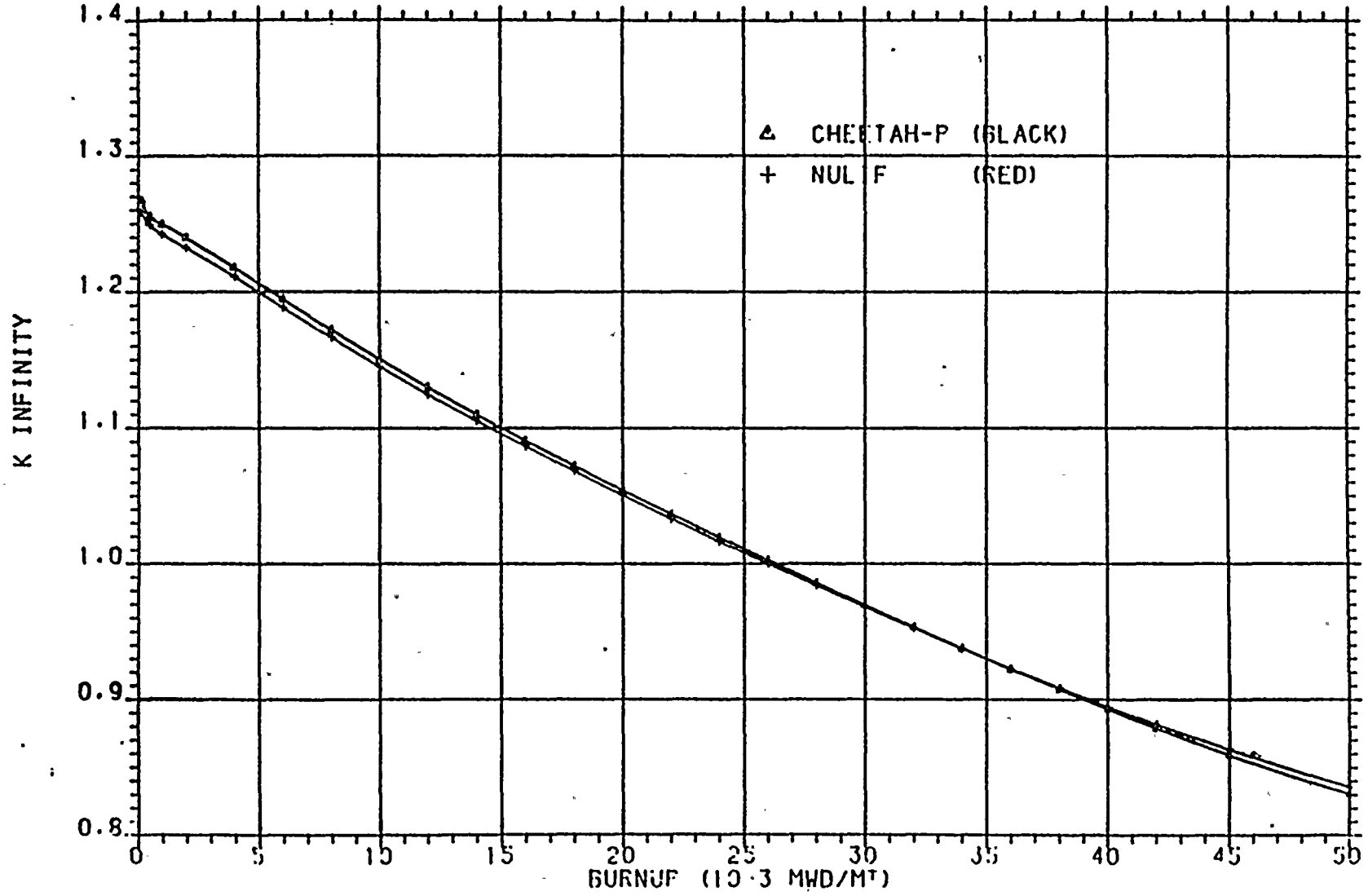

Figure 5.27

SL 1 Nuclear Unit

K infinity vs burnup at 3.67% enrichment

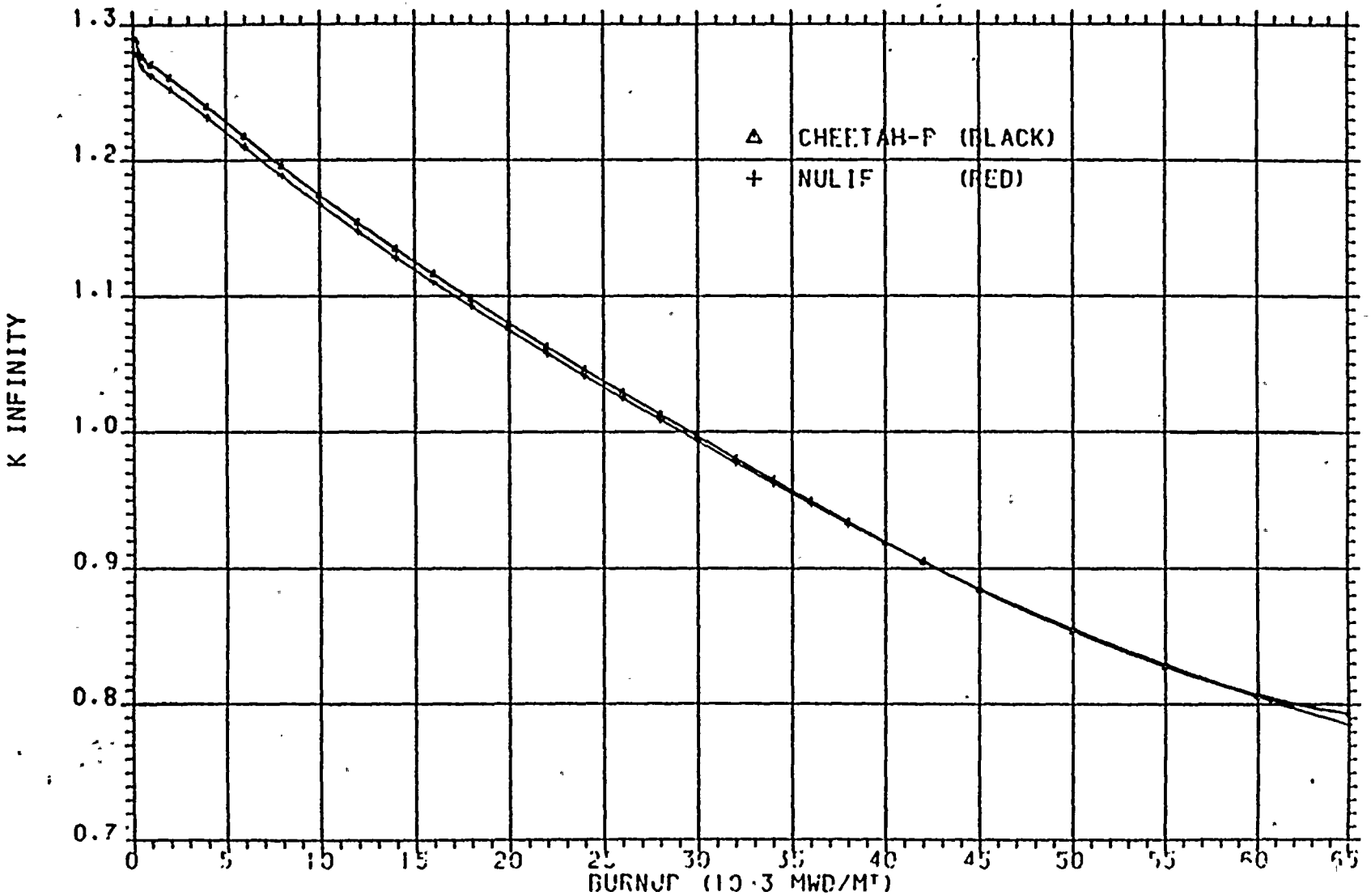

Figure 5.28

SL 1 Nuclear Unit

K infinity vs burnup at 4.00% enrichment

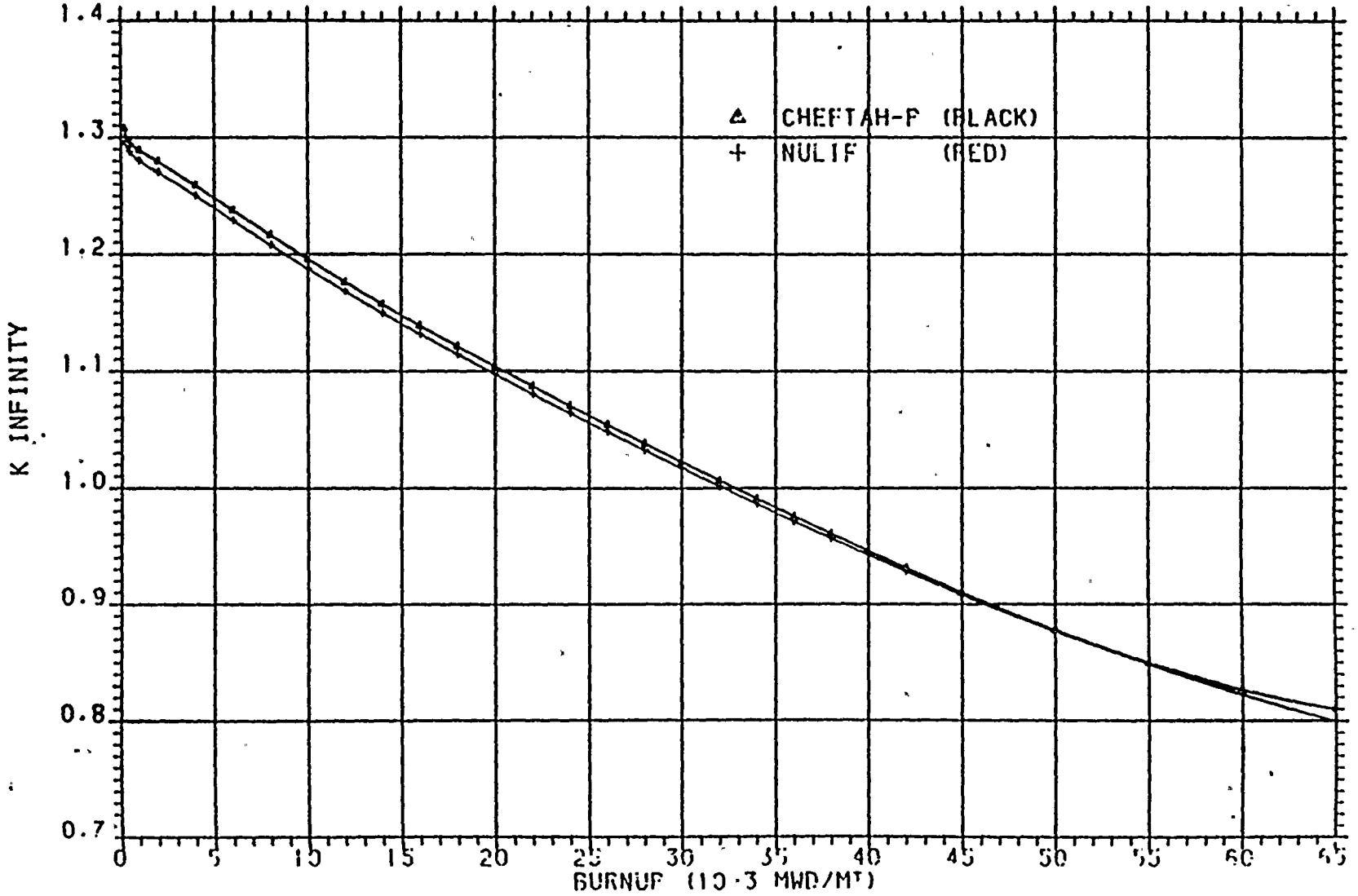

Figure 5.29

SL 1 Nuclear Unit

K infinity vs burnup at 4.5% enrichment

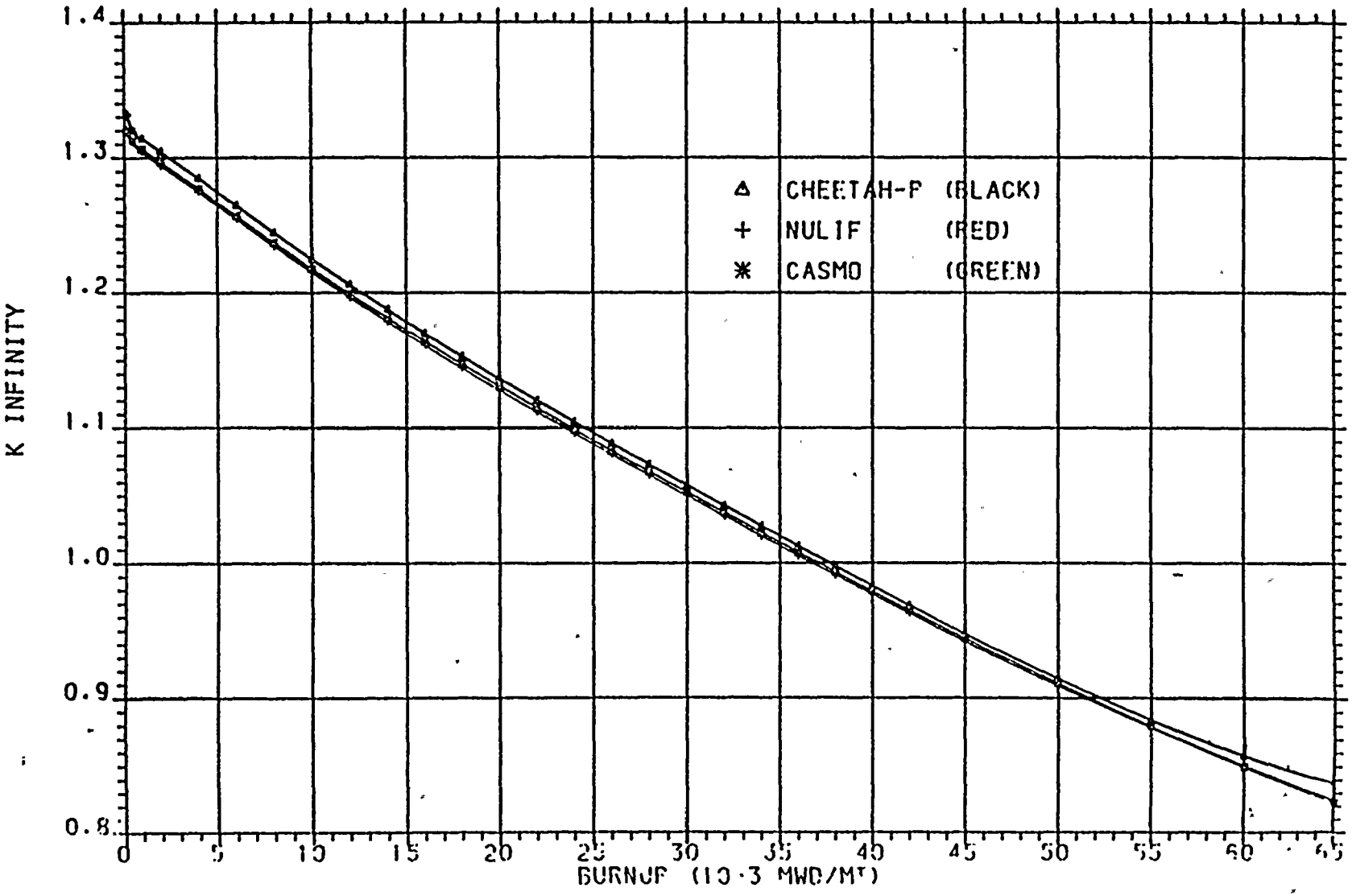

Figure 5.30

TP 4 Nuclear Unit

K infinity vs Enrichment at 150 MWD/MTU Burnup

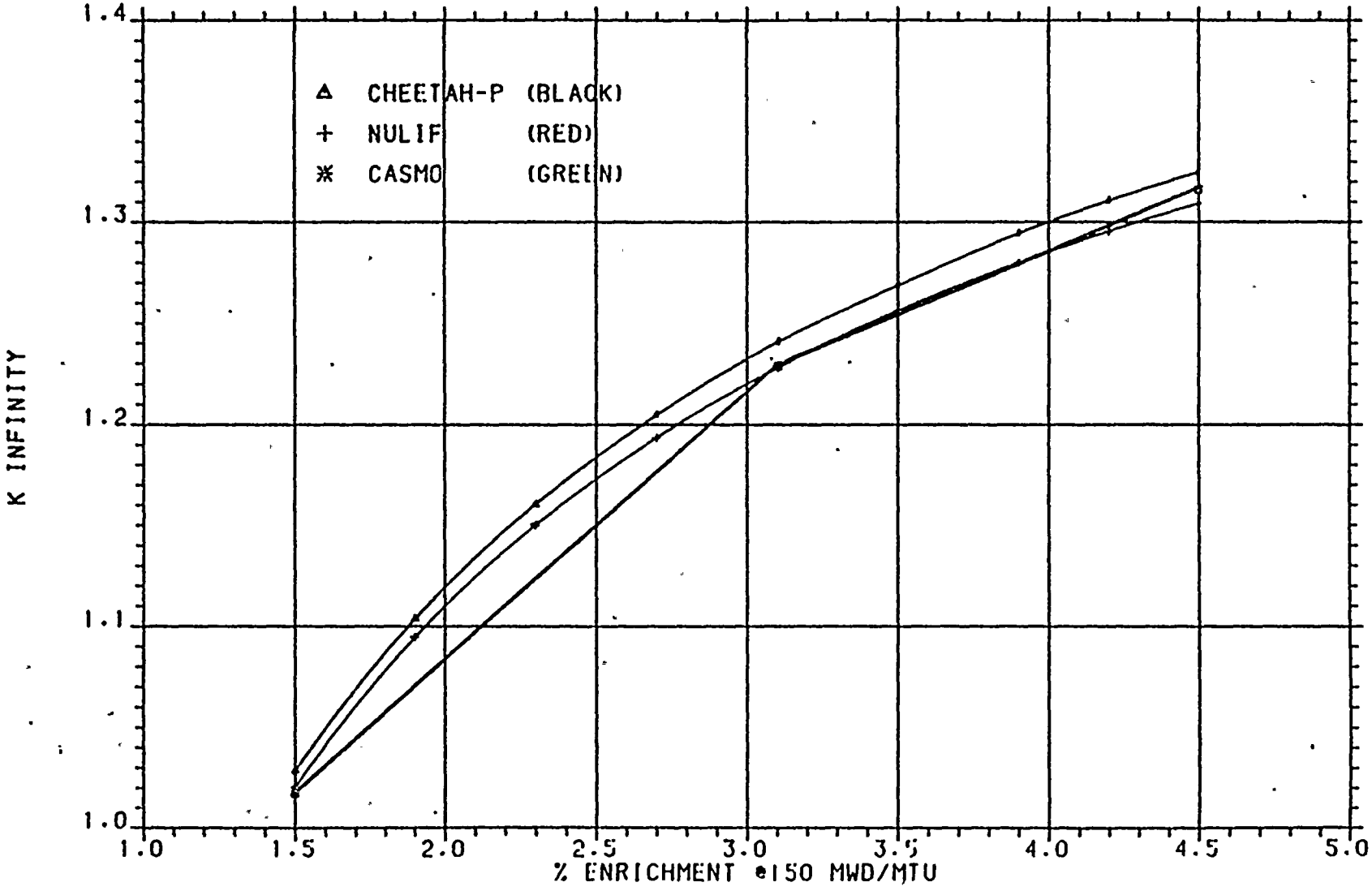

Figure 5.31

TP 4 Nuclear Unit

K infinity vs Enrichment at 50,000 MWD/MTU Burnup

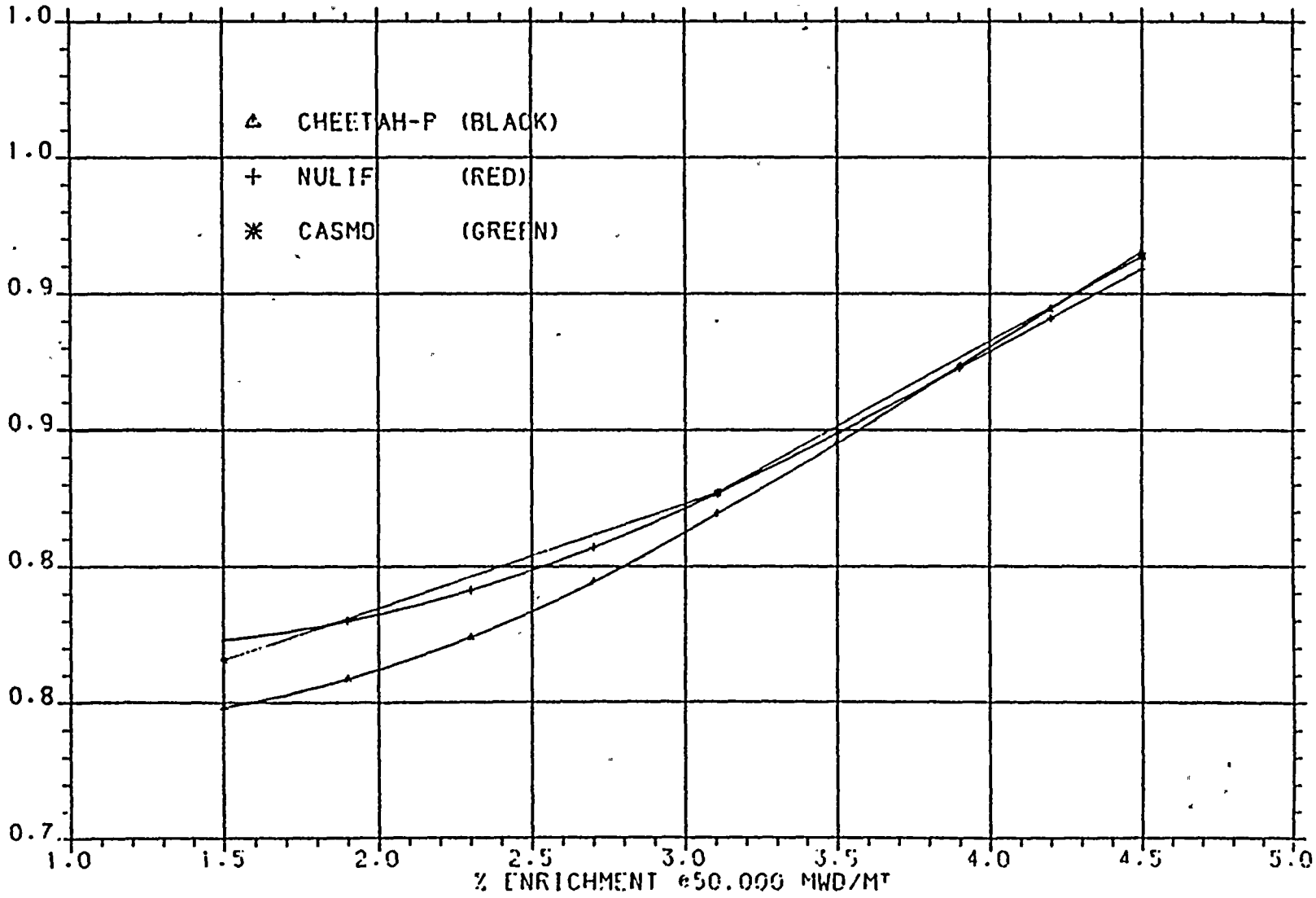

Figure 5.32

SL 1 Nuclear Unit

K-infinity vs Enrichment at 150 MWD/MTU Burnup

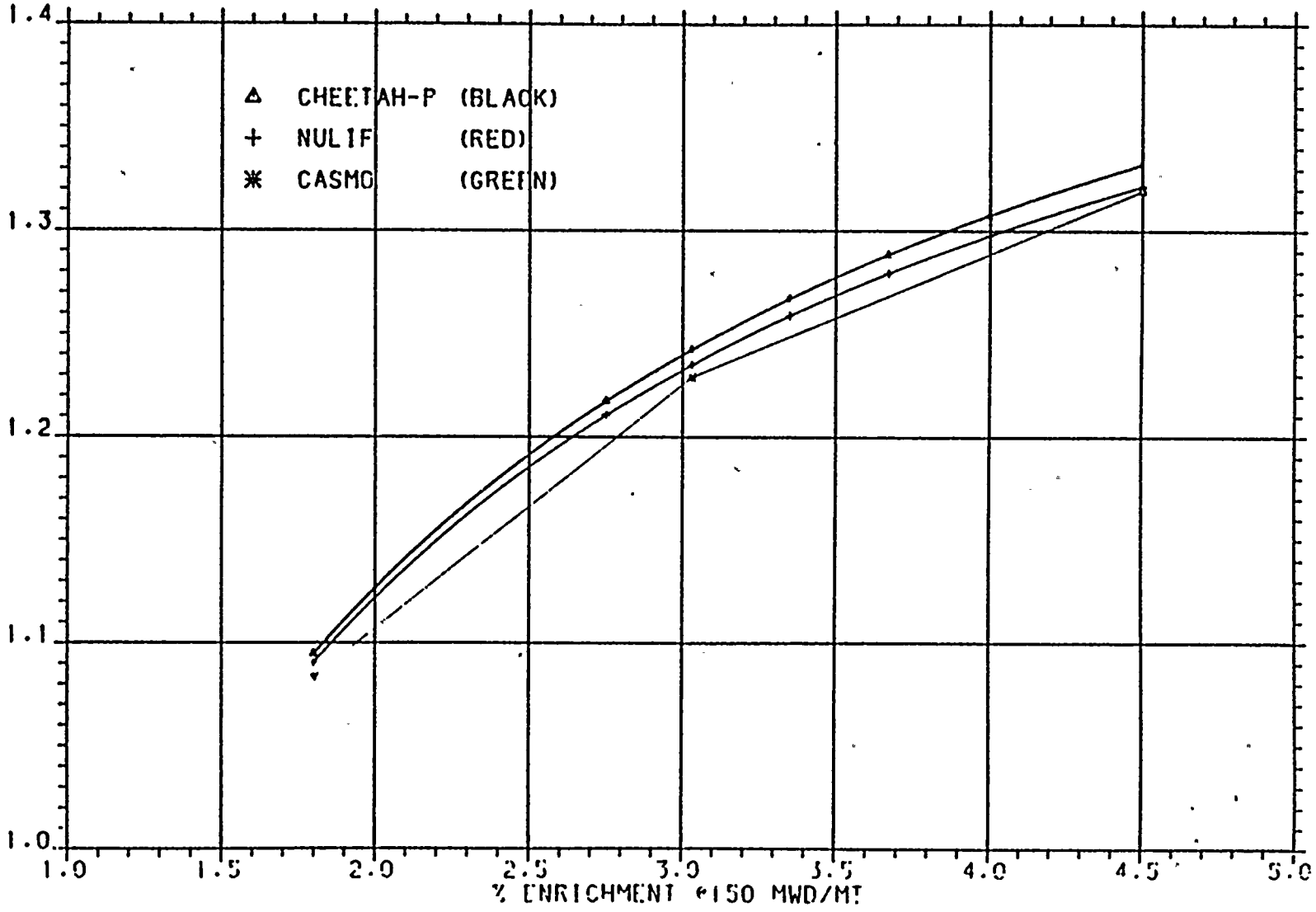

Figure 5.33

SL 1 Nuclear Unit

K-infinity vs. Enrichment at 50,000 MWD Burnup / MTU

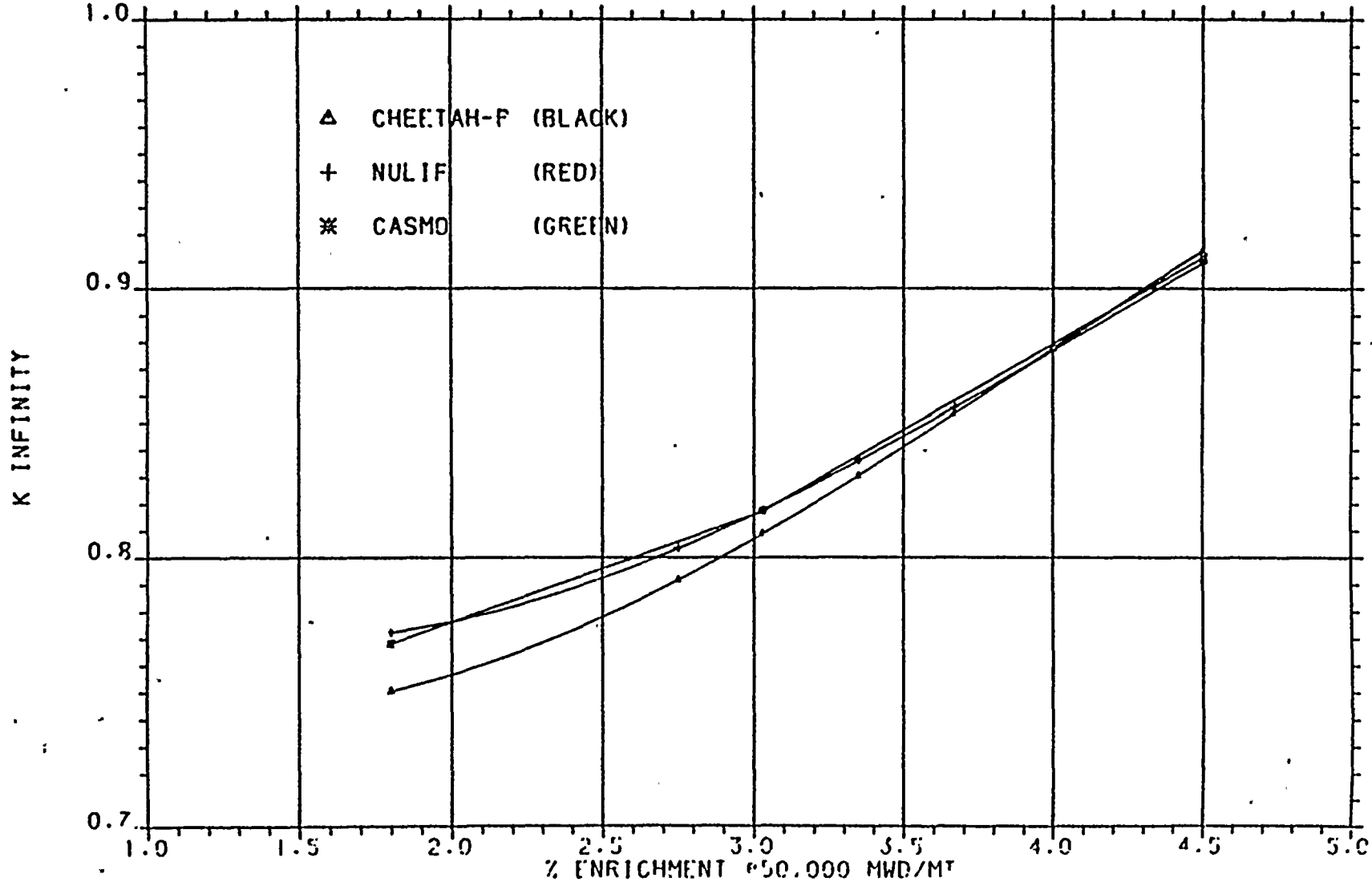

Figure 5.34

TP 4 Nuclear Unit

Discharge U-235 vs Burnup at 1.5% enrichment

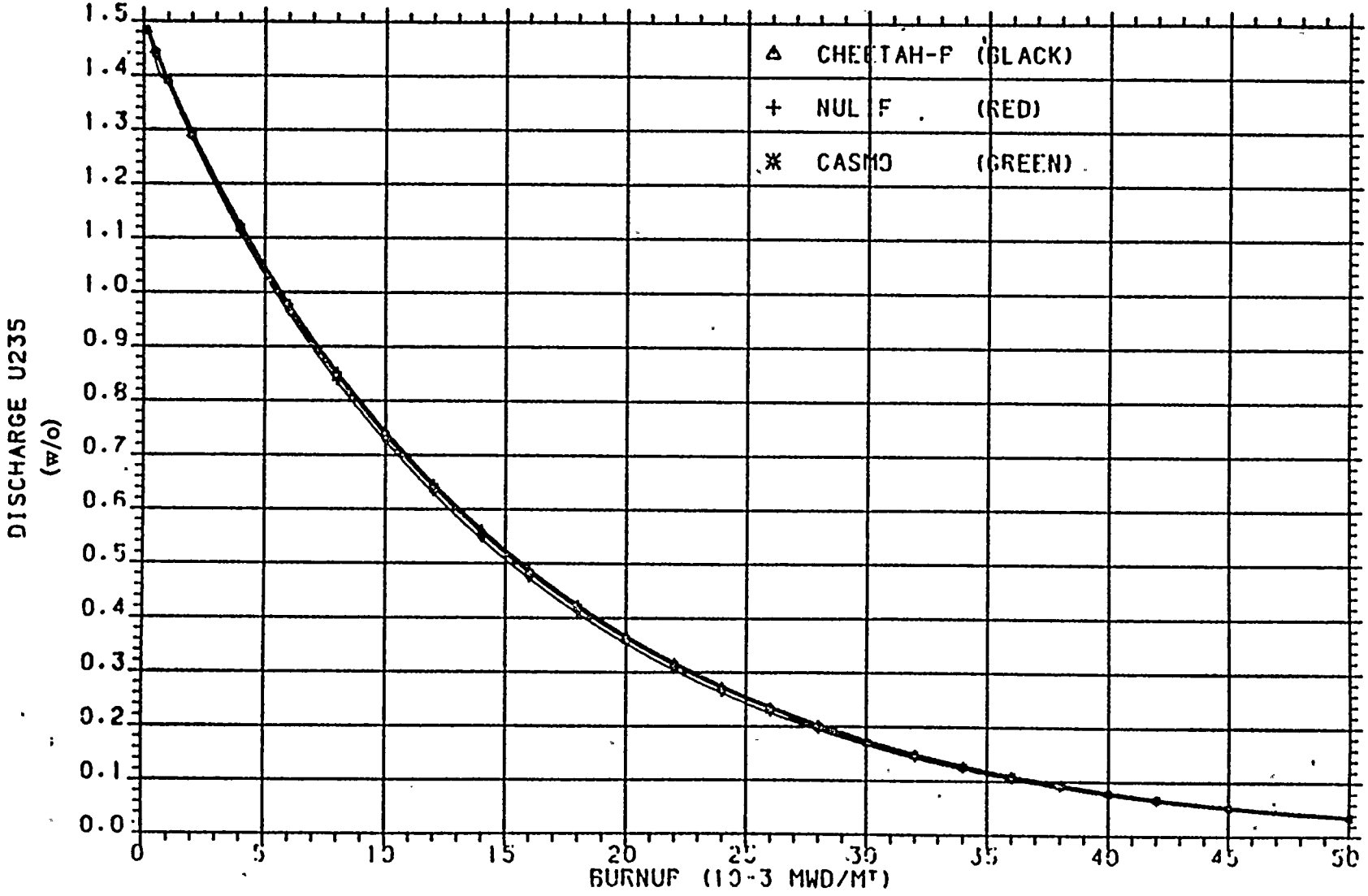

Figure 5.35

TP 4 Nuclear Unit

Discharge Fissile Plutonium vs. Burnup at 1.5% enrichment

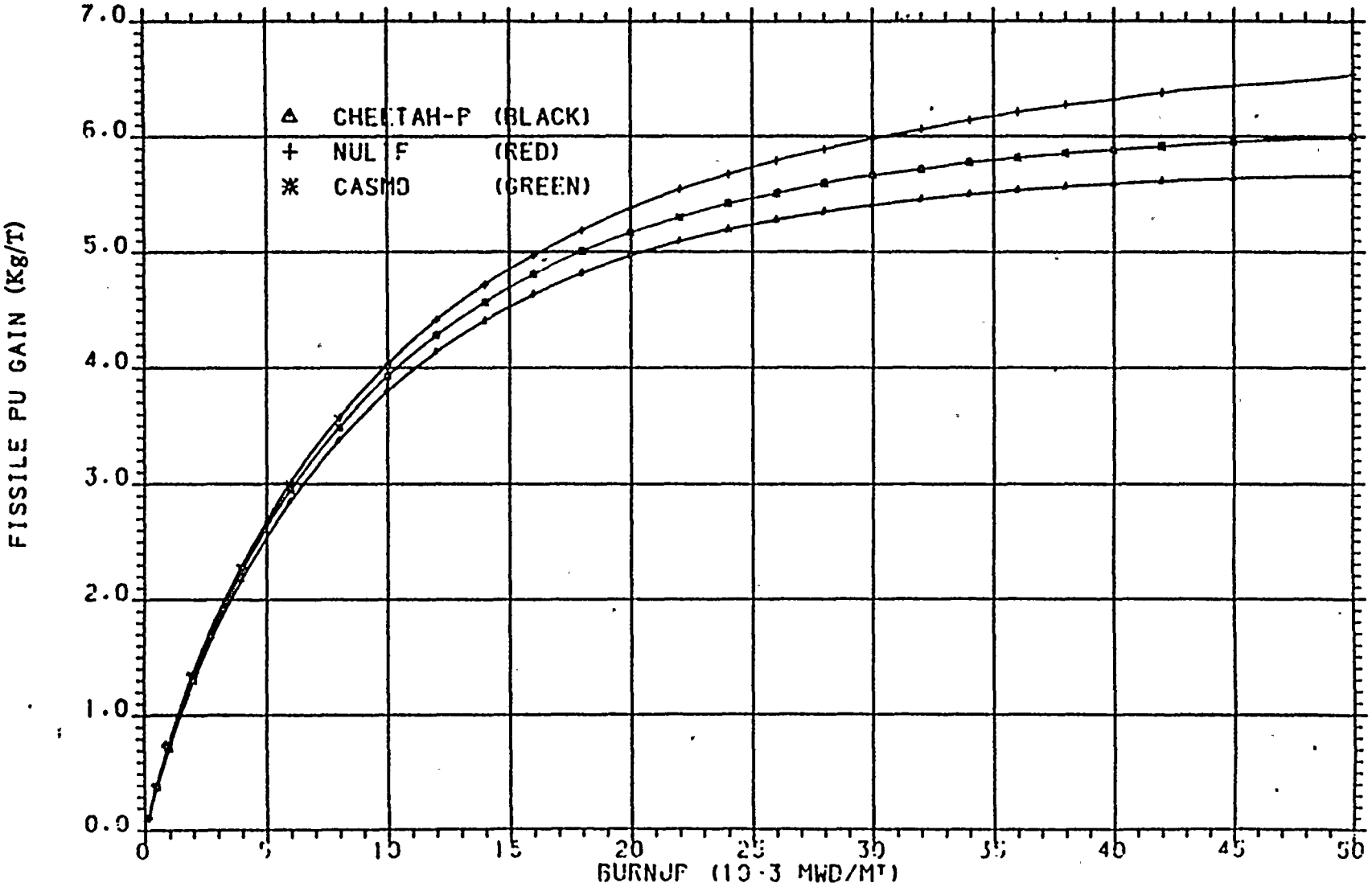

Figure 5.36

TP 4 Nuclear Unit

Discharge U-235 vs. Burnup at 2.3% enrichment

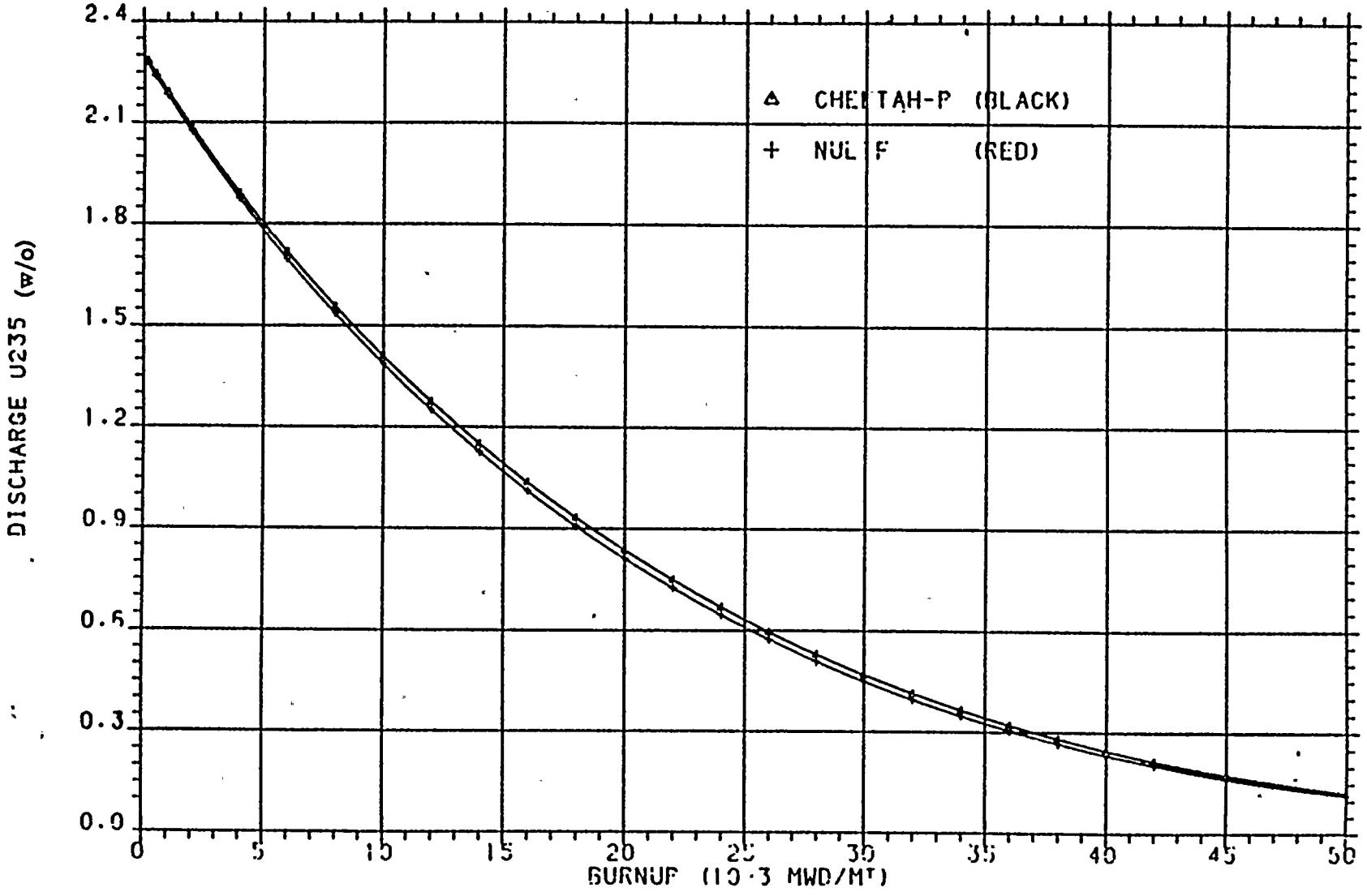

Figure 5.37

TP 4 Nuclear Unit

Discharge Fissile Plutonium vs Burnup at 2.3% enrichment

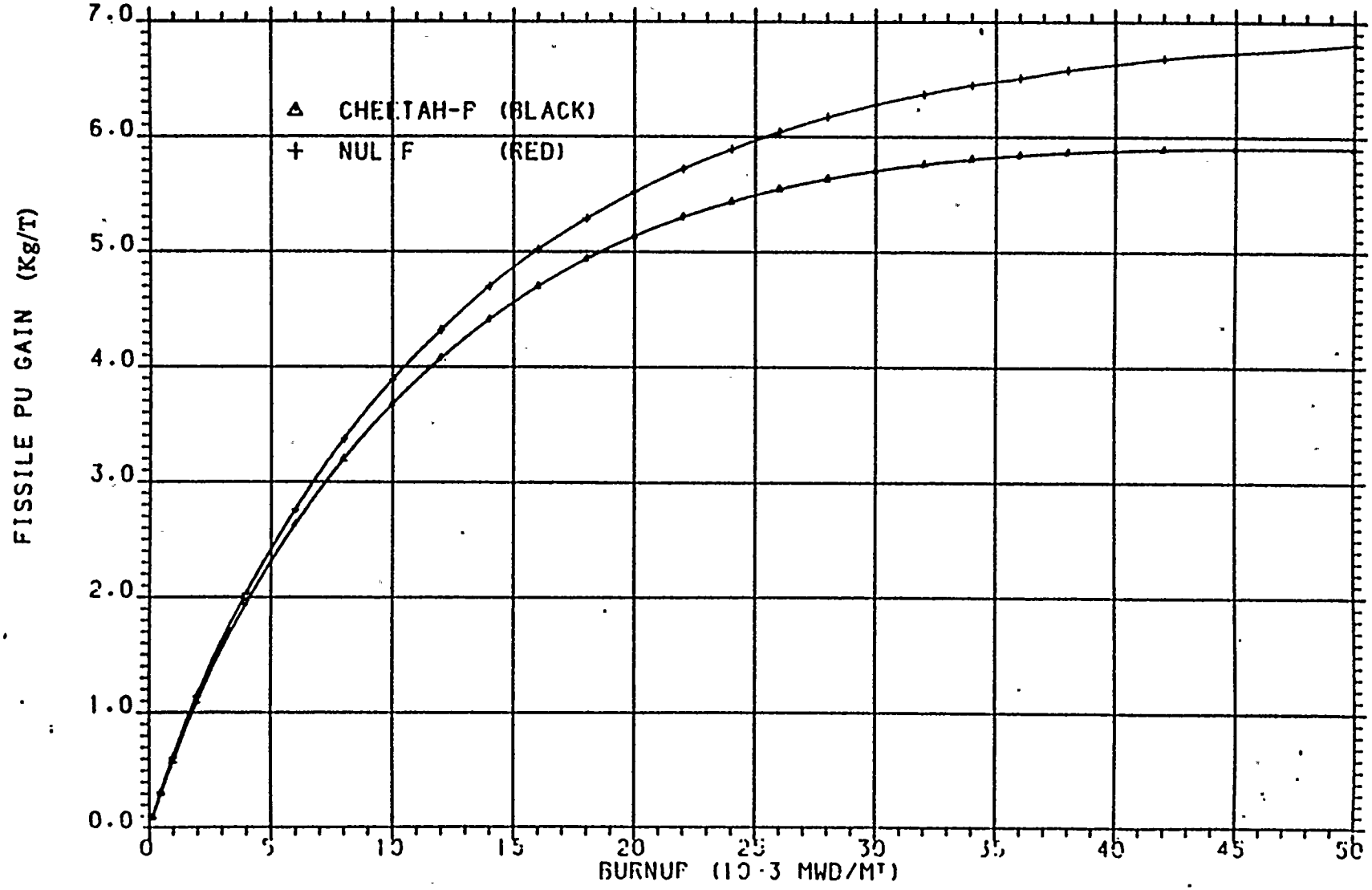

Figure 5.38

TP 4 Nuclear Unit

Discharge U-235 vs Burnup at 3.104% enrichment

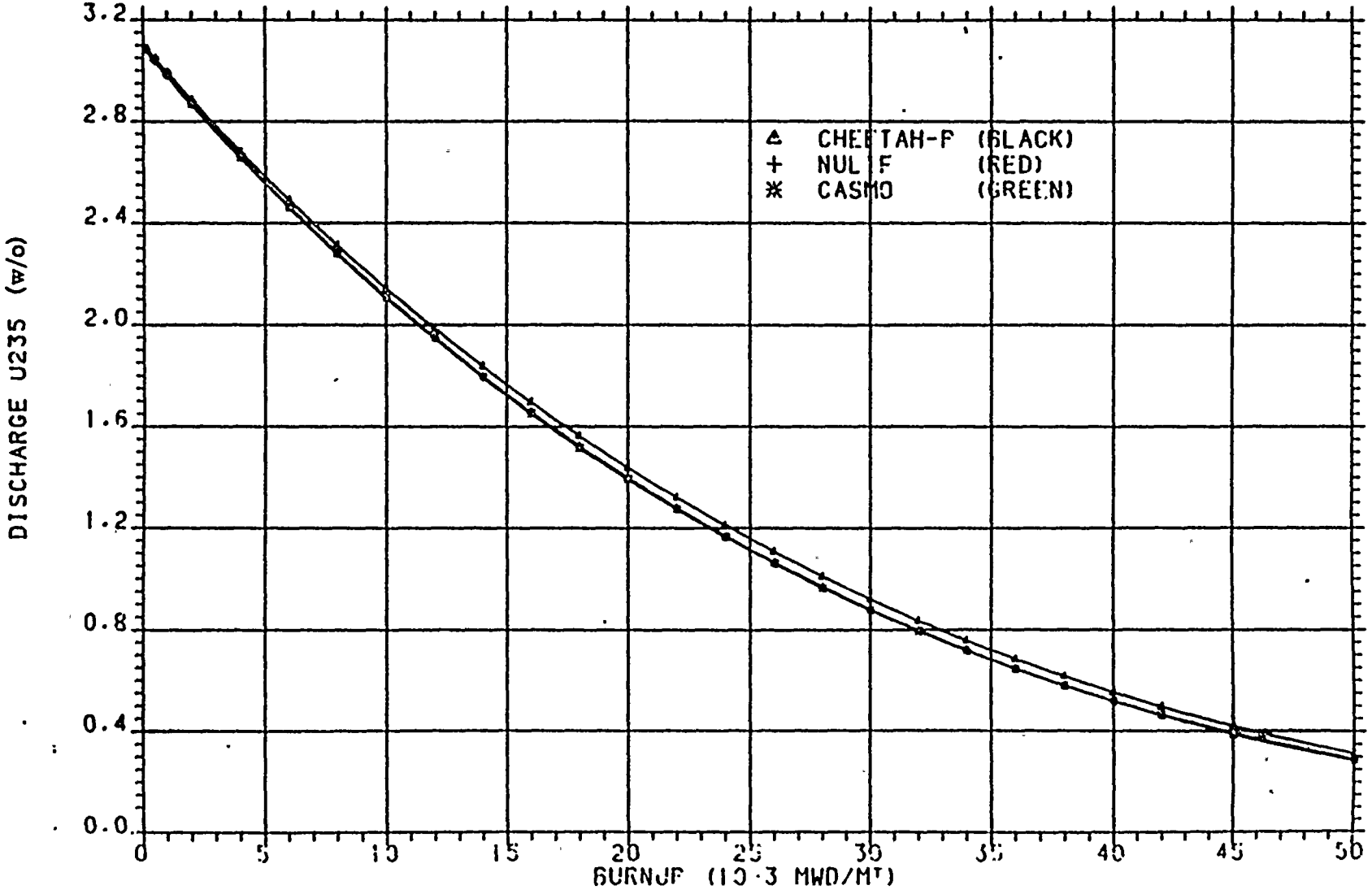

Figure 5.39

TP 4 Nuclear Unit

Discharge Fissile Plutonium vs Burnup at 3.104% enrichment

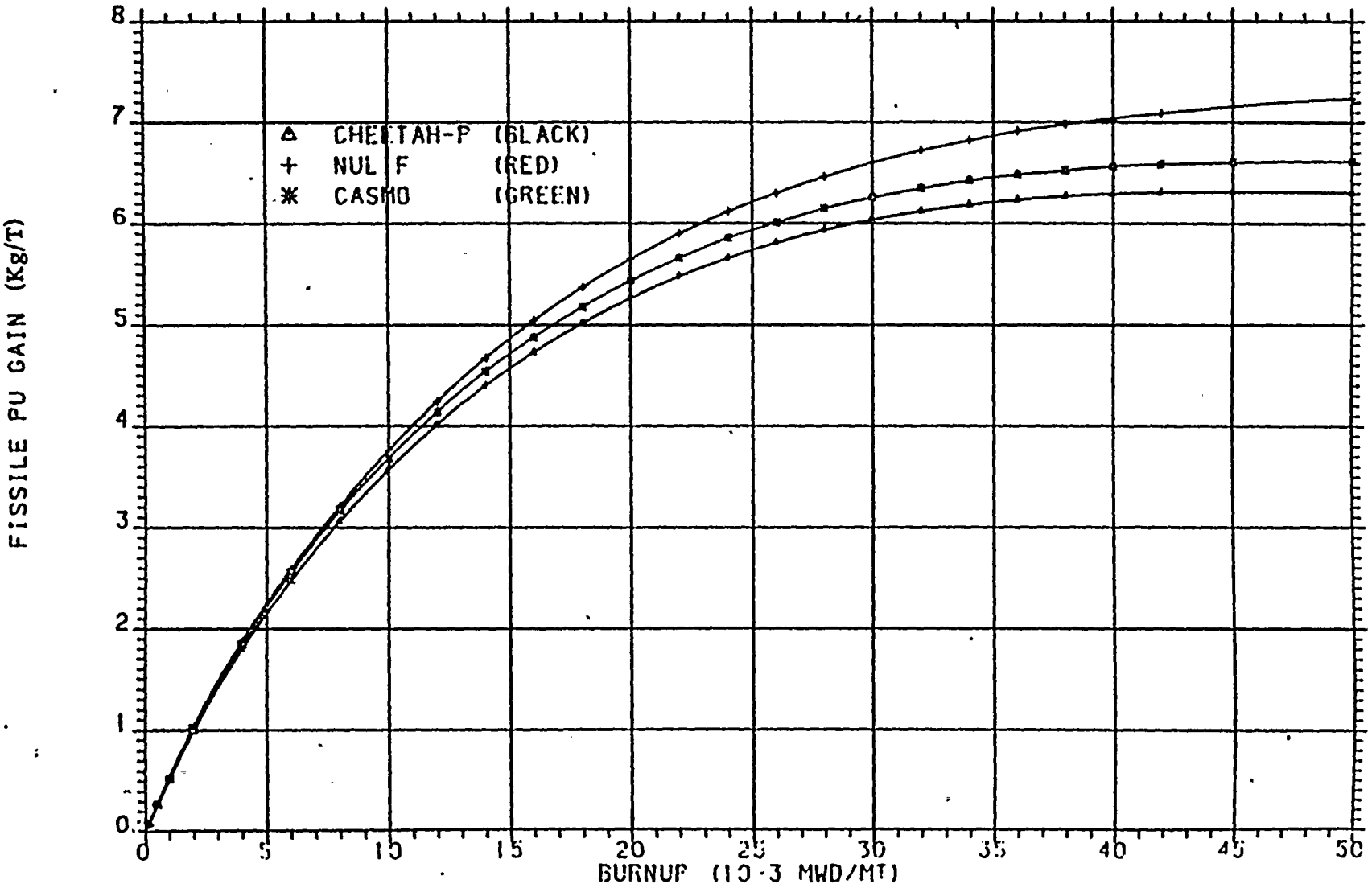

Figure 5.40

TP 4 Nuclear Unit

Discharge U-235 vs Burnup at 3.9% enrichment

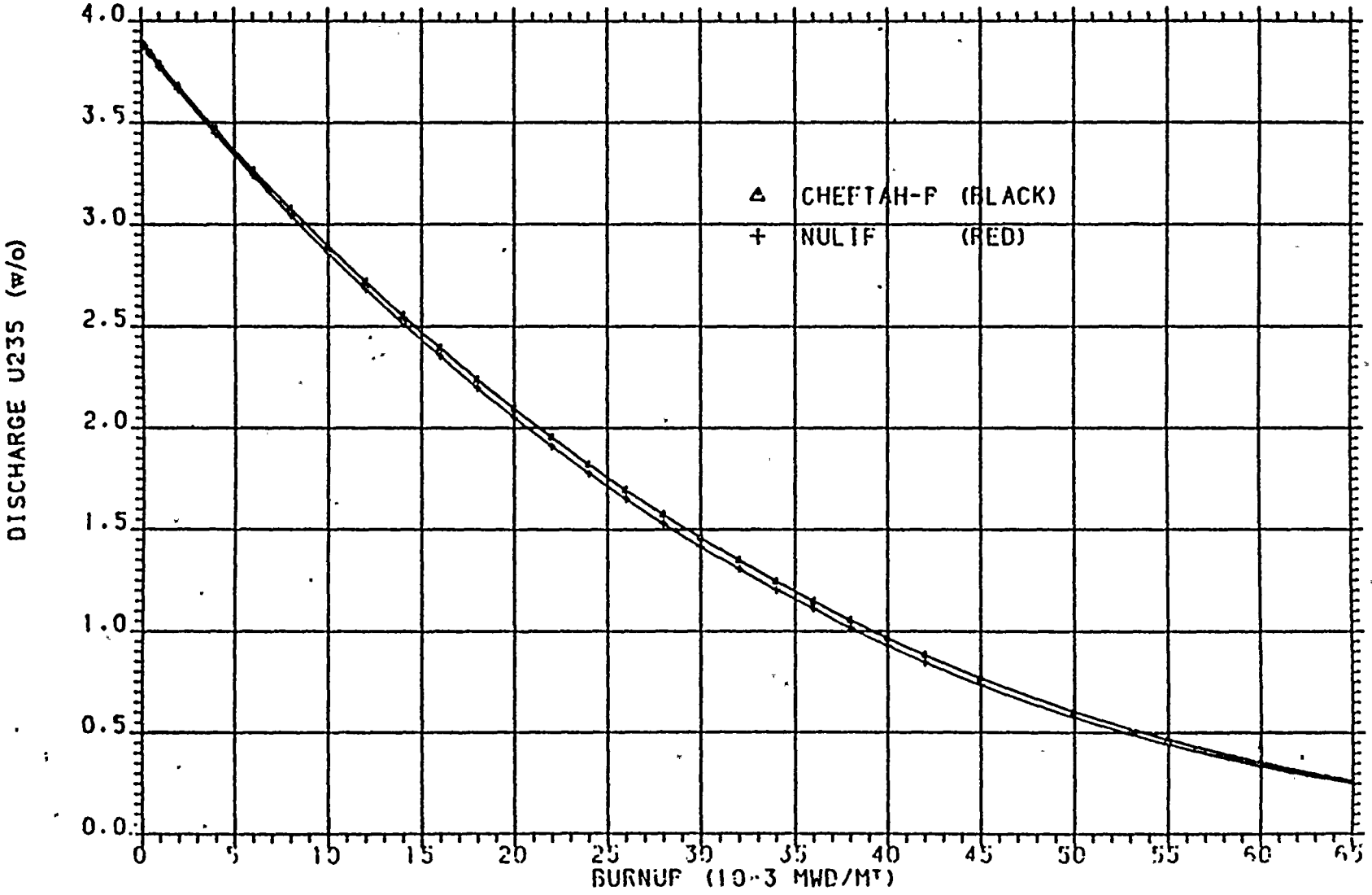

Figure 5.41

TP 4 Nuclear Unit

Discharge Fissile Plutonium vs Burnup at 3.9% enrichment

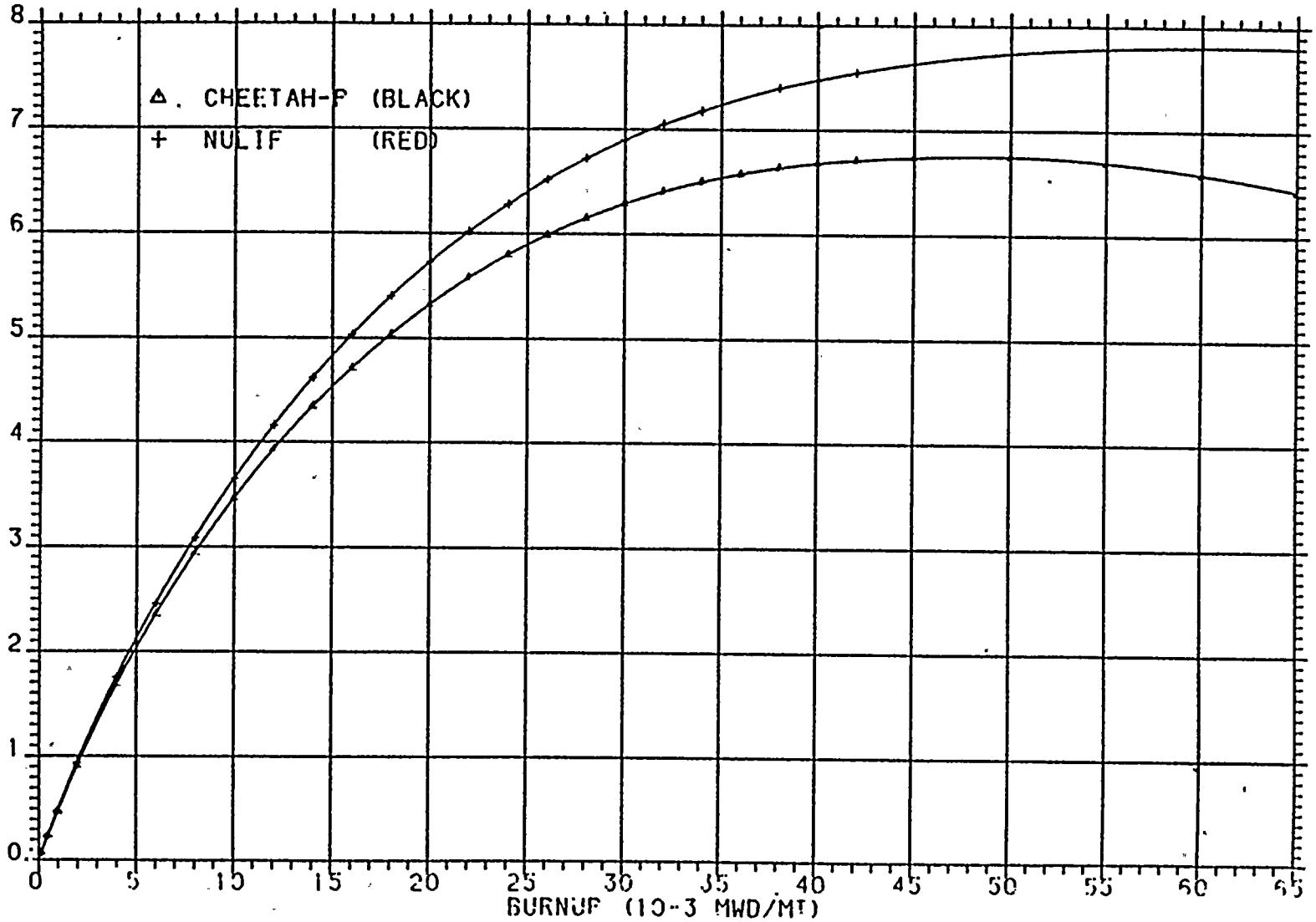

Figure 5.42

TP 4 Nuclear Unit

Discharge U-235 vs Burnup at 4.5% enrichment

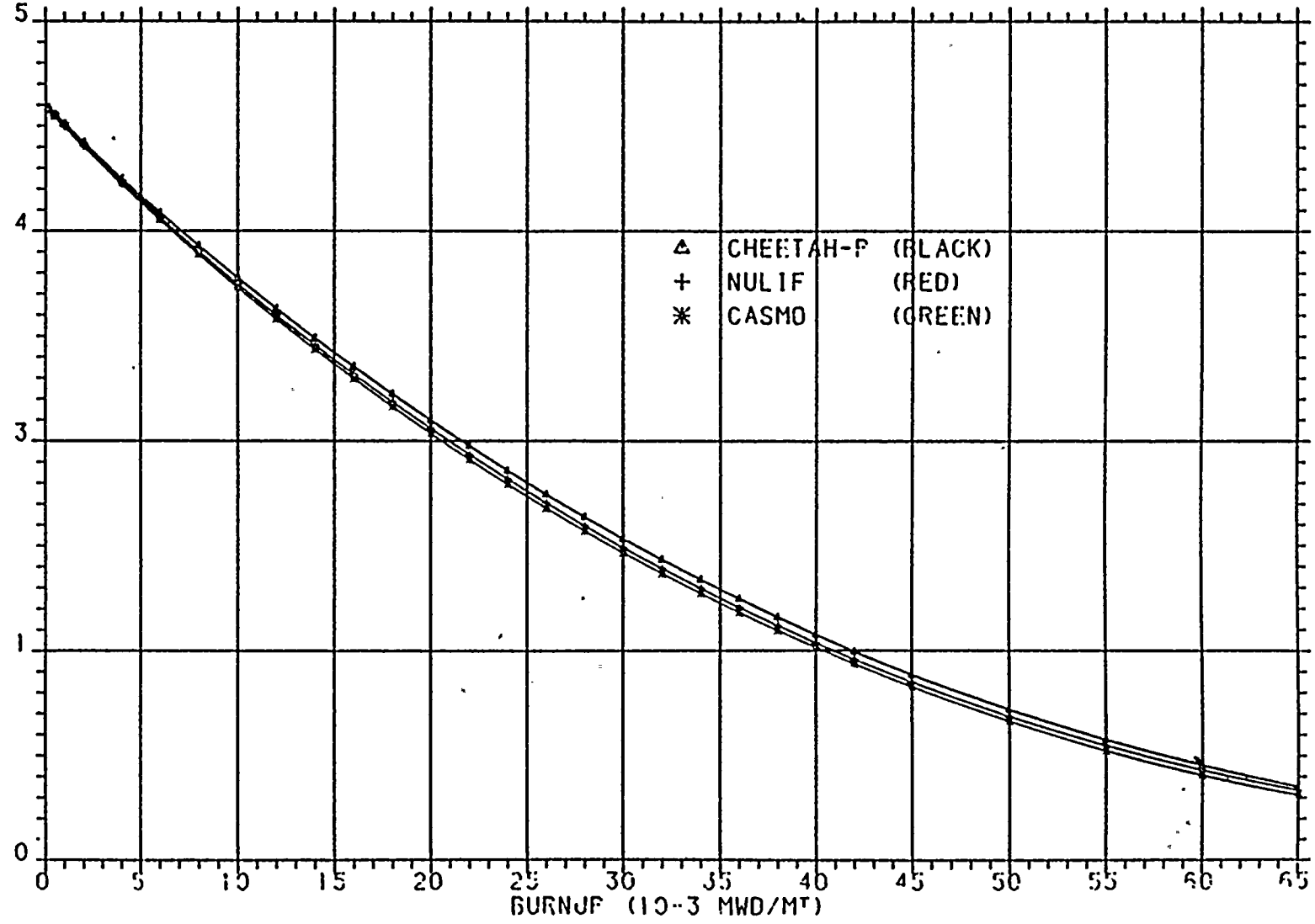

Figure 5.43

TP 4 Nuclear Unit

Discharge Fissile Plutonium vs. Burnup at 4.5% enrichment

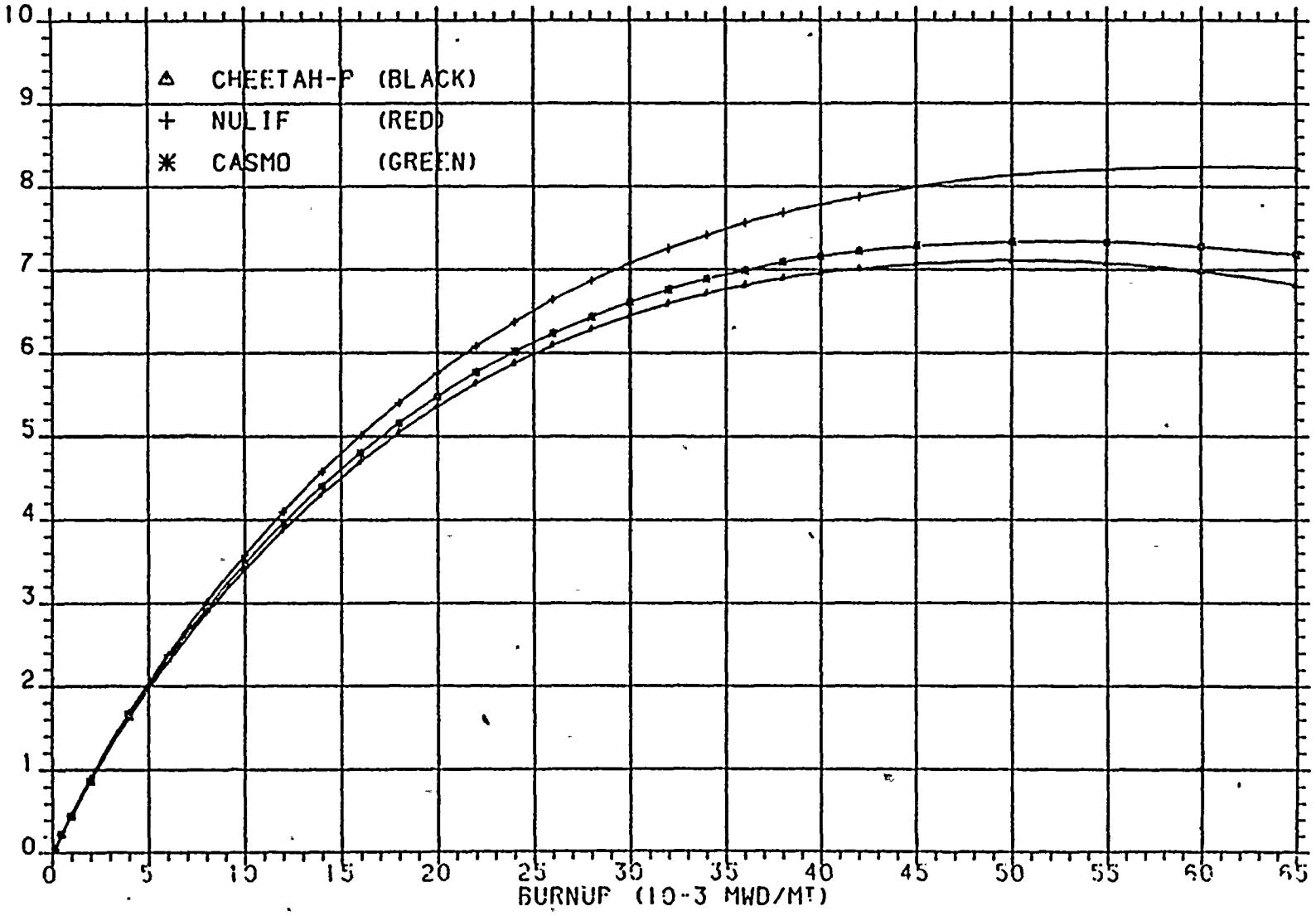

Figure 5.4-1

SL1 Nuclear Unit

Discharge U-235 vs. Burnup at 1.8% enrichment

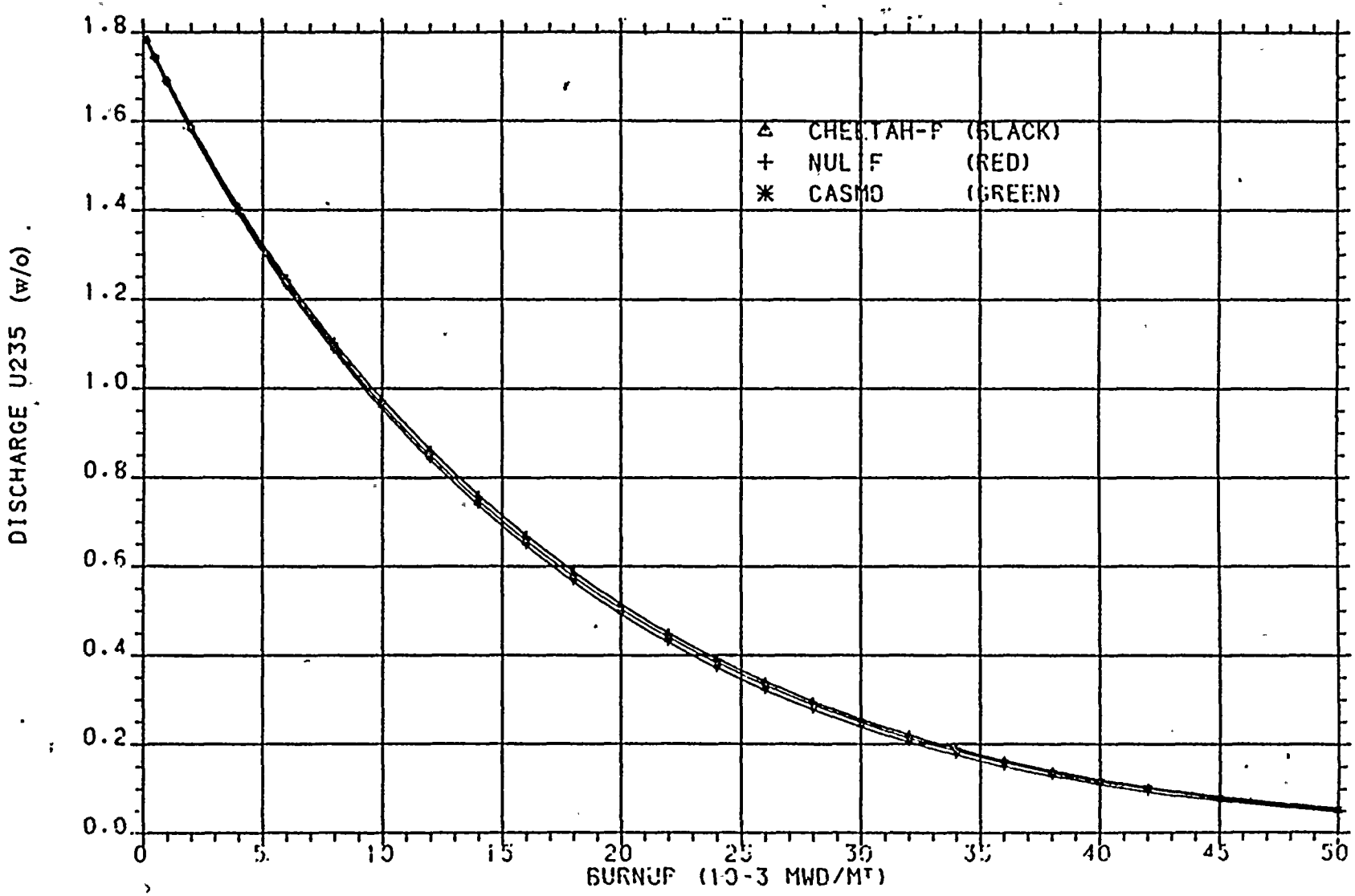

Figure 5.45

SL1 Nuclear Unit

Discharge Fissile Plutonium vs. Burnup at 1.8% enrichment

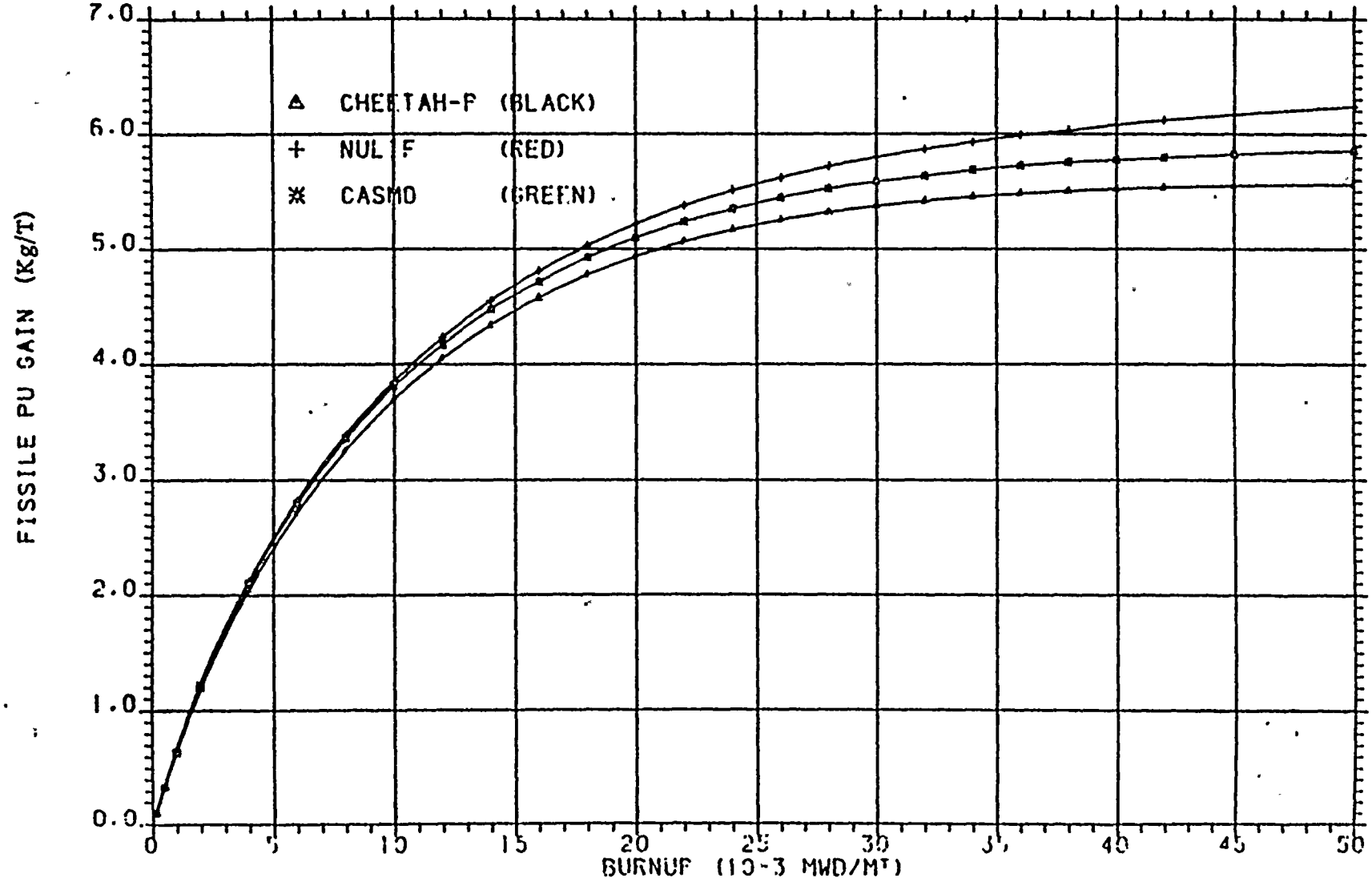

Figure 5.46

SL1 Nuclear Unit

Discharge U-235 vs. Burnup at 3.031% enrichment

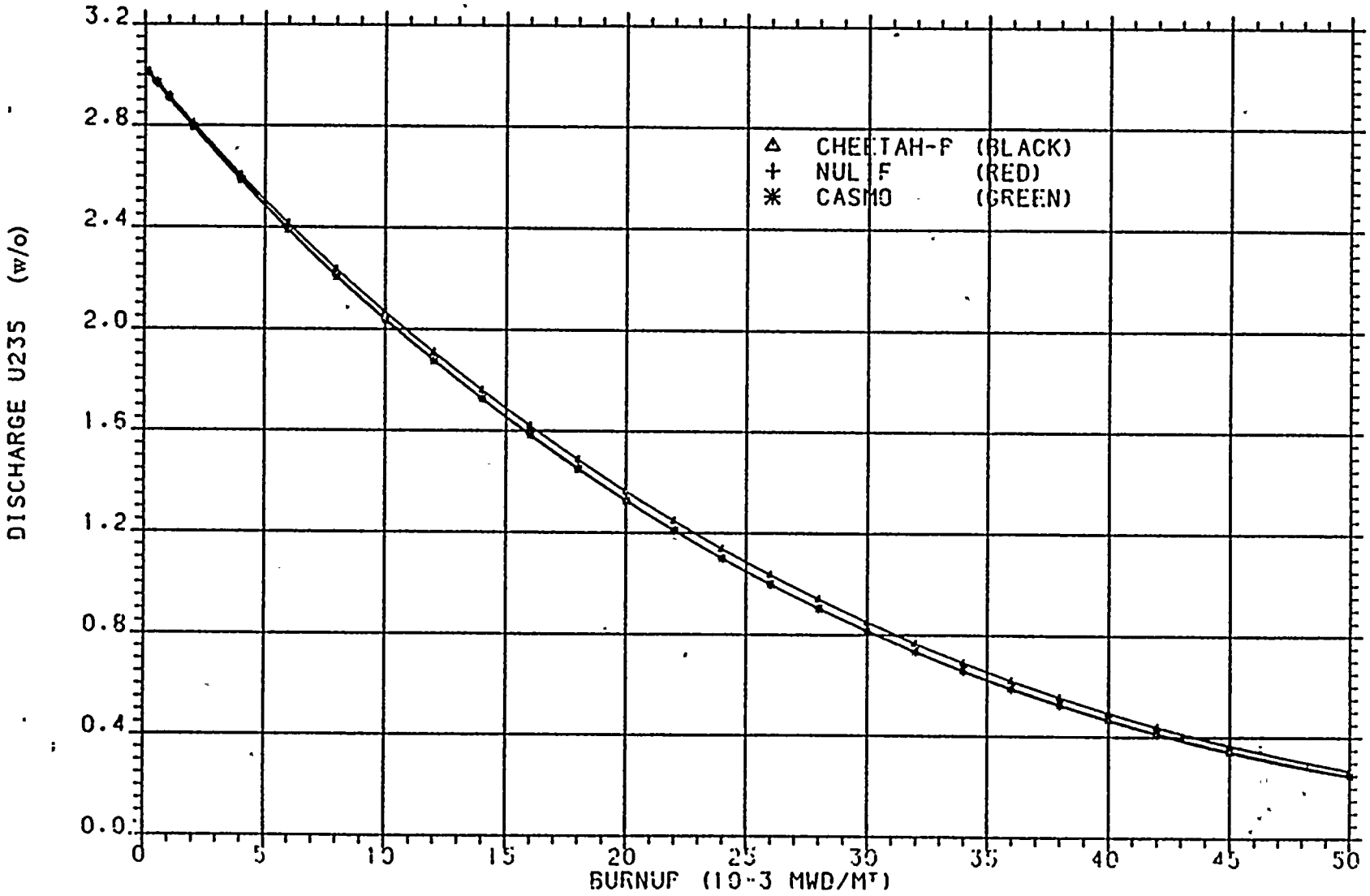

Figure 5.47

SL 1 Nuclear Unit

Discharge Fissile Plutonium vs. Burnup at 3.031% enrichment

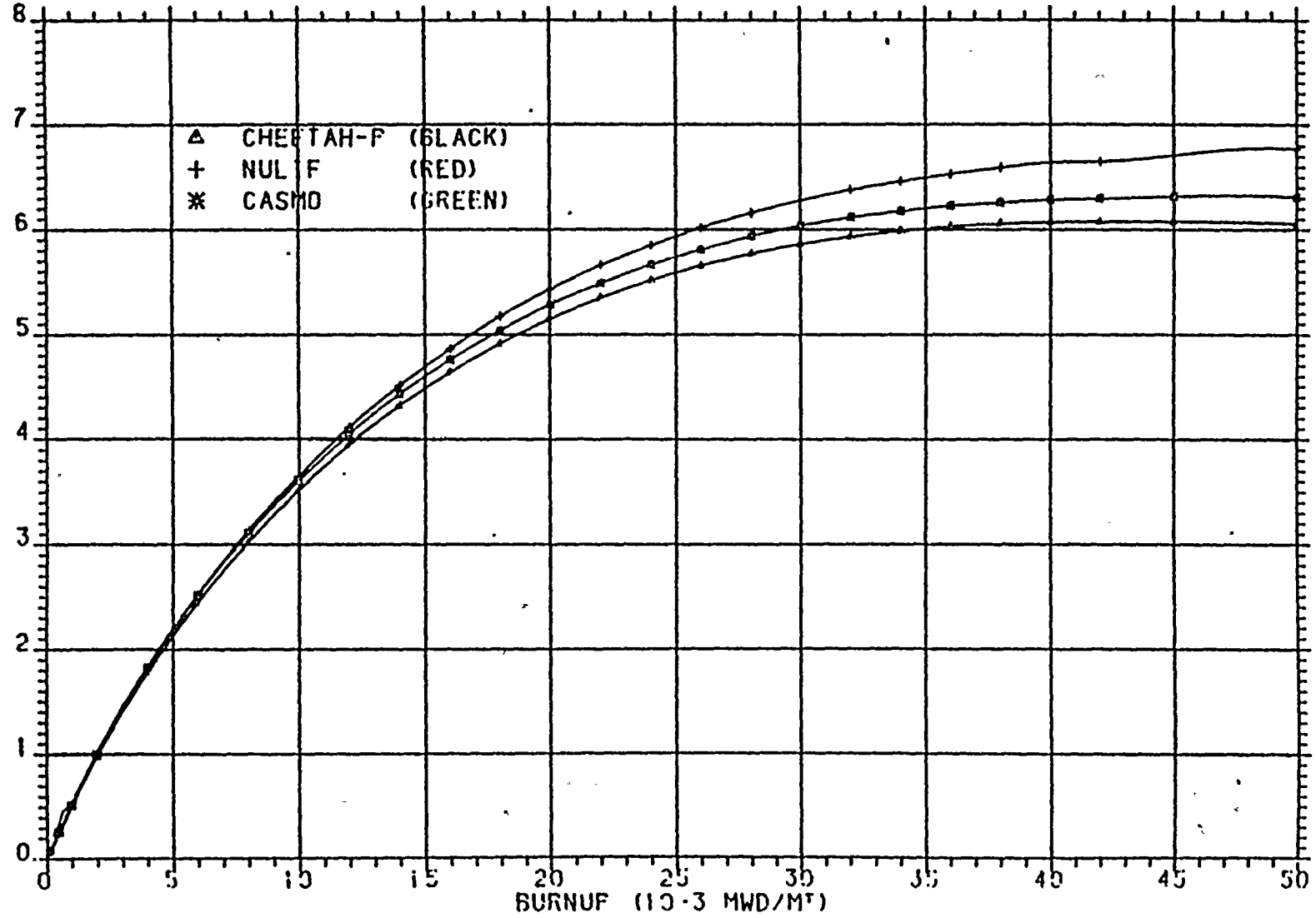

Figure 5.48

SL1 Nuclear Unit

Discharge U-235 vs. Burnup at 3.67% enrichment

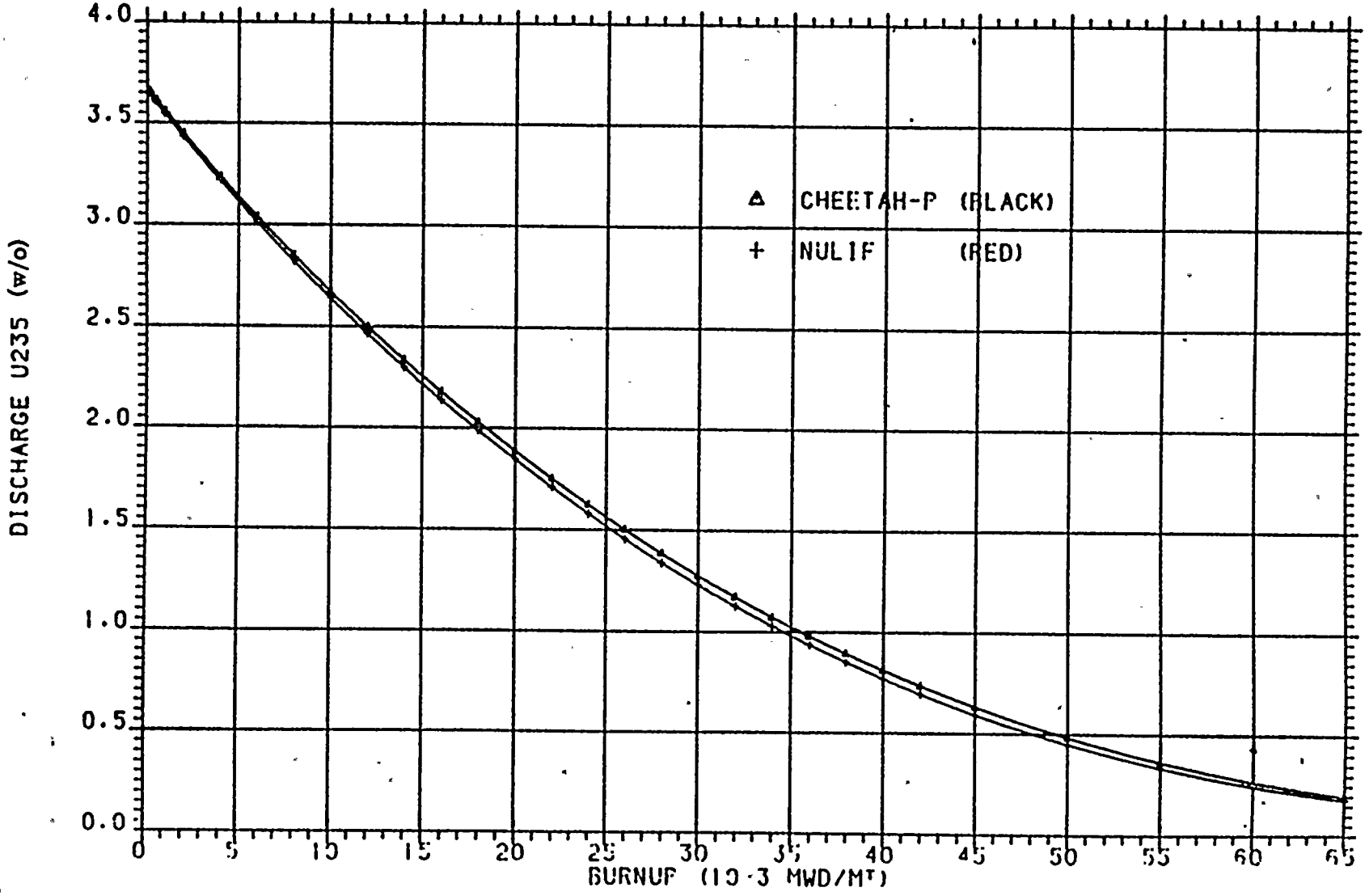

Figure 5.49

SL1 Nuclear Unit

Discharge Fissile Plutonium vs. Burnup at 3.67% enrichment

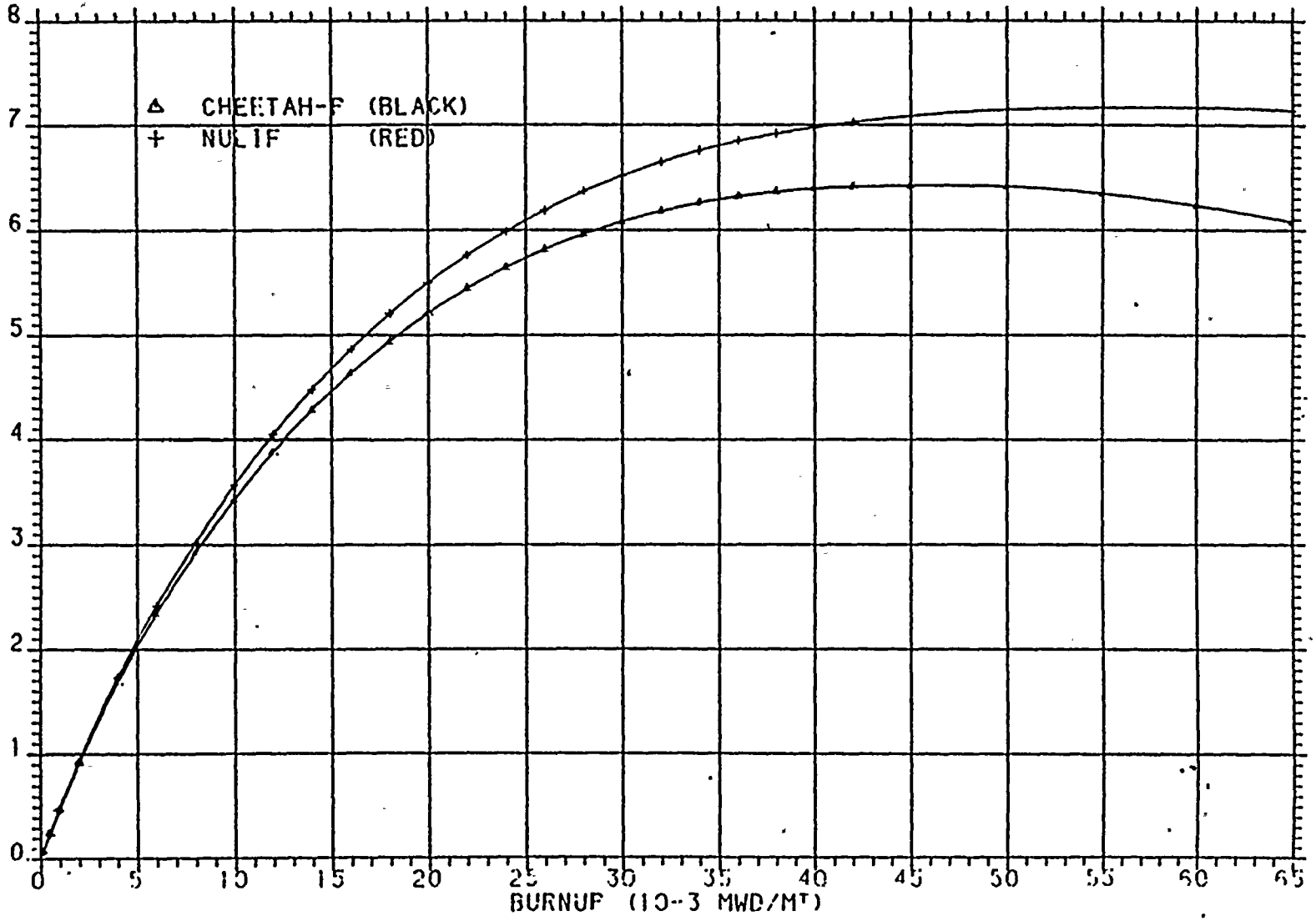

Figure 5.50

SL1 Nuclear Unit

Discharge U-235 vs. Burnup at 4.5% enrichment

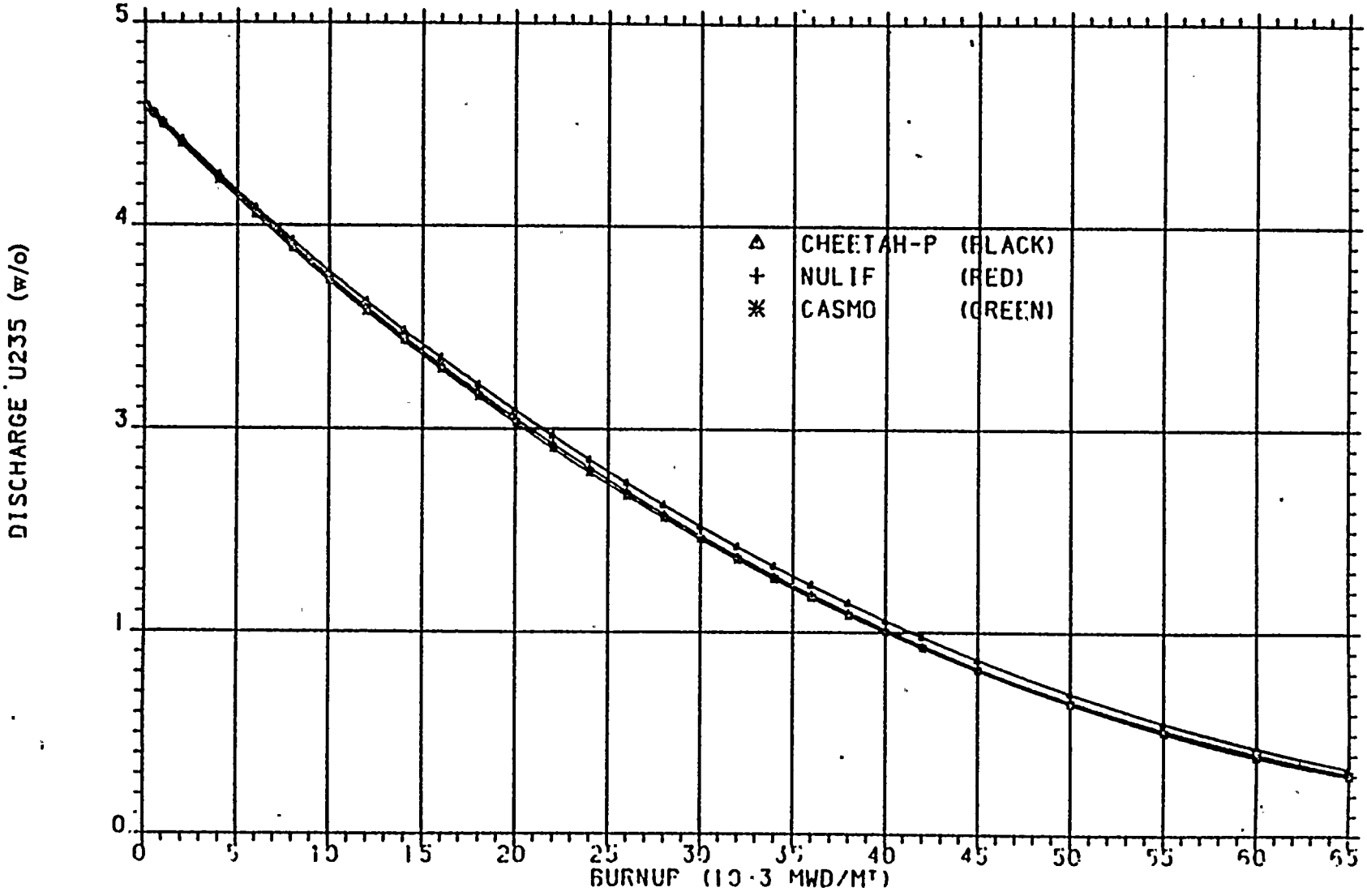

Figure 5.51

SLI Nuclear Unit

Discharge Fissile Plutonium vs. Burnup at 4.5% enrichment

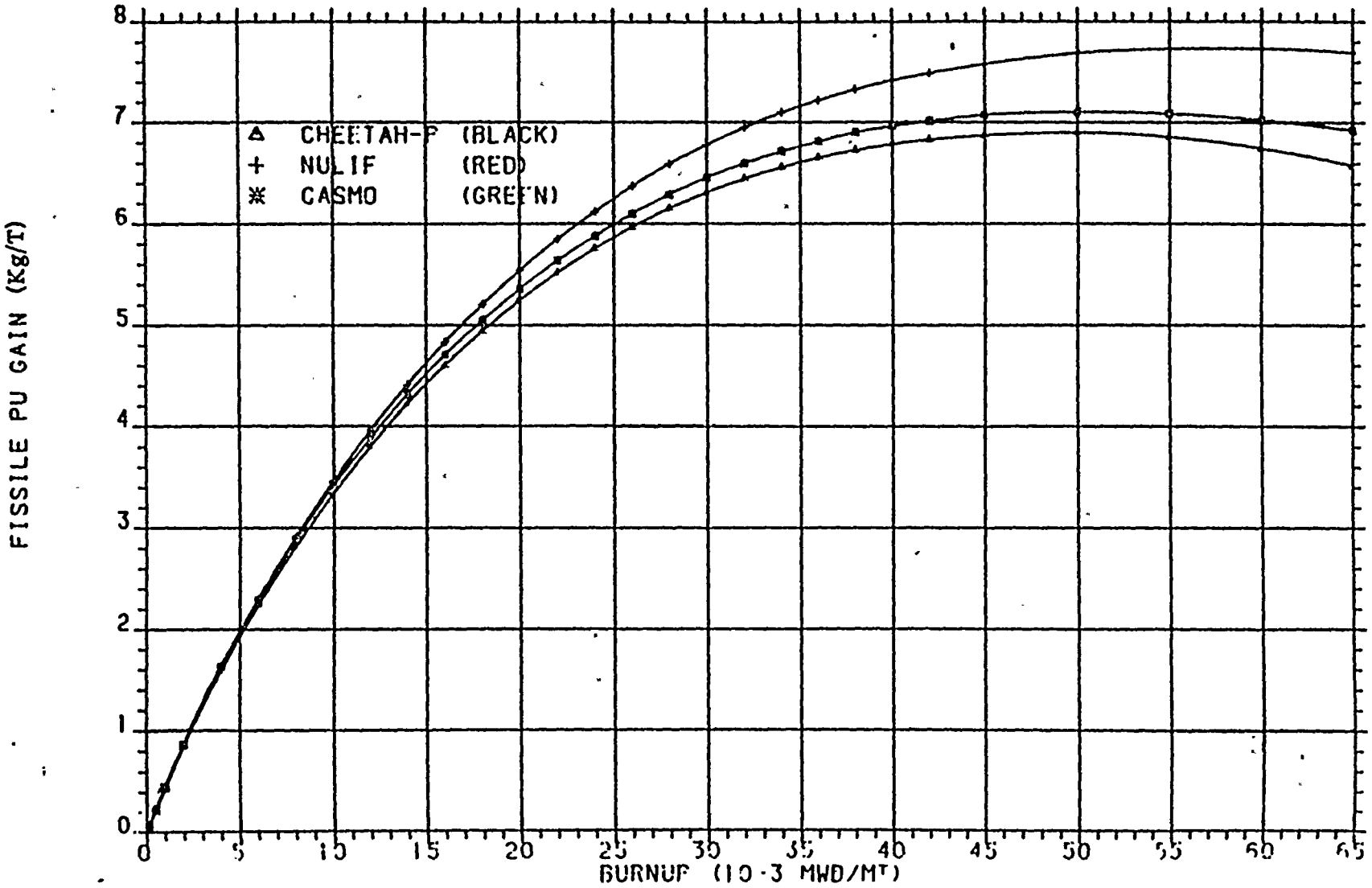

6.0 REFERENCES

1. Updated Final Safety Analysis Report, Turkey Point Plant Units 3 & 4, Florida Power & Light Company.

2. Updated Final Safety Analysis Report, St. Lucie Plant, Unit No. 1., Florida Power & Light Company.

3. Final Safety Analysis Report, St. Lucie Plant, Unit No. 2, Florida Power & Light Company.

4. "NAI Modified LEOPARD," Revision 2, NAI Report 71-13, Nuclear Associates International Corporation (December 10, 1973) (Proprietary Document).

5. "CHEETAH-P" report module within the LEAHS Nuclear Fuel Management and Analysis Package, Publication No. 84004100, Nuclear Associates International Corporation (July, 1974) (Proprietary Document).

6. R. F. Barry, "LEOPARD - A Spectrum Dependent Non Spatial Depletion Code for the IBM-7094," WCAP-3269-26, Westinghouse Electric Corporation, Pittsburgh (September, 1963).

7. H. Bohl, E. Gelbard and G. Ryan, "MUFT-4 - Fast Neutron Spectrum Code For the IBM-704," WAPD-TM-72 (July, 1957).

8. H. Amster and R. Suarez, "The Calculation of Thermal Constants Averaged Over a Wigner-Wilkins Flux Spectrum: Description of the SOFOCATE Code," WAPD-TM-39 (January, 1957).

9. R. J. Breen, "A One-Group Model For Thermal Activation Calculations," Nucl. Sci. Engr., Vol 9, 91-93 (January, 1961).

10. A. Amouyal, P. Benoist and J. Horowitz, "New Method of Determining the Thermal Utilization Factor in a Unit Cell," J. Nuclear Energy, Vol. 6, 79-98 (1957).

11. L. E. Strawbridge, "Calculation of Lattice Parameters and Criticality for Uniform Water Moderated Lattices," WCAP-3742 (September, 1963).

12. L. E. Strawbridge and R.F. Barry, "Criticality Calculations in Uniform Water-Moderated Lattices," Nucl. Sci. Engr., Vol. 23, 58-73 (September, 1965).

13. E. Hellstrand and G. Lundgren, "The Resonance Integral for Uranium Metal and Oxide," Nucl. Sci. Engr., Vol. 12, 435-439 (March, 1962).

14. E. Hellstrand, "Measurements of the Effective Resonance Integral in Uranium Metal and Oxide in Different Geometrics," J. Applied Physics, Volume 28, 1493 (December, 1957).

15. E. Hellstrand, P. Blomberg and S. Horner, "The Temperature Coefficient of the Resonance Integral For Uranium Metal and Oxide," Nucl. Sci. Engr., Volume 8, 497-506 (December, 1960).

16. A. Sauer, "Approximate Escape Probabilities," Nucl. Sci. Engr., Vol. 16, 329-335 (July, 1963).

17. H. Aisu and G. H. Minton, "Effective Surface in Lattices in the Calculation of Resonance Integrals," Nucl. Sci. Engr., Vol. 19, 468-471 (August, 1964).

18. H. A. Risti, "Unit Cell Homogenization For Reactor Depletion Studies," WCAP-6060, Westinghouse Atomic Power Division (1964).

19. O. J. Marlowe and P. A. Ombrellaro, "CANDLE - A One-Dimensional Few-Group Depletion Code for the IBM-704," WAPD-TM-53 (May, 1957).

20. Callaway-1 Licensing Application for Expanded Spent Fuel Storage Rack, Docket 50-483, Table 9.1A-3.

21. Babcock & Wilcox, Standard Nuclear Steam System, B-SAR-205, Vol. 2, p. 4.3-37 (Table 4.3-15).

22. W. L. Orr, H. I. Sternberg, P. Deramaix, R. H. Chastain, L. Binder, and A. J. Impink, "Saxton Plutonium Porgram, Nuclear Design of the

Saxton Partial Plutonium Core," WCAP-3385-51, (December 1965) (Also EURAEC-1490.)

23. R. D. Leamer, W. L. Orr, R. L. Stover, E. G. Taylor, J. P. Tobin, and A. Bukmir, "PuO_2-UO_2 Fueled Critical Experiments," WCAP-3726-1 (July, 1967).

24. R. J. Nodvik, "Evaluation of Mass Spectrometric and Radiochemical Analyses of Yankee Core I Spent Fuel," WCAP-6068 (March, 1966).

25. R. B. Davis, "Data Report for the Nondestructive Examination of Turkey Point Spent Fuel Assemblies B02, B03, B17, B41 and B43," HEDL-TME 79-68, Hanford Engineering Development Laboratory (March, 1978).

26. R. B. Davis and V. Pasupathi, "Data Summary Report For the Destructive Examination of Rods G7, G9, J8, I9, and H6 From Turkey Point Fuel Assembly B17," HEDL-TME 80-85, Hanford Engineering Development Laboratory (April, 1981).

27. S. D. Atkin, "Destructive Examination of 3-Cycle LWR Fuel Rods From Turkey Point Unit 3 For the Climax - Spent Fuel Test," HEDL-TME 80-89, Hanford Engineering Development Laboratory (June, 1981).

28. W. A. Wittkopf, J. M. Tilford, J. B. Andrews, II, G. Kirschner, N. M. Hassan and P. N. Colpo, "NULIF-Neutron Spectrum Generator, Few-

Group Constant Calculator and Fuel Depletion Code," BAW-426, Babcock & Wilcox Power Generation Group, Lynchburg (August, 1976).

29. M. Edenius, A. Ahlin and H. Haggblom, "CASMO-2: A Fuel Assembly Burnup Program," Users Manual, Studsvik Report NR-81/3, Studsvik Energiteknik AB (March, 1981).

30. Edward E. Pilat, "Methods for the Analysis of Boiling Water Reactors Lattice Physics," YAEC - 1232, Yankee Atomic Electric Company, Framington, Massachusetts (December 1980).

APPENDIX A

RESULTS OF CALCULATIONS OF CRITICAL EXPERIMENTS WITH FPL CHEETAH MODEL

Table A.1

Results of Analysis of Selected Strawbridge and Barry Critical Experiments with the CHEETAH Program.

Experiment Number	k_{eff}[1]	Enrichment (w/o)	Fuel Density (gm/cm^3)	Pitch (in.)	B^2 (cm^{-2})	Boron (ppm)	H_2O/U
1	1.0062	1.311	7.53	.8681	.002837	0	3.02
2	1.0091	1.311	7.53	.9287	.003017	0	3.95
3	1.0071	1.311	7.53	.9890	.002906	0	4.95
4	1.0068	1.311	7.52	.6134	.002528	0	3.93
5	1.0072	1.311	7.52	.6504	.002521	0	4.89
6	1.0083	1.311	10.53	.6134	.003259	0	2.88
7	1.0087	1.311	10.53	.6504	.003547	0	3.58
8	1.0083	1.311	10.53	.7110	.003422	0	4.83
9	1.0064	2.700	10.18	.4050	.004075	0	2.18
10	1.0096	2.700	10.18	.4350	.005323	0	2.93
11	1.0083	2.700	10.18	.4700	.006326	0	3.86
12	1.0117	2.700	10.18	.5730	.006564	0	7.02
13	1.0124	2.700	10.18	.6150	.006007	0	8.49
14	1.0063	2.700	10.18	.6650	.005292	0	10.38
15	1.0056	2.700	10.18	.4180	.00475	0	2.50
16	1.0024	2.700	10.18	.4930	.00688	0	4.51
17	1.0071	3.699	10.37	.4180	.00683	0	2.50
18	1.0081	3.699	10.37	.4930	.00951	0	4.51
19	1.0065	3.699	10.37	.4930	.009568	0	4.51
20	1.0022	3.699	10.37	.4930	.007464	455.4	4.51
21	1.0006	3.699	10.37	.4930	.006366	708	4.51
22	0.9992	3.699	10.37	.4930	.004099	1259	4.51
23	0.9985	3.699	10.37	.4930	.003839	1330	4.51
24	0.9972	3.699	10.37	.4930	.003338	1472	4.51
25	0.9957	4.020	9.46	.5950	.00880	0	2.55
26	1.0017	4.020	9.46	.5950	.00172	3389	2.55
34	0.9897	4.020	9.46	.5709	.00790	0	2.14
37	1.0215	2.459	10.24	.5950	.007010	0	2.84
42	0.9962	3.000	9.28	.6122	.005075	0	2.64
43	0.9772	3.000	9.28	.8653	.006881	0	8.16
44	1.0035	4.020	9.45	.6122	.006925	0	2.59
45	0.9991	4.020	9.45	.6630	.008552	0	3.53
46	1.0041	4.020	9.45	.8653	.009284	0	8.02
47	0.9858	4.020	9.45	.9374	.009179	0	9.90
50	1.0140	2.459	10.24	.5950	.00202	1674	2.84
51	1.0152	2.070	10.38	.8558	.00580	0	2.06
52	0.9940	2.070	10.38	.9469	.00806	0	3.09
53	0.9949	2.070	10.38	1.0300	.00857	0	4.12
54	1.0018	2.070	10.38	1.1768	.00770	0	6.14
55	0.9989	2.070	10.38	1.3092	.00616	0	8.20

Note 1: Measured bucklings were used in CHEETAH.

Table A.2

Results of Analysis of SNUPPS Zirconium Clad Critical Experiments with the CHEETAH Program.

Experiment Number	k_{eff}[1] (1-D)	Enrichment (w/o)	Fuel Density (gm/cm^3)	Pitch (in.)	B^2 (cm^{-2})	Boron (ppm)	H_2O/U
1	1.0012	2.719	10.42	0.600	.008793	0	3.04
2	1.0054	2.719	10.42	0.690	.009725	0	4.93
3	1.0014	2.719	10.42	0.848	.008637	0	8.87
4	0.9981	2.719	10.42	0.976	.006458	0	12.66
5	1.0015	2.719	10.42	0.600	.007177	306	3.04
6	1.0016	2.719	10.42	0.600	.006244	536.4	3.04
7	1.0011	2.719	10.42	0.600	.005572	727.7	3.04
8	1.0014	2.719	10.42	0.600	.008165	104	3.04
9	1.0008	2.719	10.42	0.600	.007599	218	3.04
10	1.0003	2.719	10.42	0.600	.007106	330	3.04
11	0.9989	2.719	10.42	0.600	.006661	446	3.04
12	1.0014	2.719	10.42	0.600	.005809	657.1	3.04
13	1.0003	2.719	10.42	0.848	.007320	104	8.87
14	0.9970	2.719	10.42	0.848	.006073	218	8.87

Note 1: The k_{eff} results are for one-dimensional calculations using CHEETAH diffusion equation coefficients and material bucklings from Reference 20.

Table A.3

Results of Analysis of Mixed Oxide Critical Experiments with the CHEETAH Program.

Experiment Number	k_{eff}[1] (1-D)	Enrichment (w/o)	Fuel Density (gm/cm^3)	Pitch (in.)	B^2 (cm^{-2})	Boron (ppm)	H_2O/U
1	1.0065	5.74	10.19	0.52	0.01176	0	3.166
2	1.0150	5.74	10.19	0.56	0.01271	0	4.076
3	1.0123	5.74	10.19	0.792	0.01368	0	10.68
4	1.0214	6.6 (8.6)	10.35	0.52	0.01088	0	3.532
5	1.0211	6.6 (8.6)	10.35	0.56	0.01221	0	4.547
6	1.0259	6.6 (8.6)	10.35	0.735	0.01596	0	9.872
7	1.0252	6.6 (8.6)	10.35	0.792	0.01593	0	11.92
8	1.0199	6.6 (8.6)	10.35	1.04	0.01284	0	22.59
9	1.0065	2.0 (7.7)	9.54	0.9758	0.01059	0	7.819
10	1.0050	2.0 (7.7)	9.54	1.0607	0.00984	0	9.742
11	1.0037	2.0 (7.7)	9.54	0.9758	0.00837	261	7.819
12	1.0007	2.0 (7.7)	9.54	0.9758	0.00631	526	7.819
13	1.0121	2.0(23.5)	9.54	0.9758	0.00795	0	7.823
14	1.0101	2.0(23.5)	9.54	1.0607	0.00733	0	9.746

Note 1: The k_{eff} results are for one dimensional calculations using CHEETAH diffusion equation coefficients and measured axial bucklings.

Note 2: Enrichments quoted for Experiments 1 through 3 are for UO_2; enrichments quoted for Experiments 4 through 14 are the PuO_2 content (w/o) with Pu-240 (w/o) in parenthesis. All PuO_2 is in natural UO_2.